ANTIMALARIAL SECONDARY METABOLITES

FROM *MORINDA LUCIDA*

A thesis submitted in fulfilment of the requirements

for the degree of

MASTER OF SCIENCE

of

Rhodes University

By

BERTHA CHITHAMBO

FEBRUARY 2017

ABSTRACT

Antimalarial activities of secondary metabolites from *Morinda lucida* (Rubiaceae), were investigated. Even though *M. lucida* is traditionally used to treat malaria, diabetes, jaundice, hypertension, dysentery and many other diseases, the compounds in this plant have not yet been fully investigated and characterised. Most of the studies that have been done on this plant focused on the medicinal properties of the crude extracts but have not gone further to isolate and characterise the compounds.

In this study, the methanol – dichloromethane crude extract from the bark of *M. lucida* was fractionated into fractions 1–8. Fractions 2–5 were purified in order to isolate active secondary metabolites. The isolated pure compounds were characterised and identified. An *in vitro* antimalarial assay was carried out on the crude extract, fractions, pure compounds and solutions made from different combinations of pure compounds using the parasite lactate dehydrogenase (pLDH) assay. An IC_{50} done on the methanolic crude extract gave a value of 25 µg/mL. The % cell viability for the crude extract in cell toxicity assay remained at 100%. Each of the pure compounds tested had very little activity. Their activities were increased when samples from the different compounds were mixed. One of these mixtures reduced malaria viability to about 22 % at 20 µM and gave an IC_{50} value of 17 µM. Antibacterial assays were also carried out on the crude extract and fractions. Fractions 2 and 3 were relatively active (MIC values ranging between 125-1000 µg/mL) against *M. cattarhalis* and *E. faecalis.* Fraction 2 was also the most active on *S. typhimurium* and *S. aureus* (MIC value of 1000 µg/mL) compared with the other fractions. This same fraction also showed some activity against *M. tuberculosis* with MIC_{90} and MIC_{99} values of 40.9 and 46.3 µg/mL respectively in an anti-tuberculosis assay.

The following compounds, comprising of iridoids (asperuloside and asperulosidic acid), terpenoids (stigmasterol, β-sitosterol, campesterol, lanosterol and cycloartenol) and anthraquinones [5,15-O-dimethylmorindol, 1,7-dihydroxy-2-methoxy-5-(methoxymethyl) anthraquinone and 1,6-dihydroxy-2-methoxy-5-(methoxymethyl)anthraquinone], were isolated. All these compounds have been isolated from different plants before with the exception of 1,7-dihydroxy-2-methoxy-5-(methoxymethyl)anthraquinone and 1,6-

dihydroxy-2-methoxy-5-(methoxymethyl)anthraquinone which were tentatively assigned the structures due to insufficient data. To the best of our knowledge, this is the first report on the identification of all of the mentioned compounds, with the exception of β-sitosterol and stigmasterol, from *M. lucida*.

Molecular docking was performed on one of the isolated anthraquinones (5,15-O-dimethylmorindol) to check if it can bind to cytochrome bc_1, a known target for atovaquone. This compound interacted with the same amino acids that atovaquone, a well known antimalarial agent, interacted with on cytochrome bc_1 indicating a possible similar mode of action.

ACKNOWLEDGEMENTS

I am very grateful to a lot of people who have helped me in different ways to achieve this MSc. My father's voice still echoes in my mind on the importance of education and I can still remember my mother's pinch on my earlobe for some misdemeanour in class as she was at one time my teacher. I salute you my parents and all my teachers who helped make me who I am today.

Prof Rui Krause, my supervisor, thank you for accepting me as a member of your expansive group. Even with your hectic schedule, you found time to explain those concepts that I could not understand no matter how much I consulted the books or literature. Thank you for your meticulous feedback on my work.

Dr Xavier Siwe Noundou, thank you for the endless support and feedback throughout this research, for the many lessons on extraction techniques, eluting a column, TLC, running and analysing NMR, MS and IR experiments, reading through initial writing etc. Your help is greatly appreciated.

Thank you to all members of the Chemistry Department, both academic and technical staff. Dr R Klein and Dr D S Khanya, thank you for the constructive criticism during our group meetings as well as during the Departmental presentations. Thank you to Prof P Kaye for helping me with the IUPAC nomenclature of some of the compounds, Dr K Lobb for lessons on running and analysing NMR spectra, Dr P Kempgens for NMR training, Mr L Sigauke for lessons in molecular docking which even run over the weekends and the help in editing my docking report, thank you. Mr F Chindeka, thank you for running the elemental analysis. Thank you to Rhodes University for the support and facilities as well as the South African Medical Research Council (MRC) with funds from National Treasury under its Economic Competitiveness and Support Package. A special thank you to Prof. Hopper and Prof. P. Kaye for allowing us to have our samples tested using their research facilities and Mrs Michelle Isaacs for performing the anti-malarial and toxicity assays. Mr Dondashe, thank you for all your help at the stores. Thank you to Prof. Sandy van Vuuren for the help with performing the antimicrobial assay and use of her laboratory at University of Witwatersrand, School of

Pharmacy and Mrs Phumzile Madondo, laboratory technician in Prof S van Vuuren's laboratory who helped us with carrying out the bioassay and showed us the way around the laboratory. Thank you to Dr Ronnett Seldon of the Drug Discovery and Development Centre (H3-D), Chemistry Department at the University of Cape Town, for performing the anti-tuberculosis assay.

Thank you to all F22 members for the friendship and support. Special thanks to Mr M Manyeruke, for introducing me to the column as well as TLC and rota vap and just being there responding to every little query I had without a grumble, Dr Gaelle Ngnie and Mr Treoneste Umumararungu - for running my NMR samples when I first started, Dr Dereck T Ndinteh - for the first lesson in TLC, Dr Yollande Fomogne for helping me get to grips with the techniques of running an IR experiment and analysing NMR spectra, Mr Gervase Makoni who was always willing to help and give ideas even though he had an overflowing schedule, thank you. Thank you to Ms Nozuko Makayonke for willing to help with my very first departmental presentation. Thank you to Mr Khethobole Sekgota, Mr Victor Hakizimana, Ms Christiana Adeyemi, Mrs Omobola Jesumoroti, Ms Maureen Gumbo, Mr Mpho Ngoepe, Mr Yemi Oderinlo, Dr S Majumder, Mr Yusuf Hassan, Mr Hilary Hezuruike, Mrs Gugu Msane and Ms Nokuthula Ngomane for your continuous help in different ways. Colleagues in G12, F12, S3, S4 and S22, thank you for your help.

My friends and family, thank you for pushing me on and encouraging me to keep on going when I thought I couldn't manage. Makaiko, my husband, for the continuous supply of chocolates to boost my morale and all the help and support, thank you. My children Sungeni, Tamani and N'lamwai, thank you for the encouragement and support. My sisters and brothers, I know I was normally if not always in your prayers, thank you.

"Whatever you do, do all to the glory of God", 1 Corinthians 10 vs. 31 (RSV). May His name be glorified for ever.

LIST OF ABBREVIATIONS

1D	1 dimensional
2D	2 dimensional
3D	3 dimensional
Acetyl-CoA	Acetyl coenzyme A
AcOH	Acetic acid
AcONa	Sodium acetate
AD4 atom types	Autodock 4 atom types
ADT	Autodock tools
ATCC	American Type Culture Collection
CC	Column chromatography
CDC	Centre for disease control
$CDCl_3$	Deuterated chloroform
CD_3OD	Deuterated methanol
COSY	Correlated spectroscopy (^1H-^1H)
CQ	Chloroquine
δ_H	Delta (Chemical shift of proton)
δ_C	Delta (Chemical shift of carbon)
d	Doublet
DBE	Double bond equivalence
DCM	Dichloromethane
DEPT	Distortionless enhancement by polarization transfer
Disc	Discovery studio
DMSO	Dimethyl sulfoxide
DMSO-d_6	Deuterated dimethyl sulfoxide
DNA	Deoxyribonucleic acid
EtOAc	Ethyl acetate
FT-IR spectroscopy	Fourier-transform infrared spectroscopy
HeLa cells	Human cervix adenocarcinoma cells
HR-ESI-MS	High resolution electrospray ionisation mass spectrometry
HMBC	Heteronuclear multi-bond coherence (^1H-^{13}C)

HSQC	Heteronuclear single quantum coherence (^{1}H-^{13}C)
IC_{50}	50% Inhibitory concentration
INT	Iodonitrotetrazolium chloride solution
IR	Infrared
LD_{50}	Median lethal dose
m	Multiplet
MeOH	Methanol
MHz	Megahertz
MIC	Minimum inhibitory concentrations
MIC_{90}	90% Inhibitory concentration
MIC_{99}	99% Inhibitory concentration
mg	Milligram
mL	Millilitre
ML	*Morinda lucida*
mM	Millimolar
m.p	Melting point
MS	Mass spectrometry
NBT	Nitrotetrazolium Blue chloride
NMR	Nuclear magnetic resonance
NOE	Nuclear overhauser effect
NOESY	Nuclear overhauser effect spectroscopy (^{1}H-^{1}H)
PES	Phenazine ethosulphate
PDB (or pdb)	Protein data bank
$Pd(OAc)_2$	Palladium acetate
PE	Petroleum ether
pLDH assay	Parasite lactate dehydrogenase assay
PPh_3	Triphenyl phosphate
ppm	Parts per million
q	Quartet
RBC	Red blood cells
s	Singlet

t	Triplet
TEA	Triethanolamine
TLC	Thin layer chromatography
µL	Microlitre
UV	Ultraviolet
VCC	Vacuum column chromatography
WHO	World Health Organisation,

CONTENTS

1. INTRODUCTION

1.1 Malaria

Malaria is an infection caused by different species of the genus *Plasmodium* (Abraham and Rotella, 2010; Kumar et al, 2014). Three of the species named *P. vivax*, *P. falciparum* and *P. malariae* are widely distributed (Abraham and Rotella, 2010; Kumar et al, 2014). Another species, *P. ovale,* is mainly a parasite found in tropical Africa (Abraham and Rotella, 2010). A fifth species, *P. knowlesi* is also emerging (Manguin et al, 2010; Villalobos et al, 2013). *Plasmodium falciparum* is the most lethal species (Kessl et al, 2007; Villalobos et al, 2013; Kumar et al, 2014, Sharma et al, 2015) and is quite problematic in the tropics (Dan and Bhakat, 2015).

The *Plasmodium* species keeps on changing its genetic make up to adapt to some malarial drugs (Noedl et al, 2003). It is therefore becoming resistant to drugs (Noedl et al, 2003; Van Tyne et al, 2013; Dan and Bhakat, 2015). This has caused a global loss of the effectiveness of some drugs like chloroquine (Perez-Sacau et al, 2005; Hrycyna et al, 2014; Dan and Bhakat, 2015). *Plasmodium falciparum* is responsible for more than 90 % of all cases of malaria (Kumar et al, 2014; Sharma et al, 2015) and 90 % of all deaths that occur due to malaria infections (Kumar et al, 2014).

In 2015, between 149 and 303 million people worldwide were infected with malaria (WHO, 2015) and more than 400 thousand people died of it (WHO, 2015). Nearly 40 % of the world population is at risk of being infected with malaria (Pinheiro et al, 2003; Abraham and Rotella, 2010; Unekwuojo et al, 2011) and about 90 % of the infections affect children in Africa (Unekwuojo et al, 2011; Sharma et al, 2015; WHO, 2015). Malaria control and therapy continue to be complicated by parasite resistance to drugs (Van Tyne et al, 2013; Dan and Bhakat, 2015; Sharma et al; 2015, WHO, 2015) and by mosquito resistance to insecticides (Wang and Jacobs-Lorena, 2013; Kumar et al, 2014; WHO, 2015). There is still no effective vaccine for malaria (Villalobos et al, 2013; Wang and Jacobs-Lorena, 2013; Kumar et al, 2014).

Malaria is introduced to humans by an infected female anopheles mosquito (Pinheiro et al, 2003; Muthas et al, 2005; Wang and Jacobs-Lorena, 2013). **Figure 1** shows a detailed as well as a summerised life cycle of *Plasmodium* within mosquito and human (Manguin et al, 2010; Robert et al, 2002). The mosquito injects *Plasmodium* sporozoites (reproductive cells) into the human's blood stream during feeding (Toole and Toole, 1999; Abraham and Rotella, 2010). These sporozoites are transported to the liver through the blood circulatory system (Abraham and Rotella, 2010; Manguin et al, 2010). In the liver (liver stage), the sporozoites invade liver cells (hepatocytes) where they undergo cell division and mature into schizonts (Toole and Toole, 1999; Abraham and Rotella, 2010). The schizonts rupture the liver cells and release merozoites (Toole and Toole, 1999; Abraham and Rotella, 2010). One schizont can release as many as 30 merozoites (Abraham and Rotella, 2010; Manguin et al, 2010). From the liver, these merozoites then travel back into the blood stream where they enter the erythrocytes i.e. red blood cells [RBC (Abraham and Rotella, 2010; Manguin et al, 2010)]. In the RBC (erythrocytic stage), the merozoites undergo different developmental stages first to form trophozoites which mature into schizonts again (Abraham and Rotella, 2010; Manguin et al, 2010). When the schizonts are mature within the RBC, the RBC rapture and release new merozoites into the blood stream (Toole and Toole, 1999; Abraham and Rotella, 2010; Manguin et al, 2010).

The cycle continues when a female anopheles mosquito feeds on the human's infected blood (Toole and Toole, 1999; Abraham and Rotella, 2010; Wang and Jacobs-Lorena, 2013). The anopheles mosquito is the main host for the parasite where sexual reproduction of the parasite takes place and sporozoites are produced (Abraham and Rotella, 2010; Manguin et al, 2010; Wang and Jacobs-Lorena, 2013). These sporozoites travel to the salivary glands and can again be injected into another human while the mosquito is feeding (Toole and Toole, 1999; Manguin et al, 2010; Wang and Jacobs-Lorena, 2013).

When a person has been infected with the malaria parasite, they show a number of symptoms in a specific order (Toole and Toole, 1999; Abraham and Rotella, 2010). For malaria caused by *P. vivax*, *P. falciparum* and *P. ovale*, these symptoms are repeated every third day hence the name tertian malaria (Abraham and Rotella, 2010). This is in unison to times when parasites mature into schizonts in the RBC (Toole and Toole, 1999; Abraham

and Rotella, 2010). For *P. malariae*, the symptoms are repeated every fourth day, giving the malaria that occurs the name quartan malaria (Abraham and Rotella, 2010). This type of malaria is normally mild compared to the malignant tertian malaria (Abraham and Rotella, 2010).

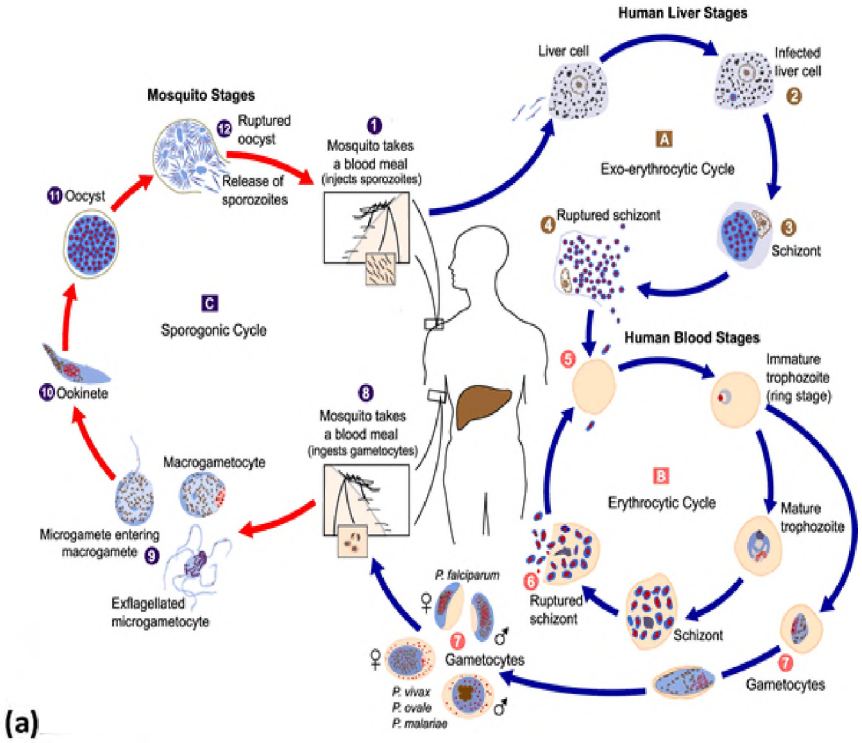

(a)

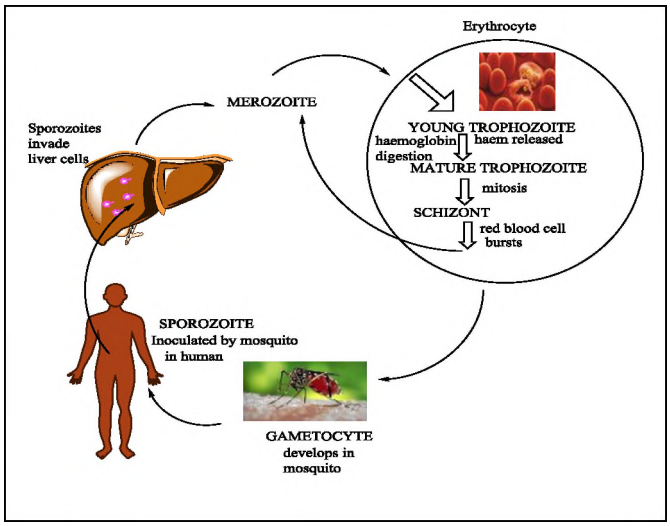

(b)

Figure 1: **Life cycle of *Plasmodium* within mosquito and human (a) a detailed cycle (Manguin et al, 2010) (b) a summarised cycle (Robert et al, 2002).**

Plasmodium vivax, the agent of benign tertian malaria, and *P. falciparum*, the one that causes malignant tertian malaria, are responsible for the great majority of cases and deaths attributed to malaria throughout the world (Abraham and Rotella, 2010; Sharma et al, 2015; WHO, 2015).

Most antimalarial drugs act on the pathogens at the erythrocytic stage of the disease (Ginsburg et al, 1998; Sharma et al, 2015). This is the stage when the malaria parasites attack the host's RBC's cytoplasmic matrix (cytosol) by ingesting it (Ginsburg et al, 1998). The RBC's cytosol is mostly haemoglobin (Ginsburg et al, 1998). This haemoglobin is broken down by the parasites to obtain amino acids for protein synthesis (Ginsburg et al, 1998; Rosenthal, 1998 and 2004). Haem is produced during this process (Ginsburg et al, 1998; Sanchez et al, 2008). Haem is toxic to the parasite and so the parasite polymerises some of this haem to an insoluble compound called haemozoin to protect itself (Sanchez et al, 2008; Ettari et al, 2010). The haem that is not converted to haemozoin can move across membranes into the parasite's or host's cytosol where it is detoxified (Ginsburg et al, 1998). Some of the drugs that act on the parasites during this stage either prevent the polymerisation of the haem or inhibit the degradation of the haem by the parasite (Ginsburg et al, 1998; Ettari et al, 2010). This allows for the accumulation of the haem in the parasite and so killing the parasite (Ginsburg et al, 1998). However, a few drugs like primaquine, act during the liver stage (Abraham and Rotella, 2010).

1.2 Plants as a source of antimalarial drugs

Plants were once a primary source of almost all the medicines in the world (Van Wyk and Wink, 2004; Dike et al, 2012). They still continue to provide humankind with new phytochemicals that are used as medicines for different sicknesses (Van Wyk and Wink, 2004; Dike et al, 2012; Olasehinde et al, 2014). Several secondary metabolites are responsible for the biological activity (such as antimalarial activity) of plants (Dewick, 2002; Evans, 2002). These secondary metabolites are synthesised in plants for their survival (Evans, 2002). Most of these metabolites are synthesised from building blocks derived from acetyl coenzyme A (acetyl-CoA) (**Fig. 2a**), mevalonic acid (**Fig. 2b**) as well as shikimic acid (**Fig. 2c**) and are used respectively in the acetate, mevalonate and shikimate biosynthetic pathways (Dewick, 2002).

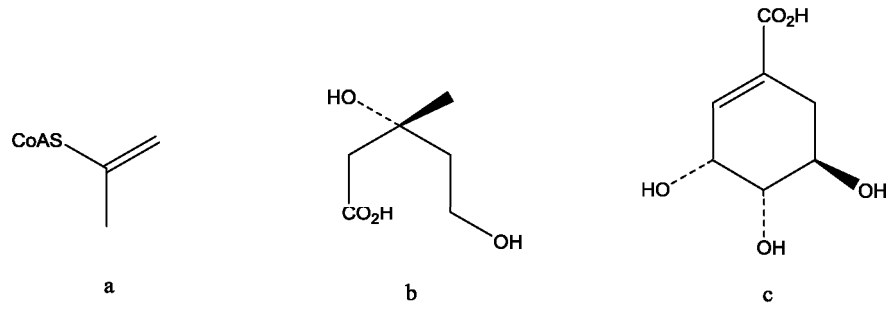

Figure 2: Chemical structure of (a) Acetyl-CoA (b) Mevalonic acid (c) Shikimic acid

Through these biosynthetic pathways, secondary metabolites like phenols, alkaloids and terpenoids are produced (Dewick, 2002). Most antimalarial compounds are derived from alkaloids, terpenes and some phenolic compounds (Evans, 2002; Sudhanshu et al, 2003).

1.2.1 Alkaloids

Alkaloids are organic nitrogenous bases found mainly in plants (Evans, 2002; Sudhanshu et al, 2003). More than 10 000 alkaloids have been isolated from plants of different families (Evans, 2002) and while they can be crystalline or amorphous, it is rare to find coloured alkaloids (Evans, 2002). In addition to carbon, hydrogen and nitrogen, most alkaloids contain some oxygen atoms (Dewick, 2002; Evans, 2002). There are heterocyclic (typical) and non-heterocyclic (atypical) alkaloids that are further classified into groups according to their structure (Evans, 2002).

Quinine (**Fig. 3a**), the first widely used antimalarial drug (Sanchez et al, 2008; Dinio et al, 2012), is an example of a plant alkaloid (Dewick, 2002; Evans, 2002; Dinio et al, 2012). It is extracted from the bark of the cinchona tree, *Cinchona pubescens* and from several other species of the genus *Cinchona* (Dewick, 2002; Evans, 2002; Dinio et al, 2012). These plants are still cultivated in many parts of the world (Van Wyk and Wink, 2004). For more than 300 years, these plants provided the only effective remedy for malaria (Van Wyk and Wink, 2004; Sanchez et al, 2008). Quinine is still used effectively in most parts of the world but many strains of *P. falciparum* have some resistance to quinine (Sanchez et al, 2008; Dinio et al, 2012). To avoid complete resistance in the future, quinine derivatives with improved activity and lower median inhibitory concentrations (IC_{50}) values are constantly being developed (Dinio et al, 2012).

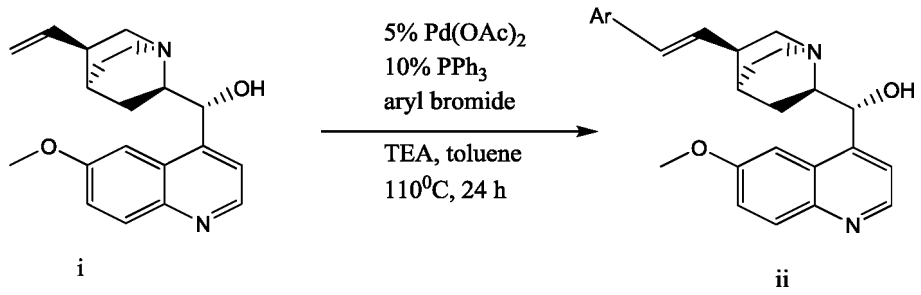

Figure 3a: Conversion of (i) quinine into (ii) derivatives of quinine

Figure 3a shows one of the processes used to modify quinine through the Heck reaction (Dinio et al, 2012). In this figure, palladium (II) acetate (Pd $(OAc)_2$), triphenylphosphate (PPh_3), bromobenzene, dry toluene and triethanolamine (TEA) were used in a reaction to add different aromatic groups on the quinuclidine alkene of the quinine (Dinio et al, 2012).

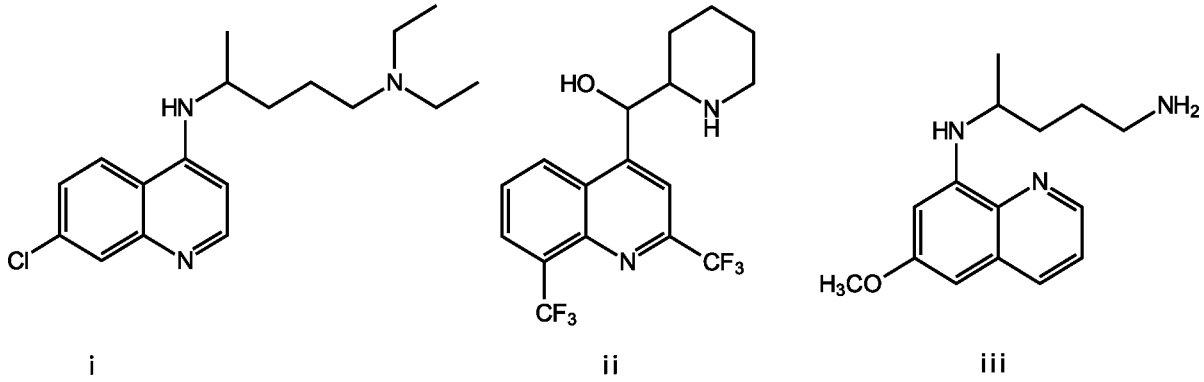

Figure 3b: Chemical structure of synthetic quinolines: (i) Chloroquine, (ii) Mefloquine (iii) Primaquine

Quinine served as the model for the development of a number of synthetic aminoquinoline drugs that are in use today and being developed further (Abraham et al, 2010; Unekwuojo et al, 2011). Chloroquine (CQ, **Fig. 3b**) is an important synthetic antimalarial drug that has been in use for a long time (Abraham et al, 2010; Ettari et al, 2010; Unekwuojo et al, 2011). It was developed as an alternative to quinine and wide spread resistance to it has led to its removal as a first line treatment against malaria (Abraham et al, 2010; Ettari et al, 2010; Unekwuojo et al, 2011).

Mefloquine (**Fig. 3b**) is a synthetic derivative of quinine (Abraham et al, 2010; Ettari et al, 2010). It was developed to replace CQ for the use on resistant strains of the malaria parasite (Abraham et al, 2010). Its mode of action is believed to be similar to that of quinine and its

derivatives (Kumar et al, 2014; Abraham et al, 2010). The absorption of mefloquine, however, appears to be reduced in severe malaria (Abraham et al, 2010) and resistance to this drug has also been reported in some areas of the world (Ettari et al, 2010; Unekwuojo et al, 2011).

Primaquine (**Fig. 3b**), an aminoquinoline, is another quinine analog (Abraham et al, 2010; Kumar et al, 2014). This drug is active against all parasite stages in humans but its mode of action is not yet completely known (Abraham et al, 2010). It is one of a few drugs that is believed to act during the liver stage but it is very toxic (Abraham et al, 2010; Ettari et al, 2010).

Quinine and its derivatives act on the erythrocytic stage of the parasite by inhibiting the crystallisation of haem into haemozoin (Sanchez et al, 2008; Abraham et al, 2010). Quinine is toxic and has been found to induce an abnormal rhythm of the heart beat, a condition called arrhythmia (Abraham et al, 2010). These days quinine is mainly used to treat complicated severe malaria (Sanchez et al, 2008; Abraham et al, 2010; Olasehinde et al, 2014). Chemo resistance to quinine monotherapy is slowly developing and consequently the drug is being used with other anti-malarial agents in combination therapy (Abraham et al, 2010).

1.2.2 Terpenoids

Terpenoids form another large group of plant phytochemicals (Van Wyk and Wink, 2004). Monoterpenes, sesquiterpenes, diterpenes, steroids, tetraterpenes, triterpenes and polyterpenes form this group (Dewick, 2002; Van Wyk and Wink, 2004). Even though terpenes have simple building blocks, their structures are complex because of the range of functional groups and secondary ring formations (Van Wyk and Wink, 2004).

Terpenes are probably best known for their aroma in flowers and essential oils, but there are some with medicinal activity (Abraham et al, 2010). Artemisinin (**Fig. 4**), from *Artemisia annua L*, is a sesquiterpene lactone endoperoxide antimalarial that is currently in widespread use (Dewick, 2002; Abraham et al, 2010). It was discovered during the screening of indigenous plants with anti-malarial properties in China during the Vietnam War (Krishna

et al, 2004; Abraham et al, 2010). The use of this plant to reduce fevers was recommended as early as the 340 AD but it was difficult to confirm the anti-malarial activities from aqueous extracts of *A. annua* (Abraham et al, 2010). It was later discovered that the active compound was extracted with ethyl ether at low temperatures (Abraham et al, 2010). A number of artemisinin's derivatives (**Fig. 4**) have been synthesised (Golenser et al, 2006; Abraham et al, 2010; Santos et al, 2014).

The activity of artemisinin is increased by modifying the structure of artemisinin to give C-10 derivatives (Kumar et al, 2014; Santos et al, 2014). The modified compounds have improved aqua-solubility as well compared to artemisinin which has very low solubility (Kumar et al, 2014; Golenser et al, 2006). This low solubility limits the methods of its administration (Golenser et al, 2006; Dewick, 2002). Synthesis of artemisinin is complex so it is normally extracted from *A. annua* and semi-synthesis of its derivatives is performed on these extracts (Evans, 2002).

A number of mechanisms of action of artemisinins have been proposed (Evans, 2002; Golenser et al, 2006; Shandilya et al, 2013). One of the mechanisms suggests that the endoperoxide group on the artemisinin reacts with the iron in haem (Evans, 2002; Golenser et al, 2006). This reaction gives highly reactive free radicals (Evans, 2002; Meshnick, 2002) that react with proteins in the parasite, hence killing the parasite (Evans, 2002). Haem-artemesinin complexes have been isolated in cultures of *P. falciparum* that had been treated with artemesinin (Golenser et al, 2006).

Artemisinins have gametocidal properties as well (Krishna et al, 2004; Abraham et al, 2010). This property of artemisinin is of importance as killing gametocytes reduces malaria transmission (Krishna et al, 2004; Abraham et al, 2010).

Recurence (recrudence) of malaria normally a month after treatment with artemisinin and its derivatives is a problem (Meshnick, 2002; Abraham et al, 2010). Because of the fast acting nature of this group of drugs, not all parasites are killed after treatment (Meshnick, 2002; Abraham et al, 2010). Recombination therapy with other groups of drugs like mefloquine is normally administered (Meshnick, 2002; Evans, 2002). Artemisinin- resistant

strains of *Plasmodium* are developing (Van Tyne et al, 2013; Dan and Bhakat, 2015; WHO, 2015). Gene mutations associated with drug resistance is beginning to alter the sensitivity of the parasites to some of the derivatives of artemisinin (Golenser et al, 2006; Unekwuojo et al, 2011).

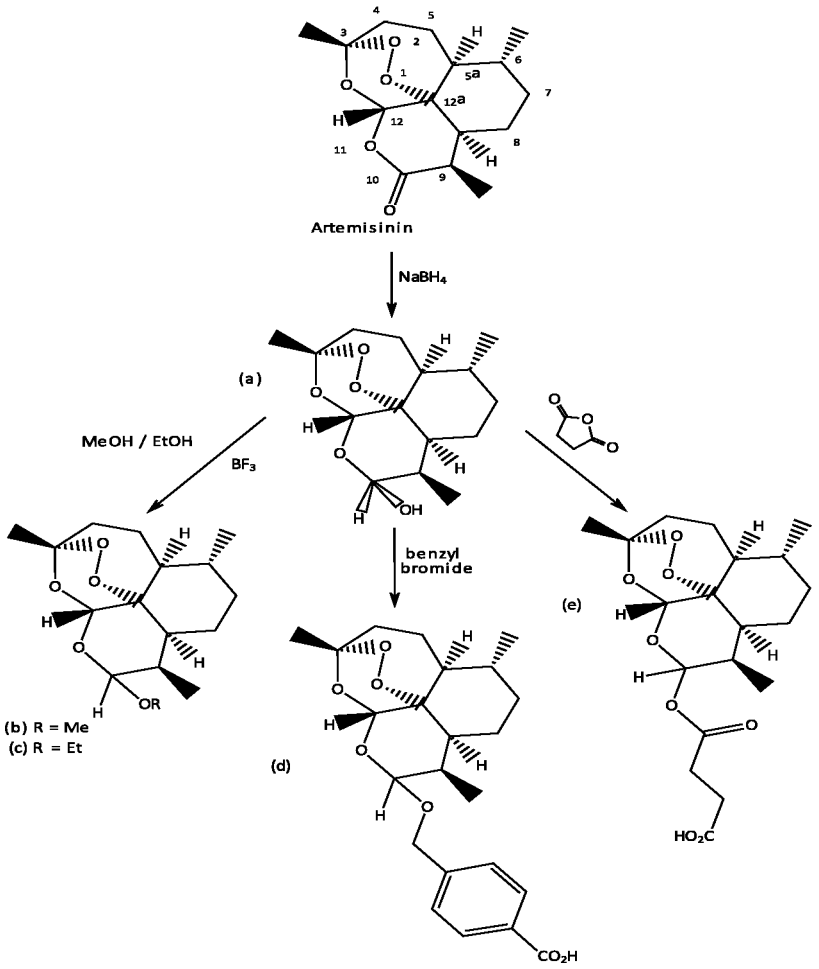

Figure 4: Some of the derivatives of artemisinin: (a) dihydroartemisinin (b) artemether (c) arteether (d) artelinic acid (e) artesunic acid

1.2.3 Phenolic compounds (Phenazines)

This group of secondary metabolites have aromatic moieties giving a range of compounds from those with one ring to some with complex polyaromatic structures (Evans, 2002). Aromatic antiprotozoal compounds have been isolated from plants (Dewick, 2002; Evans, 2002). Examples include naphthoquinones, flavonoid glycosides as well as some polyphenolic compounds (Dewick, 2002; Evans, 2002), but most antimalarial aromatic compounds are synthetic (Evans, 2002).

The quinone lapachol (**Fig. 5a**), has been isolated from a plant, *Tabebuia rosea*, and other species of the *Bignoniaceae* family (de Andrade-Neto et al, 2004). Lapachol itself is a weak antimalarial drug, but a number of its synthetic derivatives (e.g. **Fig. 5b**) are active (de Andrade-Neto et al, 2004). This applies to β-lapachone as well (**Fig. 5c**), a naturally occurring quinone which can easily be synthesised (de Andrade-Neto et al, 2004).

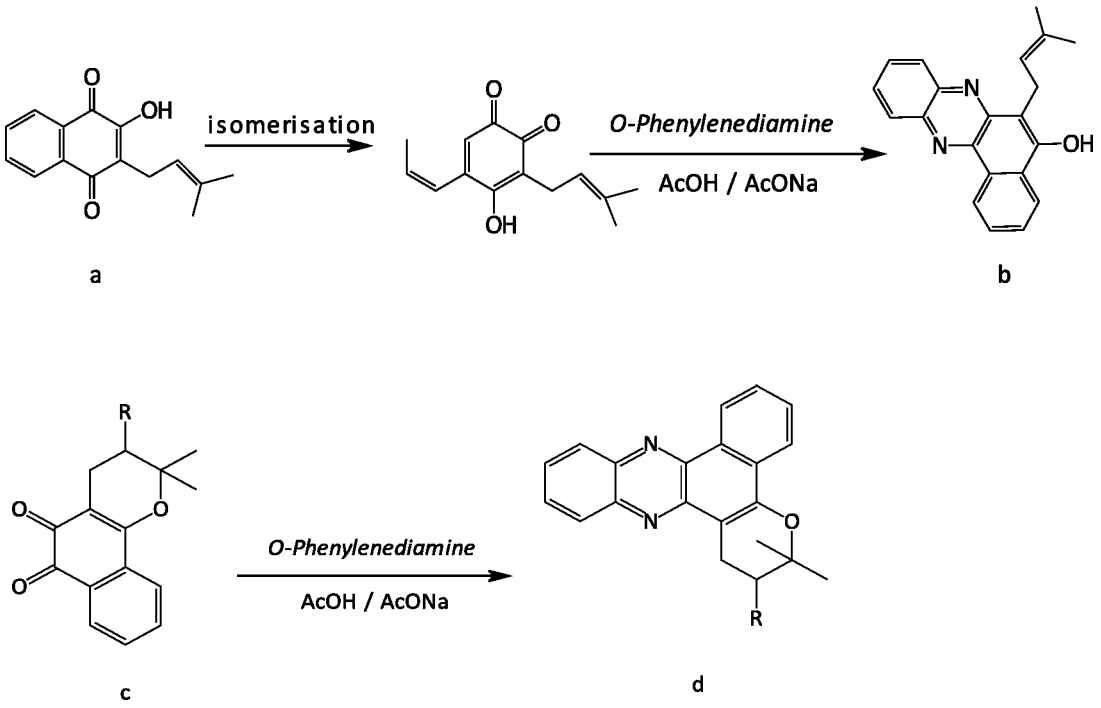

Figure 5: The synthesis of derivatives of (a) Lapachol (c) β-Lapachone

When the antimalarial activity of the derivatives of lapachol and β-lapachone were performed, a sulfonide derivative (**Fig. 5d**) was found to be the most active both in vivo as well as in vitro against malaria (de Andrade-Neto et al, 2004).

Atovaquone (**Fig. 6a**), a synthetic naphthoquinone, was developed from lapachol derivatives (Baggish and Hill, 2002). Atovaquone alone is less effective in treating drug-resistant infections of malaria caused by *P. falciparum* (Baggish and Hill, 2002) but it is highly effective when combined with another drug called proguanil (**Fig. 6a**) in a drug combination called Malarone™ (Yeo et al, 1997; Baggish and Hill, 2002). Atovaquone and proguanil act synergistically, enhancing the activity against *P. falciparum* (Yeo et al, 1997; de Andrade-Neto et al, 2004). Atovaquone inhibits electron transport by cytochrome complex bc_1 in the mitochondria of *Plasmodium* species (Baggish and Hill, 2002; Kessl et al, 2007). The

inhibition of the electron transport system leads to the inhibition of other parasite enzymes like dihydroorotate dehydrogenase which is responsible for the synthesis of pyrimidines (Baggish and Hill, 2002). This leads to the inhibition of DNA synthesis and so causes the death of the parasite (Baggish and Hill, 2002).

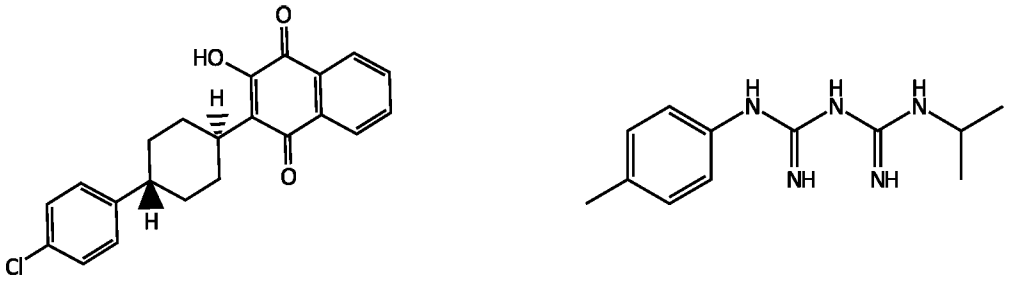

i ii

Figure 6a: Synthetic phenolic compounds: (i) atovaquone (ii) proguanil

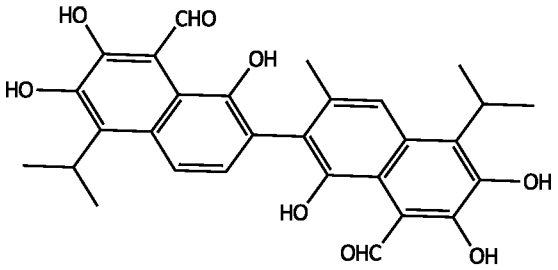

Figure 6b: Gossypol

Gossypol (**Fig. 6b**) is another phenolic compound active against *P. falciparum* (Dewick, 2002). It has been isolated from cotton seeds of *Gossypium* species (Dewick, 2002; Evans, 2002). Even though gossypol is active against *Plasmodium*, it is mostly used as a male contraceptive in China (Evans, 2002).

1.2.4 Phytochemical screening

All these classes of secondary metabolites can be identified in a sample by use of different qualitative tests (Evans, 2002) listed here as well as characterisation methods (Wu et al, 2013).

1.2.4.1 Tests for alkaloids

The following methods are used to test the presence of alkaloids in extracts:

(a) Mayer's Test

Approximately 1 mL of extract is added to 1 mL of Mayer's reagent (potassium mercuric iodide solution). A positive test gives a whitish or cream coloured precipitate (Evans, 2002; Chukwuemeka et al, 2013).

(b) Wagner's Test

The extract (1 mL) is added to 2 mL of Wagner's reagent (solution of iodine in potassium iodide). A reddish-brown precipitate indicates the presence of alkaloids (Evans, 2002; Chukwuemeka et al, 2013).

(c) Hager's Test

The extract (1 mL) is added to 3 mL of Hager's reagent (a saturated solution of picric acid). This gives a yellow precipitate in the presence of alkaloids (Evans, 2002; Chukwuemeka et al, 2013).

(d) Drangendorff's Test

The Dragendorff's reagent is first prepared as follows: 40 mg of potassium iodide are dissolved in 100 mL of distilled water (solution A). An 850 mg of bismuth subnitrate is dissolved in 50 mL of 20 % (v/v) acetic acid (solution B). Immediately before use, a mixture of 10 mL of solution A, 10 mL of solution B, and 20 mL of glacial acetic acid are mixed and diluted with distilled water to 100 mL (Dragendorff's reagent, solution C) [Kuwoyama et al, 2005; Askal et al, 2008]. A few drops of Draggendorff's reagent (solution C) are added to 1 mL of extract. The presence of a precipitate indicates the presence of alkaloids (Kuwoyama et al, 2005).

1.2.4.2 Tests for terpenoids

Salkowski's test is used to check the presence of terpenoids in an extract, where 3 mL concentrated sulphuric acid is added to a mixture of 5 mL extract and 2 mL chloroform. A reddish-brown colouration on the interface indicates the presence of terpenoids in an extract (Edeoga et al, 2005; Mir et al, 2013).

Another test for terpenoids is the Liebermann-Burchard's test which is carried out by mixing 2 mg of sample with 1 mL of acetic anhydride in a glass vial. The mixture is heated until it

boils then cooled in ice. A few drops of concentrated sulphuric acid are added along the sides of the vial. A pink colour gives a positive test for terpenoids (Siwa, 2012).

1.2.4.3 Tests for phenolic compounds

Different tests can be done to check the presence of the different aromatic compounds in an extract. For a general test, the extract is dissolved in 5 mL of distilled water. A few drops of neutral 5 % ferric chloride solution are added to this mixture. A dark green colour indicates the presence of aromatic compounds (Wankhar et al, 2015). For flavonoids, 4 mL of extract is mixed with 1.5 mL of 50 % methanol solution then warmed. A magnesium ribbon is added to the warmed solution followed by 5–6 drops of concentrated hydrochloric acid. A red colour indicates the presence of flavonoids and orange colour for flavones (Saikia et al, 2013).

1.2.4.4 Tests for reducing sugar

The extract (1 mL) solution is added to 1 mL of water and 5–8 drops of Fehling's solution is added to the mixture. A brick-red precipitate indicates the presence of reducing sugar (Saikia et al, 2013).

1.2.4.5 Test for carbohydrates

A few drops of Molisch's reagent are added to 2 mL of a water extract. A small quantity of concentrated sulphuric acid is then added and the mixture is shaken. After shaking, the mixture is left to stand for 2 minutes and then diluted with 5 mL of water. A purple precipitate indicates the presence of carbohydrates (Yisa, 2009).

1.2.5 Plants with antimalarial properties

A wide variety of plants are traditionally used to treat malaria (Evans, 2002; Van Wyk and Wink, 2004; Boonphong et al, 2007; Dike et al, 2012; Iwu, 2014). Some of these plants are listed in **Appendix 1**. It can be seen that these plants have one or two groups of the secondary metabolites discussed above which gives the plant its antimalarial activity.

1.3 *Morinda lucida*- a plant considered to have antimalarial compounds

Morinda lucida (Benth.) of the Rubiaceae family is a medium-sized tree which can grow up to 15 m high (Lawal et al, 2012; Iwu, 2014). It has a scaly grey bark, short branches and

shining foliage (Lawal et al, 2012; Adeyemi et al, 2014; Iwu, 2014). The plant is known by different names in parts of West and Central Africa (Lawal et al, 2012; Adeyemi et al, 2014; Iwu, 2014). It is called *Sangogo*, *Ewe amake*, *Oruwo* or *Ruwo* and its English name, *Brimstone*, is derived from the yellow wood of *M. lucida* (Lawal et al, 2012; Iwu, 2014). The plant produces white flowers in January to July and then September to October (Adeyemi et al, 2014; Iwu, 2014).

In Central and West Africa, infusions and decoctions of root, bark and leaves are used as treatment against different fevers, including yellow fever, malaria, trypanosomiasis and feverish conditions during childbirth (Lawal et al, 2012; Iwu, 2014). The plant is also used in cases of insomnia, diabetes, hypertension, cerebral congestion, dysentery, stomach-ache, ulcers, jaundice, leprosy and gonorrhoea (Lawal et al, 2012; Iwu, 2014). The powdered root bark as well as plasters made from stem or root bark is used as a dressing against itch and ringworm as well as wound infections and abscesses (Lawal et al, 2012). Leaves and twigs are sold in markets as a medicinal tonic for young children (Lawal et al, 2012). Apart from oral teas from the leaves being used as a general febrifuge, they are also used as analgesics and laxatives (Lawal et al, 2012). The leaves are also used to treat infertility and irregular menstruation in women of some parts of West Africa (Lawal et al, 2012).

Phytochemical tests on the aqueous and methanol stem bark (Odutunga, 2010), aqueous leaf (Adeyemi et al, 2014) and ethanol leaf extract (Chukwuemeka et al, 2013) of *M. lucida* have indicated the presence of tannins, steroids, glycosides, saponins and alkaloids (Odutunga, 2010; Chukwuemeka et al, 2013; Adeyemi et al, 2014).

The iridoid oruwacin (**Fig. 7a**), anthraquinones like damnacanthal (**Fig. 7b**), nordamnacanthal (**Fig. 7c**), alizarin-1-methyl ether (**Fig. 7d**), digitolutein (rubiadin-1-methyl ether) (**Fig. 7e**), rubiadin (**Fig. 7f**), soranjidiol (**Fig. 7g**), 1-hydroxy-2-methyl-anthraquinone (**Fig. 7j**) and 1-methoxy-2-methyl-anthraquinone (**Fig. 7k**) and anthraquinols like oruwal (**Fig. 7h**) and oruwalol (**Fig. 7i**) have been isolated from *M. lucida* (Adesogan, 1973; 1979; Lawal et al, 2012). The iridoid, oruwacin, was isolated from a petroleum extract of the leaves and crystallised from methanol as colourless needles (Adesogan, 1979; Lawal et al, 2012). For the anthraquinones and anthraquinols, two samples from the stem of *M. lucida* harvested

from different areas were used (Adesogan, 1973). One sample gave both anthraquinones and anthraquinols whereas the other sample from a different location had no anthraquinols (Adesogan, 1973). This indicated that *M. lucida*, just like other plants, can have different chemical compositions depending on the location of the plant (Adesogan, 1973). A mixture of β-sitosterol and stigmasterol was also isolated from a methanol and water extract of the leaves (Nweze, 2012). A number of essential oils like sabiene, *β*-pinene, 1,8-cineole and *α*-tepinyl acetate, have also been isolated from *M. lucida* (Owolabi et al, 2014).

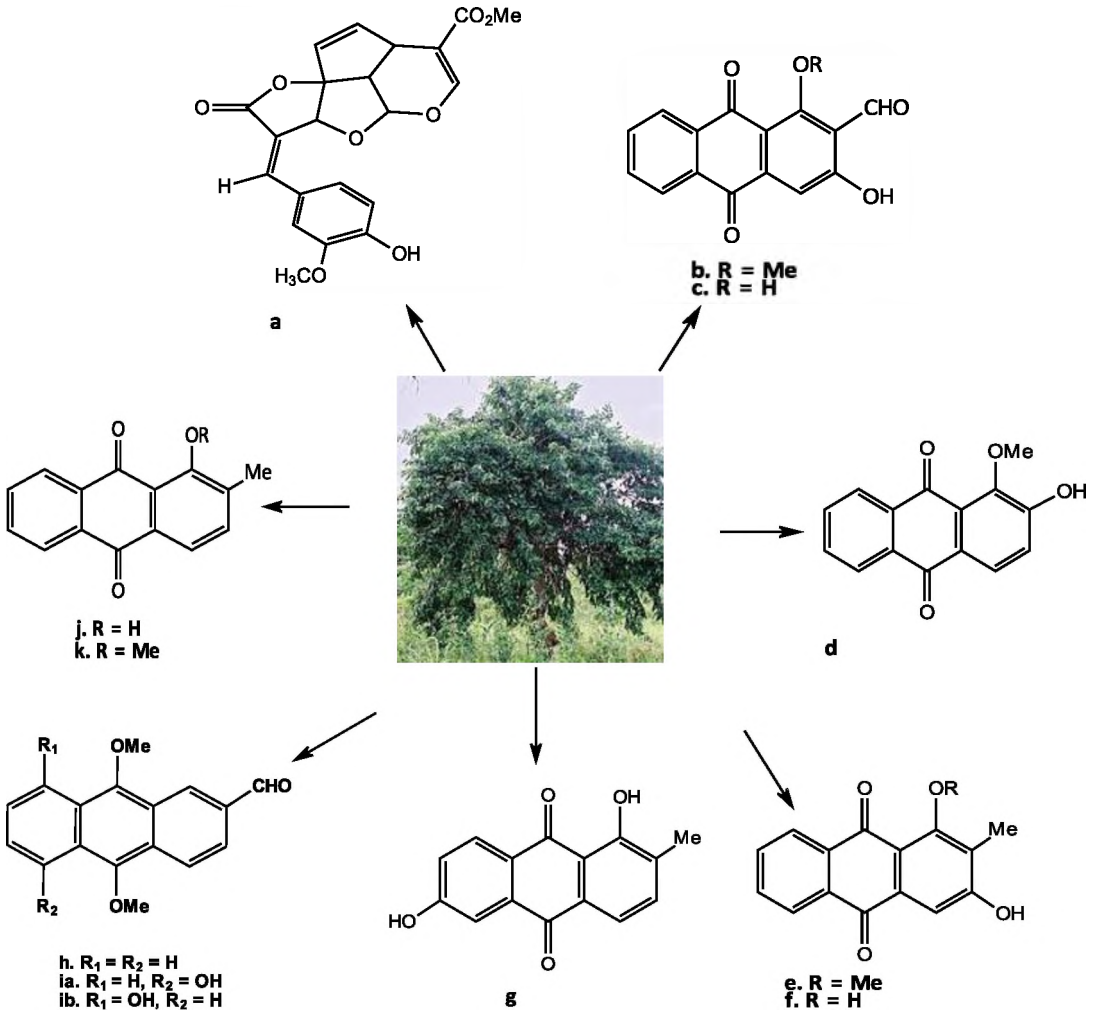

Figure 7: Some of the compounds that have been isolated from *M. lucida* (Adesogan, 1973; 1979; http://database.prota.org, 2015).

A number of *in vivo* and *in vitro* tests to check the activities of different extracts from *M. lucida* have been done (Oduola et al, 2010; Ashafa and Olunu, 2011; Balogun et al, 2011; Unekwuojo et al, 2011; Umar et al, 2013). *M. lucida* has been found to be non-toxic

(Balogun et al, 2011). Tests done on albino rats gave low bilirium concentration in the blood (Balogun et al, 2011). This indicated that the methanol leaf extracts did not cause haemolysis and liver damage (Balogun et al, 2011). Another study on an acute oral toxicity test of an aqueous leaf extract suggested an oral median lethal dose (LD_{50}) of *M. lucida* to be greater than 6400 mg/kg as there was no death of Wistar albino rats when tested at this dosage (Oduola et al, 2010). In a separate study on male Wistar rats, it was found that the ethanol root extract did not show any unfavourable effects related to extract toxicity, for example, there was no restlessness of rats being tested as well as no diarrhoea (Ashafa et al, 2011). No rats died at a dosage of 2000 mg/kg body weight (Ashafa et al, 2011). The extract did not show any significant effect on the composition of the blood at dosages of 50, 100, 200 and 300 mg/kg body weight (Ashafa et al, 2011).

An aqueous leaf extract of *M. lucida* showed *in vivo* antimalarial activity of up to 85.05 % against *Plasmodium berghei NK-65* in mice at doses of 100, 200, 400 and 800 mg/kg body weight (Unekwuojo et al, 2011). Methanolic root extract suppressed parasites by 59.84, 67.72 and 81.80 % for doses of 100, 200 and 400 mg/kg body weight, respectively (Umar et al, 2013). Both leaf and root extracts were investigated in this study and higher activities were observed with the root extract than with the leaves (Umar et al, 2013). The standard drug, chloroquine, killed 95.35 % of the parasite (Umar et al, 2013). In another study, the effects of digito-lutein, rubiadin 1-methyl ether and damnacanthal extracted from the stem bark and the roots of *M. lucida* on the *in vitro* growth of *P. falciparum* were investigated (Koumaglo et al, 1992). In this study, 100 % inhibition of the malaria parasite was obtained with 30 to 40 µg of each compound tested (Koumaglo et al, 1992). IC_{50} for these compounds were done. Rudiadin-1-methyl ether gave the lowest IC_{50} value at 8.10 µg/mL (Koumaglo et al, 1992). In other studies to investigate the antimalarial activity of *M. lucida*, it was also found that a crude ethanol leaf extract inhibited the growth of *P. falciparum* with a minimum inhibitory concentration (MIC) of 0.6 mg/mL (Bello et al, 2009). Anthraquinones from a petroleum ether leaf extract were also found to be active with damnacanthal being the most active against the malaria parasite (Titanji et al, 2008).

Separate studies on the aqueous leaf extracts (Kazeem et al, 2013) and stem bark extracts (Odutuga et al, 2010) as well as methanol stem bark extract (Odutuga et al, 2010) showed

some anti-diabetic properties by inhibiting α-amylase and α-glucosidase (Kazeem et al, 2013) and lowering aspartate aminotransferase (Odutuga et al, 2010) enzymes in diabetic albino rats. Another study of a methanol extract of *M. lucida* found that a dose of 400 mg/kg body weight exhibited anti-hyperglycaemic effect in streptozontonic-diabetic rats (Olumayokun et al, 1999).

Crude aqueous and ethanol extracts of *M. lucida* root bark (250, 500, 750 and 1000 mg) showed some activity against *Escherichia coli*, *Salmonella typhi*, *Staphylococcus aureus, Bacillus subtilis, Flavobacterium* species, *Klebsiella pneumoniae and Pseudomonas aeruginosa* (Adomi et al, 2010). The ethanol extract was found to be most active on *B. Subtilis* with a maximum zone of inhibition of 19 mm compared to 28 mm zone of inhibition for the antibiotic ampiclox (Adomi et al, 2010). The aqueous extract had the least activity (Adomi et al, 2010). In a separate study, an ethanol extract of leaves was found to inhibit the *in vitro* growth of *S. aureus* and *P. aeruginosa* (Addy et al, 2013).

Antifungal tests were done on anthraquinones which were isolated from a dichloromethane root extract of *M. lucida* (Rath et al, 1995). Alizarin - 1 - methyl ether had the highest activity against *Cladosporium cucumerinum* and *Candida albicans* in this study (Rath et al, 1995).

Hot and cold crude aqueous leaf extracts of the plant have been reported to be active against *Trypanosoma brucei brucei, a protozoan* parasite that causes trypanosomiasis (Busari et al, 2014). The most effective dose was 400 mg/kg body weight from the hot aqueous leaf extract which cleared after 2 weeks of treatment (Busari et al, 2014). An earlier study also found that some fractions of a methanol and aqueous leaf extract showed *in vitro* anti-trypanosomal activities against *T. b. brucei* S427 with MIC values ranging between 6.25 to 25 µg/mL (Nweze, 2012).

A methanol stem bark crude extract has also been found to have antioxidant and ferric reducing abilities (Ogunlana et al, 2008). The ability of the extract to prevent the oxidation of β–carotene was used to check the antioxidant activity of the sample (Ogunlana et al, 2008).

Essential oils, phostoxin and primo-ban-20, from the aqueous extract of the aerial parts of *M. lucida* were found to be active against the pulse beetle, *Callosobruchus maculates* (Owolabi et al, 2014). The beetles were killed within 72 hours of being sprayed with these essential oils at a dosage of 0.20 µg/mL (Owolabi et al, 2014).

M. lucida has also been reported to have trypanocidal and aortic vasorelaxant activities (Ashafa et al, 2011).

1.4 Molecular docking

Molecular docking models the molecular interactions of drugs (ligands) with pathogen enzymes (macromolecules or proteins) using computer software (Kessl et al, 2007). Molecular docking studies provide the possible binding conformations of the ligand in an enzyme (Villalobos et al, 2013). The interactions between ligand and enzyme are then studied to check the probabilities of ligand in being able to stop the functional activities of the enzyme (Pinheiro et al, 2003).

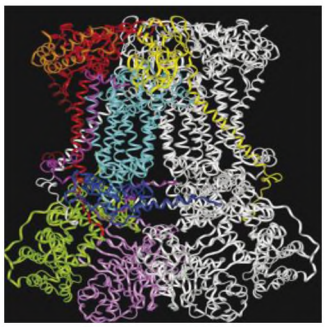

Figure 8: Ribbon structure of the yeast cytochrome bc_1 complex (PDB code 1EZV) with one of the dimmers coloured white, cytochrome b is coloured cyan, Rieske iron-sulfur protein is in yellow, cytochrome c_1 in red. The other subunits have different colours (Kessl et al, 2007).

Cytochrome bc_1 complex (**Fig. 8**) is an example of an enzyme responsible for mitochondrial respiration in some organisms like plasmodium (Baggish and Hill, 2002; Lange and Hunte, 2002; Kessl et al, 2007). It is a dimer composed of 11 subunits of which 3, namely the Rieske iron-sulfur protein ([2Fe–2S]-), cytochrome b and cytochrome c_1 are catalytically important (Kessl et al, 2007). Each monomer of the complex has a binding site with Qi site on cytochrome b and Qo site located at the interface of cytochrome b and the Rieske protein

(Hunte et al, 2000; Kessl et al, 2007). The symbol Q refered to on the names of the binding sites is from the coenmzyme Q (another name for mitochondrial protein called ubiquinone) that binds to cytochrome bc_1 (Baggish and Hill, 2002). Most crystal structures of cytochrome bc_1 complex have shown that the cluster-carrying domain of the Rieske iron-sulphur protein is mobile as it is sometimes not visible or is found in different positions in the various crystal forms of the enzyme and is dependent on the inhibitor binding the Qo site (Hunte et al, 2000).

The three-dimensional structure of *P. falciparum's* cytochrome bc_1 is not available (Villalobos et al, 2013). The one used in docking studies is from *Saccharomyces cerevisae* (**Fig. 8**), a yeast, as there is about 68% sequence identity between the *S. cerevisae* and plasmodial cytochrome bc1 within the Qo binding pocket (Kessl et al, 2007**;** Villalobos et al, 2013).

Atovaquone, an antimalarial drug, is an inhibitor of cytochrome bc_1 complex (see section 1.2.3) and targets the Qo site (Baggish and Hill, 2002; Kessl et al, 2007; Villalobos et al, 2014). **Figure 9** shows atovaquone at the cytochrome bc1 complex's binding site.

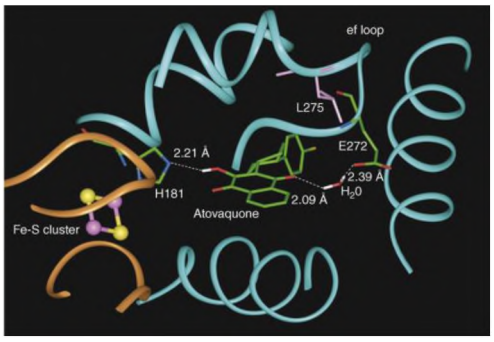

Figure 9: **Atovaquone-binding pocket in the yeast cytochrome bc1 complex. Cytochrome b is shown in cyan, and a portion of the Rieske iron-sulfur protein is in gold. Atovaquone (coloured green) is hydrogen bonded to His181 of the Rieske protein and to a water molecule that forms a bridge to Glu272 through a second hydrogen bond (Kessl et al, 2007).**

Kessl et al (2007) have reported that atovaquone binds to the Qo pocket when the mobile domain of the Rieske protein is close to cytochrome b and that it interacts directly with the iron-sulfur protein. They also concluded that atovaquone forms a hydrogen bond between the hydroxyl group on the napthoquinone ring of the inhibitor and His181 of the Rieske protein (**Fig. 9**).

Docking studies can unravel the mechanism of action of drugs and they offer guidelines for the synthesis of new derivatives with improved efficiency (Pinheiro et al, 2003; Fogel et al, 2008).

1.5 Aims of the research project

In this research, the chemical constituents in the methanol – dichloromethane extract from the stem of *Morinda lucida* were investigated. The aims of the research were to:

a) Carry out biological assays on the crude extracts and fractions from the bark of *M. lucida* to test their:
   (i) toxicity against Hela cells
   (ii) activity against *P. falciparum*
   (iii) activity against bacterial pathogens.
b) Extract and isolate pure compounds from the bark of *M. lucida* using column and thin layer chromatography.
c) Characterise and identify the isolated compounds by using MS, IR and NMR.
d) Carry out biological assays on the isolated compounds to test their:
   (i) toxicity against Hela cells
   (ii) activity against *P. falciparum*
   (iii) activity against bacterial pathogens.
e) Study how some of the isolated compounds interact with the parasite's protein using molecular docking.

2. EXPERIMENTAL MATERIALS AND METHODS

2.1 Experimental materials

Hexane, petroleum ether (PE), ethylacetate (EtOAc), methanol (MeOH), water (H_2O), dichloromethane (DCM), dimethyl sulfoxide (DMSO), deuterated chloroform ($CDCl_3$) methanol (CD_3OD), and dimethyl sulfoxide (DMSO-d_6) were the solvents that were used in this research project for the extraction and isolation processes and as the mobile phase for TLC as well as in bioassay and NMR experiments. Acetone was mainly used to clean the apparatus as well as to wash samples. DCM and PE were supplied by B&M Scientific (Cape Town), the other solvents were obtained from Protea Chemicals, Port Elizabeth and Sigma Aldrich. The hexane was further distilled in the Chemistry Department Laboratory at Rhodes University and the other solvents were used as received, unless specified.

Column chromatography was used to separate the compounds in a fraction. Different sizes of columns ranging from 10 to 40 mm in diameter were used. Silica gel 60 (0.063-0.2 mm) supplied by Macherey-Nagel GmbH & Co.KG, Germany, was used as the stationary phase with a small layer of washed sand added on top to help pack the silica in the column. A Buchi Rotavapour R-205 was used to concentrate the samples.

TLC silica gel 60 F_{254} on aluminium sheets (20 x 20 cm) supplied by Merck company from Germany, were used to run the TLC. This was visualised using ultraviolet (UV) lamp, model CM-10A with short and long wavelength UV of 254 and 365 nm respectively. Vanillin spray was used to view spots that were not visible under UV light.

NMR experiments were run on a Bruker 600 MHz NMR spectrometer and were referenced using the following residual protonated solvent signals: ^{1}H-NMR chemical shift: 7.26 ppm for $CDCl_3$, 2.50 ppm for DMSO-d_6 and 3.31 for CD_3OD, ^{13}C-NMR chemical shift: 77.00 ppm for $CDCl_3$, 39.50 for DMSO-d_6 and 49.00 for CD_3OD (Gottlieb et al, 1997). A Perkin-Elmer FT-IR Spectrum 100 spectrometer was used to run the IR spectra and a high resolution Waters API Q-TOF Ultima ESI mass spectrometer from Stellenbosch University was used to record the mass spectra. Melting points were measured using a Reicheter 281313 apparatus and the ATAGO POLAX-2L polarimeter was used to measure the optical rotation of some isolated

compounds. The concentration of solutions used to determine the optical rotations was expressed in g / mL (H_2O).

2.2 Experimental methods

2.2.1 Plant collection, extraction of plant material and fractionation of crude extract

The plant (stem bark) was collected from the Elounden Mountain, Yaoundé, in the central region of Cameroon in January 2010. It was identified as *Morinda lucida* Benth. by Victor Nana, a botanist in the National Herbarium of Cameroon (HNC) in Yaoundé. The voucher specimen (number 57202/HNC) was deposited in this same herbarium.

The ground stem bark (437 g) was soaked overnight in 2 L of DCM/MeOH (1:1) solvent system. This solvent system was used throughout the process of extracting the plant material. The mixture was filtered after 24 hours. The filtrate was evaporated using a rotary evaporator. More solvent was added to plant material after every 24 hours for the next three days and left to soak overnight. The extraction process was completed on the fourth day when plant material was filtered and evaporation was completed. A blackish brown extract of mass 46.0 g was obtained. A portion of the crude extract (5.00 g) was put aside to be used for biological assays.

The crude extract was subjected to vacuum column chromatography (VCC) on silica gel. This was eluted with hexane and the polarity was increased with EtOAc followed by MeOH. A total of 56 fractions of 200 mL each were collected. The 56 fractions were then combined according to the results of TLC to give 8 fractions, ML1 to ML8 (**Table 1**).

TLC was used to check the presence of compounds throughout the extraction and isolation experiments. The TLC plates were first viewed under short wavelength UV of 254 nm and long wavelength UV of 365 nm. The spots that were visible under UV were marked. The TLC plates were then sprayed with vanillin solution. The vanillin solution developed some of the spots that were not visible under the UV lamp. This solution was prepared by dissolving 665 mg of vanillin (2-hydroxy-3-methoxybenzaldehyde) in 100 mL of ethanol (Gorgoi et al, 2014). The vanillin / ethanol solution was slowly mixed with 2.5 mL of sulphuric acid. The TLC plate was heated for five minutes until 105 °C after being sprayed with the vanillin

solution (Gorgoi et al, 2014). Some spots that were not visible under UV light were observed.

Table 1: The eight fractions obtained from the TLC results of the different fractions after fractionation

Fraction	1	2	3	4	5	6	7	8
Combined fractions (mass in g)	1-7 (0.11)	8-15 (0.76)	16-22 (0.47)	23-31 (3.65)	32-39 (23.2)	40-46 (0.27)	47-53 (0.99)	54-56 (0.30)

2.2.2 Biological assays

The *in vitro* toxicity, antimalarial, anti-bacterial and anti-tuberculosis (anti-TB) assays on the crude extract, fractions and pure compounds were carried out. The toxicity and antimalarial assays were performed by Mrs Michelle Issacs (Bioassay Technician, Chemistry Department at Rhodes University, South Africa), the anti-bacterial assay was performed by the author and the anti-TB assay was carried out by Dr Ronnett Seldon's laboratory at Drug Discovery and Development Centre (H3-D), Chemistry Department, University of Cape Town, South Africa.

2.2.2.1 Cell toxicity and antimalarial activity

Cell cytotoxicity and antimalarial assays were perfomed on fractions ML2 to ML7. Fraction ML8 was from MeOH. The MeOH extract was not going to be considered for the antimalarial assay due to the results of preliminary antimalarial tests which were previously performed by the research group. These results indicated that the MeOH extract from *M. lucida* produced total haemolysis of red blood cells in the culture at 50 µg/mL.

HeLa cells were used to check the toxicity of the crude extract, fractions and isolated compounds as described by Keusch et al (1972). Stock solutions of crude extract, fractions (20 mg/mL) and isolated compounds (20 mM) were prepared in DMSO. These stock solutions were diluted with culture medium to 100 µg/mL (for crude extract and fractions) and 20 µM (for isolated compounds). Emetine was used as a standard at a concentration of 20 µM. The cell toxicity single dose assay was also carried out for a mixture of the isolated compounds (20 µM) mixed in different ratios as shown in **Table 2**. In the first mixture (BC1), 8 µL of each of the six compounds was used. For BC2, 16 µL of compound **2** was used where

as 8 µL was used for the other compounds. A volume of 16 µL of compound **3** and 8 µL of all the other compounds was used for BC3. The volume was doubled for one compound whereas the rest stayed the same up to mixture BC6. Some of the compounds were used up at this point. Mixtures BC7 to BC9 were mixed up in the ratios indicated in **Table 2** for those compounds that were still available. Compound **1** was not available when the assays of the mixtures were carried out.

Table 2: Composition of mixtures from 20 mM of different compounds

Mixture	Compounds in mixture (ratio, v/v)
BC1	**2**(1) +**3**(1) +**4**(1)+**5**(1)+**6**(1)
BC2	**2**(2) +**3**(1) +**4**(1)+**5**(1)+**6**(1)
BC3	**2**(1) +**3**(2) +**4**(1)+**5**(1)+**6**(1)
BC4	**2**(1) +**3**(1) +**4**(2)+**5**(1)+**6**(1)
BC5	**2**(1) +**3**(1) +**4**(1)+**5**(2)+**6**(1)
BC6	**2**(1) +**3**(1) +**4**(1)+**5**(1)+**6**(2)
BC7	**2**(1) +**3**(0) +**4**(2)+**5**(0)+**6**(2)
BC8	**2**(0) +**3**(0) +**4**(2)+**5**(1)+**6**(2)
BC9	**2**(1) +**3**(1) +**4**(0)+**5**(0)+**6**(0)

The compounds, fractions and mixtures that reduced parasite viability significantly from the single concentration assay were used in a dose response assay to determine IC_{50} values. In this assay, four-fold serial dilutions were made with culture medium to obtain concentrations between 100 and 0.00613 µM for pure compounds and between 100 and 0.00613 µg/mL for crude extract. To assess the cytotoxicity of the compounds, the compounds were incubated in duplicate 96-well plates along with approximately 1 x 10^4 HeLa cells per well for 48 hours at 37 °C in 5 % CO_2. The number of cells which survived the drug exposure was determined by using the resazurin based reagent and reading resorufin fluorescence in a multiwell plate reader. For each crude extract, fractions and pure compounds, the percentage cell viability was dertermined from the resorufin fluorescence (560 nm excitation, 590 nm emission) in compound-treated wells relative to untreated controls (Cos et al, 2006). Compounds were tested in duplicate wells, and a standard

deviation was derived. The results for this assay were expressed as % cell viability. The IC_{50} values were obtained by non-linear regression of the dose-response curve plotted using % cell viability against log of concentration of compound.

The antimalarial assay was carried out using the pLDH assay as described by Makler et al (1993) on malaria parasites, *P. falciparum* (strain 3D7). For a single concentration assay, a 100 µg/mL solution of crude or fraction was prepared the same way as in the cytotoxicity assay. For each of the isolated compounds, 20 µM concentrated solutions were also prepared as in the cytotoxicity assay. Chloroquine (20 µM) was used as the standard in this assay. The pLDH enzyme assay was performed after a 48 hour incubation period of well plate of parasites and test samples. A 20 µL of culture was removed from each incubated well and mixed with 125 µL of a mixture of Malstat and nitrotetrazolium blue chloride (NBT)/phenazine ethosulphate (PES) solutions in a sterile 96-well plate. These solutions measured the activity of the pLDH enzyme in the culture. A purple product was formed when pLDH was present, and this product was quantified in a 96-well plate reader by absorbance at 620nm. The absorbance reading in each well was an indication of the pLDH activity in that well as well as an indication of the number of parasites in the well. The pLDH assay was also carried out for incubated plates of parasite culture and mixtures of pure compounds mixed in different ratios as shown in **Table 2**. The compounds, fractions and mixtures that reduced parasite viability significantly from the single concentration assay were used in a dose response assay to determine IC_{50} values.

2.2.2.2 The antibacterial assay

The *in vitro* antibacterial assay was carried out using the serial dilution method as described by Eloff (1998) with slight modifications. **Table 3** shows the types and amounts of samples of crude extract and fractions which were tested. Acetone was used to dissolve the samples.

The crude sample and fractions were at an initial concentration of 32 mg/mL while that of ciprofloxacin (positive control), water (negative control) and the broth (culture control) were at initial concentrations of 0.01, 32 and 30 mg/mL respectively. The culture control (used to check microbe growth in culture), was prepared by mixing 30 g of tryptone soya

broth with one litre of purified water. The mixture was put in an autoclave at 121 °C for 45 minutes to sterilize it. It was cooled down to room temperature.

Table 3: Samples for the antibacterial assays

Name of sample	Purity	Quantity (mg)	Solvent (acetone) (µL)
Crude extract	Crude	32 (x2)	1000
Fractions ML2 - ML8	Un-isolated	16 (x2)	500
Compounds **1** and **3**	Pure	1	1000
Ciprofloxacin (positive control)	Pure	0.01	1000
Water (negative control)	Pure	32	1000
Broth (culture control)	Pure	30	1000

In this experiment, a total of six pathogens were used. These are listed in **Table 4** together with their American Type Culture Collection (ATCC) numbers. A 1 mL of culture solution was diluted in a test tube to 0.01 mg/mL by mixing it (in a vortex mixer) with 100 mL of broth. The top of the test tube containing the culture solution was sterilised on a flame before and after use. A 100 µL of this mixture of broth and culture was added to the sample and control wells on the plates using a multi-headed pipette. The plates were sealed with sterile adhesive sealer and placed in an incubator set at 37 °C for 24 hours.

Table 4: The different pathogens used in the antibacterial assay together with the ATCC numbers

Name of pathogen	*Staphylococcus aureus*	*Escherichia coli*	*Salmonella typhimurium*	*Enterococcus faecalis*	*Morexella cattarhalis*	*Klebsiella pneumoniae*
ATCC #	25923	8739	1403	6230434	23246	13883

The culture was added to the well plates and to the agar filled Petri dishes as well to check for pathogen vitality. The agar used in the Petri dishes was prepared by mixing 40 g of tryptone soya agar with 1 L of purified water. The same culture solution used for the plates was used for the Petri dishes.

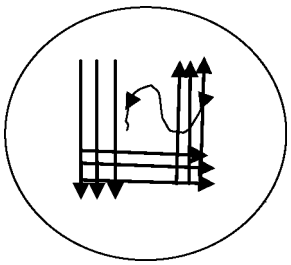

Figure 10: Patterns made with culture solution on solid agar medium

An inoculation loop was sterilised on a flame then cooled on the edge of the agar filled Petri dish then dipped into culture solution. This was then used to mark the agar in Petri dish **(Fig. 10)**. After drawing the first three lines, the loop was sterilised, three more lines were drawn from the first (without dipping the loop in culture again), in a way spreading the pathogens from the first to the second triplet of lines, from the second to the third and then to the s-shape, without touching the Petri dish edge. The Petri dish was then incubated together with the prepared plates.

After 24 hours, the Petri dishes were checked for growth of pathogens. If there was growth in Petri dishes, it showed that the pathogens were viable and that the plates were ready to be checked for activity of samples. To check the activity of samples, iodonitrotetrozaluim chloride (INT) solution was added to the plates. INT is an indicator used to check the presence or absence of bacteria in the plates. Clear wells after 4 to 6 hours of adding INT indicated the absence of bacteria and the sample was considered to be active (at that particular concentration) against that particular pathogen that was introduced in the wells. It showed that the sample was inactive when the INT changed to pink i.e. the bacteria was still alive and oxidising the INT. The INT solution was made by dissolving 0.08 mg of INT in 200 mL of purified and sterilised water. The mixture was placed in a shaker incubator (platform shaker) set at 30 $^{\circ}$C for 1 hour to completely dissolve the INT. To add the INT solution to the plates, the sealer was removed from the plates and 40 μL of the INT was added to all wells on the plate. The plates were then covered and left to stand for at least 4 to 6 hours. The reading of results was done under a lamp. The minimum inhibitory concentrations (MIC) for active samples were recorded.

2.2.2.3 The anti-tuberculosis assay

The standard broth micro dilution method, where a 10 ml culture of *Mycobacterium tuberculosis* H37RvMa:pMSP12GFP (Abrahams et al., 2012), was grown to an optical density (OD600) of 0.6–0.7 in GAST-Fe (glycerol–alanine–salts) medium pH 6.6, supplemented with 0.05% Tween-80 (De Voss et al., 2000) was used to determine the minimum inhibitory concentration (MIC). The compounds to be tested were reconstituted to a concentration of 125 μg/mL in DMSO and the culture was diluted 1:100 in GAST-Fe. Duplicate two-fold serial dilutions of the test samples were prepared in GAST-Fe, across a 96-well micro titre plate,

after which 50 µL of the 1:100 diluted *M. tuberculosis* culture was added to each well in the serial dilution. The plate layout was a modification of a previously described method (Ollinger *et al.,* 2013). Controls used were a minimum growth control (Rifampicin at 2xMIC) a maximum growth control (5% DMSO in GAST-Fe) and Rifampicin. The microtitre plate was sealed in a secondary container and incubated at 37 °C with 5% CO_2 and humidification. Relative fluorescence (excitation 485 nm; emission 520 nm) was measured using a plate reader (FLUOstar OPTIMA, BMG LABTECH), at days 7 and 14. The raw fluorescence data were archived and analysed using the CDD Vault from Collaborative Drug Discovery. Data were normalised to the minimum and maximum inhibition controls to generate a dose response curve (% inhibition), using the Levenberg-Marquardt damped least-squares method, from which the MIC_{90} was calculated (Burlingame, CA www.collaborativedrug.com). The lowest concentration of drug that inhibited the growth of more than 90 % of the bacterial population was considered to be the MIC_{90} and that which inhibited the growth of more than 99 % as the MIC_{99}.

2.2.3 Isolation and identification of compounds

Fractions ML2 to ML5 were purified by gradient CC on silica gel using different solvent systems (**Appendix 2**). These fractions were chosen as they showed activity out of the 8 fractions.

Fractions ML2 and ML3 showed some reasonable activity after the crude extract. Fraction ML2 was purified by gradient CC on silica gel using hexane and EtOAc. It yielded 148 fractions of 50 mL each. Fractions 92–105 were combined according to the TLC results and this sub-fraction was again subjected to CC by eluting with a mixture of hexane and EtOAc in a ratio of 8:1 (v/v) to yield compound **3** (5.0 mg) after washing the solid obtained with acetone. Fractions 131–148 were combined as well and separated further by CC with hexane and EtOAc in a ratio of 15:1 (v/v) to give a total of 900 fractions of 10 mL each. Compound **4** (3.8 mg) precipitated from a combination of fractions 176–491. It was washed with hexane. Fraction ML3 was purified by CC using PE followed by PE and EtOAc in a ratio of 9:1 then 4:1 (v/v). It produced 39 fractions of 50 mL each. Compound **6** (1.3 mg after washing with hexane) precipitated from a combination of fractions 4 and 5.

Isolation of compounds was also performed on fractions ML4 and ML5 as they showed some activity. Compound **1** (67.7 mg) precipitated from fraction ML4 which was a combination of fractions that had been eluted from the crude extract first with EtOAc followed by a mixture of EtOAc and MeOH in a ration of 10:1 (v/v). This compound was washed with acetone. The rest of this fraction was subjected to CC using hexane followed by hexane and EtOAc in different ratios of 15:1, 10:1, 8:1 then 6:1 (v/v) to give 24 fractions of 100 mL each. Compound **5** (1.5 mg after washing with acetone) precipitated from a combination of fractions 13 (8:1, v/v) and 14 (6:1, v/v). Fraction ML5 was subjected to gradient CC by eluting with hexane, EtOAc and MeOH. This yielded 43 fractions of 100 mL each. Fractions 36 - 38 were combined and further purified by gradient CC using EtOAc and a mixture of EtOAc and MeOH in a ratio of 10:1 (v/v) to yield 17 fractions. Fractions 1–9 were again combined and purified by gradient CC using DCM and MeOH. A mixture of DCM and MeOH in a ratio of 10:1 (v/v) was performed to obtain compound **2** (5.40 mg) which was washed with acetone.

All isolated compounds were air-dried, weighed and IR, NMR and MS experiments were carried out on each one of them. The melting point of each compound was also taken. The optical rotation as well as phytochemical tests was performed on some compounds. The unsaturation index or index of hydrogen deficiency for each compound was calculated (Lampman et al 2010).

2.2.4 Docking experiments

The ribbon structure of cytochrome bc_1 complex (with the inhibitor stigmatellin) was obtained from the Protein Data Bank (PDB) database with PDB identity number 1EZV (Hunte et al, 2000; Kessl et al, 2007).

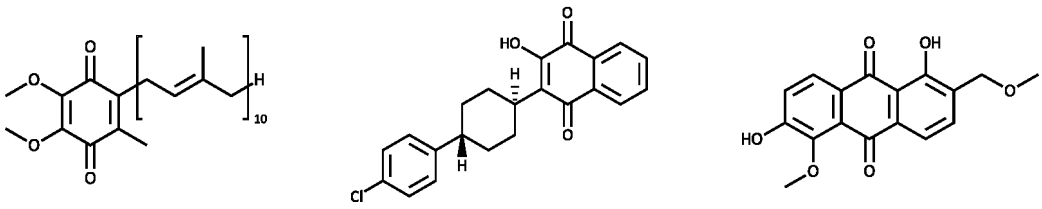

ubiquinone **atovaquone** **Compound 4**

Figure 11: Chemical structures of ligands that were used for docking

The 2-dimensional (2D) structures of the ligands to be used for docking, ubiquinone, atovaquone and compound **4** (**Fig. 11**), were drawn using ChemBioDraw Ultra 14.0 and were opened in Discovery Studio 4.1 Visualizer. In the same Discovery Studio, the protein was obtained from the PDB database and prepared by deleting water and the stigmatellin ligand after getting the coordinates of active site.

The ligands and protein were further prepared for rigid docking in AutoDock Tools (ADT) version 1.5.6. The Autodock 4.2 programme was used for docking. Using this programme, non-polar hydrogens in protein were merged. Gasteiger partial charges with a value of -13.997 were added and AD4 type atoms were assigned to the protein. The number of rotatable bonds detected in compound **4**, atovaquone and ubiquinone were three, two and thirty-one respectively. AutoGrid was used to set map types and locate the active site within a grid box. A Larmarckian genetic algorithm with 50 runs, a population of 150, a maximum number of evals (medium) of 2 500 000 and a maximum number of generations of 2 700 was used to conduct the docking for each of the ligands. The Rieske iron-sulfur protein compound was used as a guide in the docking experiments as suggested by Kessl et al (2007). The x, y and z coordinates of 17.888, 29.328 and 25.502 respectively were located in the grid box. After the docking experiments, the conformation with the lowest energy for each of the ligands was visualised using Discovery Studio Visualizer. The interactions between ligand and protein for each of the docking experiments were analysed.

3. RESULTS AND DISCUSSION

3.1 Extraction and fractionation

A blackish brown extract of mass 46 g was extracted from the 437 g of plant material. This crude extract was separated into eight fractions (**Table 5**) using column chromatography guided by visual inspection of TLC plates.

Table 5: Fractions obtained from the crude extract following chromatography

Fraction	Original fraction	Solvent system	Mass of fraction (g)
1	1 - 7	Hexane	0.11
2	8 - 15	Hexane:EtOAc (80:20)	0.76
3	16 - 22	Hexane:EtOAc (40:60)	0.47
4	23 - 31	EtOAc:MeOH (95:10)	3.65
5	32 - 39	EtOAc:MeOH (80:20)	23.2
6	40 - 46	EtOAc:MeOH (70:30)	0.27
7	47 - 53	EtOAc:MeOH (60:40)	0.99
8	54 - 56	MeOH	0.30

Figure 12: A TLC plate (Hexane:EtOA, 3:2, v/v) of fractions 2 to 8

Fractions 3 to 5 seemed to have many different compounds (**Fig. 12**). Some more dark bluish / purple spots were revealed when the TLC plate was sprayed with vanillin spray.

3.2 Biological assays

3.2.1 Cell toxicity and antimalarial parasite assays

A pLDH assay previously done by the research group (Rhodes University, unpublished results) on the hexane and DCM extracts of *M. lucida* showed activity against cultured *P. falciparum* (strain 3D7) parasites. The DCM extract had an IC_{50} value of 4.2 µg/mL where as the hexane extract had an IC_{50} value of 6.3 µg/mL (**Fig. 13**). Due to these promising preliminary results, further tests of the crude extract and fractions from *M. lucida* were perfomed and the isolation of active compounds attempted.

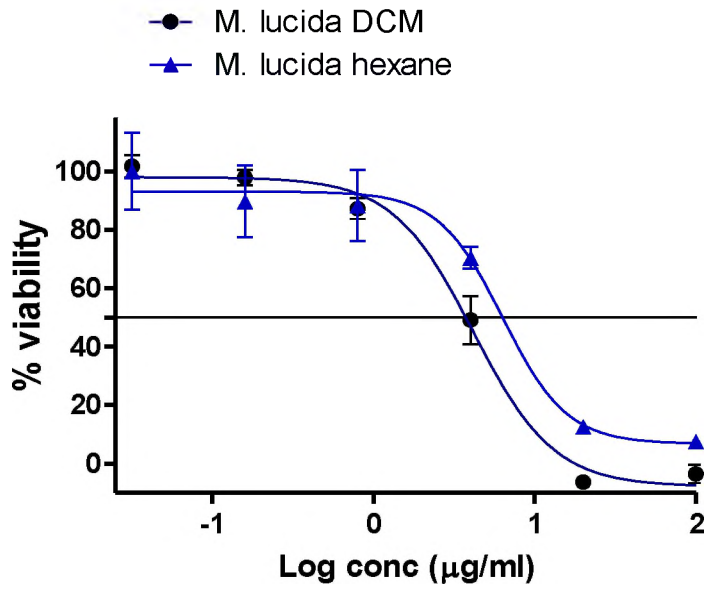

Figure 13: Dose-response plots of *M. lucida's* crude extract in DCM and hexane

The cell toxicity and pLDH assays for the crude extract and the fractions of *M. lucida* (**Fig. 14**) indicated that some fractions reduced the malaria parasite viability by approximately 50 % at 100 µg/mL while not being significantly cytotoxic. The crude extract reduced the malaria parasite viability to 0 % and was not cytotoxic (cell toxicity assay showed that cell viability remained at 100 %). The IC_{50} value of the crude sample was 25 µg/mL (**Fig. 15**). Fraction ML3 reduced malaria parasites by 50 % while the rest of the fractions were less effective. All pure compounds had very little activity by themselves (**Fig. 16**). Their activities were enhanced when 20 µM solutions of different compounds were mixed in different quantities. For example, compound **2** on its own reduced the malaria parasite viability to 93 % at 20 µM.

When 16 µL (of the 20 µM solution) of this same compound was mixed with 8 µL (at a concentration of 20 µM) of each of compounds **3** to **6** (**Fig. 17**), the mixture reduced the malaria parasites viability to 22 % and gave an IC_{50} value of 17 µM (**Fig. 19**). For comparative purposes, chloroquine was used as a standard and yielded an IC_{50} value of 0.01µM.

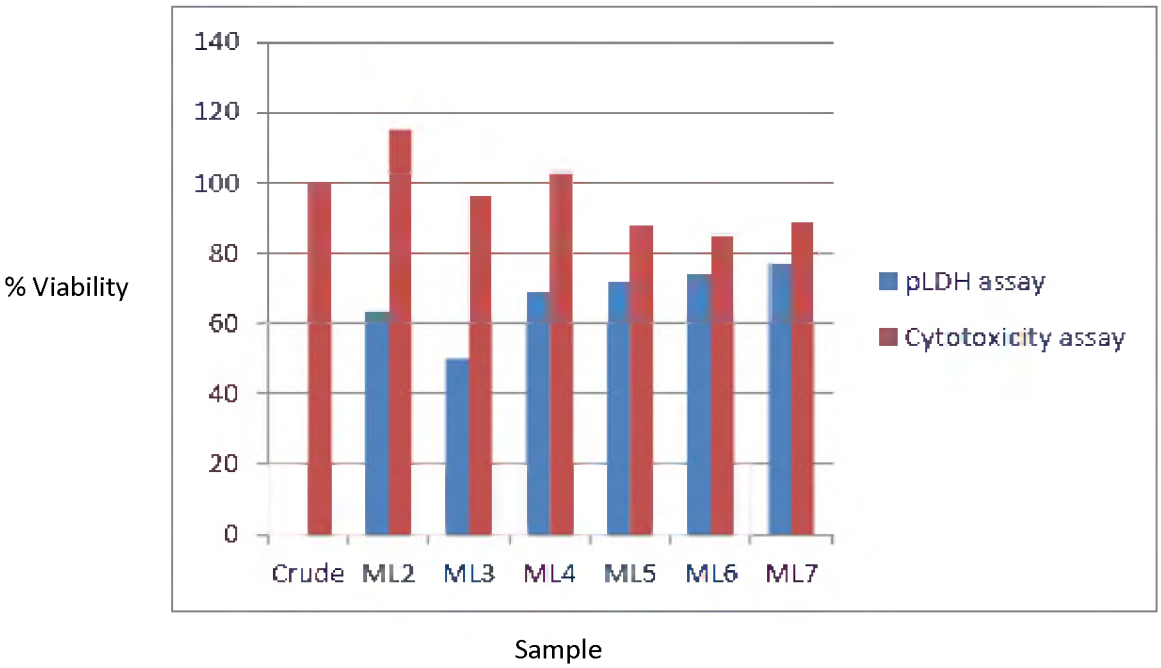

Figure 14: **Effects of crude extract and fractions 2 to 7 from *M. lucida* on pLDH and cytotoxicity assays. A 100 µg/mL of crude extract and fractions was used in each assay and cell viability in % was used to measure activity of sample.**

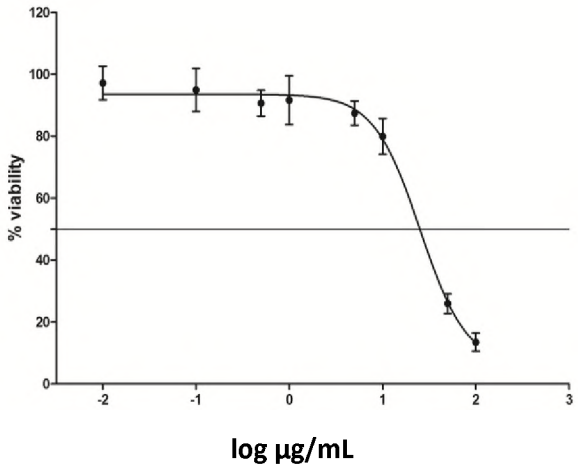

Figure 15: **Dose-response plot for the DCM/MeOH crude extract**

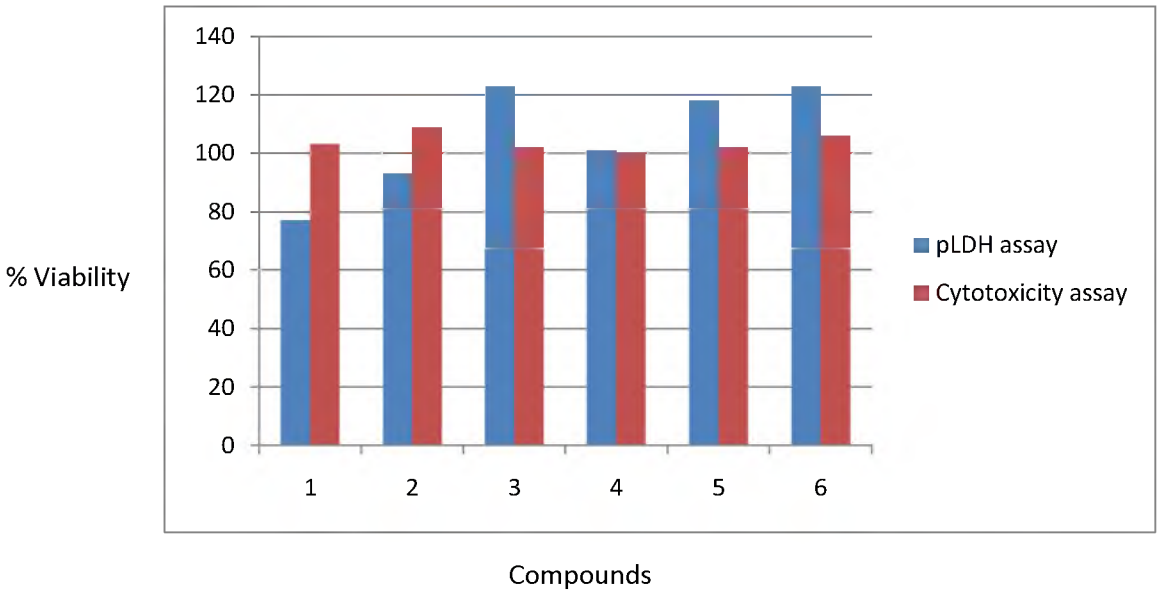

Figure 16: **Effects of compounds 1 to 6 from *M. lucida* on pLDH and cytotoxicity assays. A 20 µM of each compound was used in each assay and cell viability in % was used to measure activity of compound.**

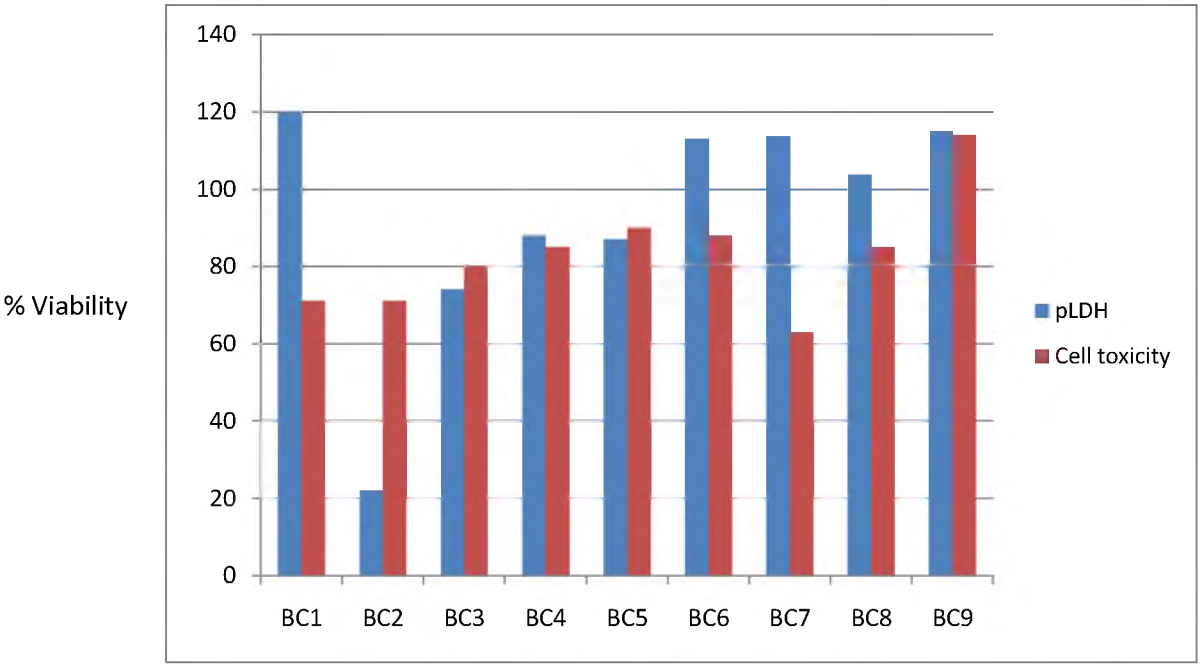

Figure 17: **Effects of a mixture of compounds 2 to 6 from *M. lucida* on pLDH and cytotoxicity assays. A 20 mM of each compound was mixed with 20 mM of other compounds in different ratios (with final mixture diluted to 20µM) and used in each assay. Cell viability in % was used to measure activity of compound.**

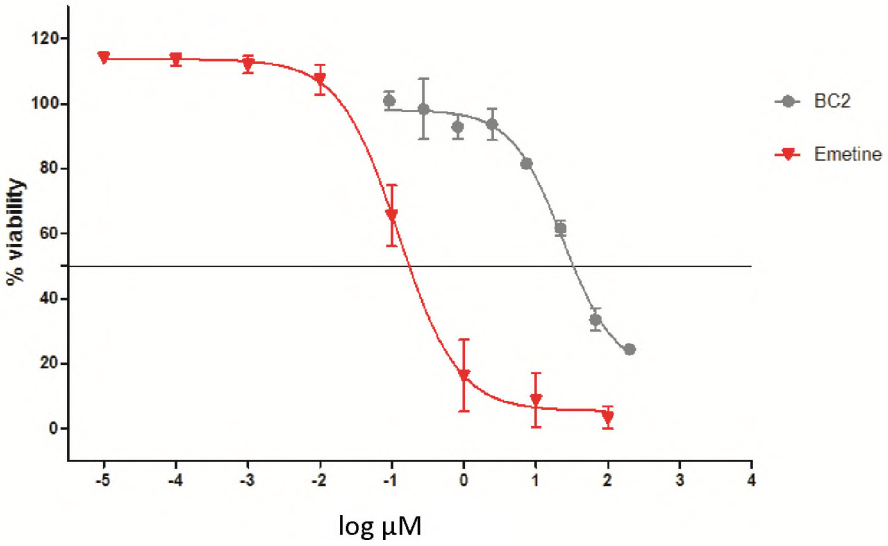

Figure 18: Dose-response plot of the toxicity assay for BC2

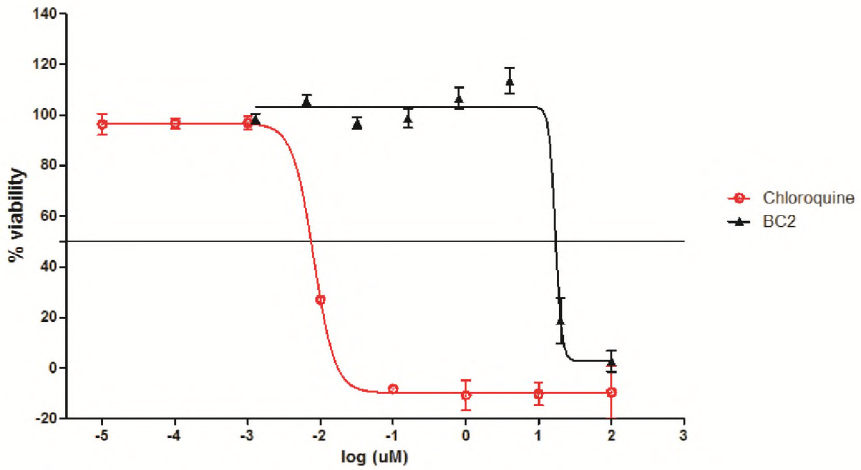

Figure 19: Dose-response plot of the pLDH assay for BC2

The IC_{50} value for the cell toxicity assay of this mixed sample was 24 µM while that of the standard drug, emetine, was 0.12 µM (**Fig. 18**). The mixtures had become more toxic to the parasite compared to the individual compounds.

IC_{50} values of the crude extracts are difficult to compare with pure compounds (the IC_{50} value of chloroquine for example was only 0.02 µM), since the crude contains many compounds that could each be active or could be acting in synergy (Hellman et al, 2010; Rasoanaivo et al, 2011). Plants normaly produce mixtures of compounds from different

classes to interefere with several targets at a time (Hellman et al, 2010), this amplifies the efficiency of the compounds and is thought to reduce the risk of resistance development by the pathogens (Hellman et al, 2010). In traditional medicine, whole plants or mixtures are used instead of isolated compounds (Rasoanaivo et al, 2011). Different types of interactions between different components within the crude extract occur to give the synergistic effect on the pathogens (Hellman et al, 2010; Rasoanaivo et al, 2011).

3.2.2 Antibacterial assay

Antibacterial assays are often a way to identify malarial drugs (Baggish and Hill, 2002). Some of the antimalarial drugs like atovaquone (Baggish and Hill, 2002) and some sulphonamides like prontosil (Abraham and Rotella, 2010), were first used for the treatment of bacterial infections. Many of the ethnopharmacology uses of *M. lucida* are for anti-fever i.e. anti-infection (Lawal et al, 2012) hence the rationale for carrying out antibacterial assays. If the samples have anti-microbial activity, there is a high probability of them having antimalarial activity as well.

Fractions 2 and 3, the first two fractions obtained from the crude extract, were relatively active against some bacterial pathogens compared to the crude sample and the other fractions. This is not surprising as these two fractions were also relatively active against the malaria parasite. They were both mildly active (MIC values ranging between 0.125-1.00 mg/mL) against *M. cattarhalis* and *E. faecalis.* Fraction 2 was also the most active on *S. typhimurium* (MIC value of 1.00 mg/mL) compared to Fraction 3. It acted better on *S. aureus* (MIC value of 1.00 mg/mL) than Fraction 3. Both fractions were not as active against *E. coli* **(Table 6)**. Even though compound **3** was isolated from Fraction 2 which showed some activity, compound **3** itself was inactive against all pathogens. The same was the case with compound **1**. A possible reason for the non-activity of the crude sample and some of the fractions might have been due to the insolubility of these samples in acetone. Acetone was used to dissolve all samples. Most of these samples were insoluble in this solvent. Methanol could have been a better solvent but it was not used as it is considered to have activity on most of the pathogens.

Table 6: MIC (mg/mL) of extracts from *Molinda lucinda* on selected bacteria pathogen

Sample	Code	Starting conc. (mg /mL)	*Enterococcus faecalis* ATCC # 6230434	*Salmonella typhi* ATCC # 1403	*Escherichia Coli* ATCC # 8739	*Staphylococcus aureus* ATCC # 25923	*Morexella cattarhalis* ATCC # 23246	*Klebsiella pneumoniae* ATCC # 13883
ML Crude	B1	32	>8	>8	>8	>8	>8	>8
Fraction 2	B2	32	0.5	1	2	2	0.5	
Compound **3**	B3	1	>0.25	>0.25	>0.25	>0.25	>0.25	
Fraction 3	B4	32	0.5	1	2	1	0.5	
Fraction 4	B5	32	>8		>8	>8	>8	
Compound **1**	B6	1	>0.25	>0.25	>0.25	>0.25	>0.25	
Fraction 5	B7	32	>8	>8	>8	>8	>8	
Fraction 6	B12	32	>8	>8	>8	>8	>8	
Fraction 7	B13	32	>8	>8	>8	>8	>8	
Fraction 8	B14	32	>8	>8	>8	>8	>8	
Ciprofloxacin	+C	0.01	0.313µg/mL	0.02µg/mL	0.313µg/mL	0.625µg/mL	1.25µg/mL	0.313µg/mL
Water	- C	32						
Broth	CC	30						

3.2.3 Anti-tuberculosis assay

In this assay, fraction 2 was relatively active against the *M. tuberculosis* pathogens with MIC90 and MIC99 values of 40.9 and 46.3 µg / mL respectively (**Table 7**) compared to the crude sample and the other fractions. This is the same fraction that was also relatively active against the malaria parasite and some of the bacterial pathogens. As Pauli et al (2005) reported that the MIC of a crude or fraction of natural extract may or may not be a reliable indicator of the chances for success in isolating a potent antimycobacterial agent. An extract with a relatively low MIC (high activity) may contain large quantities of few moderately active major constituents, an extract with moderately active crude materials could lead to the isolation of a small number of compounds with high activity (Pauli et al, 2005). The active compound or compounds in fraction 2 might be in small quantities whose effects are slightly sensed by the microbes. Isolating and testing the compounds responsible for the activity would give a good indication on the activity of compounds.

Table 7: MIC (mg/mL) of crude extract and fractions from *M. lucinda* on *M. tuberculosis*

Sample name	GPF-Assay- 10pt DR: MIC90 (µg / mL)	GPF-Assay- 10pt DR: MIC90 (µg / mL)
ML-Crude	> 125	> 125
ML2	40.9	46.3
ML3	> 125	> 125
ML4	> 125	> 125
ML5	> 125	> 125
ML6	> 125	> 125
Rifampicin	0.00676 (µM)	0.0108 (µM)

3.2.4 Medicinal properties of isolated compounds

The proposed structures of compounds **1** and **2** have the iridoid skeleton. Iridoids are normally found in plants belonging to Rubiaceae, Apocynaceae, Lamiaceae,

Scrophulariaceae and Verbenaceae families (Viljoen, 2012). Plants from these families are used as anti-inflammatorries (Van Wyk et al, 2004; Viljoen, 2012). Inflammations occur as a product of different ailments such as arthritis, atherosclerosis and Alzheimer's disease (Viljoen, 2012). Apart from being used as anti-inflammatories, iridoids have shown a wide range of pharmacological activities against diseases such as cardiovascular, hypoglaecemia and cancer (Viljoen, 2012).

Asperuloside (compound **1**) has been found to have anti-obesity effects (Hirata et al, 2011). It decreases body weight, white adipose tissue levels, levels of triglyceride in plasma as well as total cholesterol levels (Hirata et al, 2011). The presence of asperuloside in M. lucida is probably the reason why the plant is traditionally used in the treatment of hypertension (Lawal et al, 2012).

A group of steroids have also been identified in this study (sample **3**). Sterols are an important group of chemicals in all living organisms as they are structural components of plasma membranes (Suzuki et al, 2006; Ohyama et al, 2009) and precursors of steroidal hormones (Suzuki et al, 2006). Phytosterols have been found to have cancer preventive biological-active substances (Careri et al, 2001). β-sitosterol (present in sample **3**) has been shown to have cholesterol lowering property, anti-inflammatory, anti-oxidant and immune-modulating activities (Careri et al, 2001; Patra et al, 2010). Gomes et al (2007) have also reported on the anti-snake venon activity of β-sitosterol and stigmasterol (also identified in sample **3**).

Different anthraquinones have been isolated in this study. Different derivatives of anthraquinones are usually found in families of Rubiaceae, Polygonaceae, Rhamnaceae, Fabaceae, Hypericaceae and Asphodelaceae (Van Wyk et al, 2004; Lawal et al, 2012). This group of secondary metabolites are known for their purgative action as well as their antioxidant effect and antitumor activities (Evans, 2002; Ishak et al, 2010; Subramani et al, 2015).

3.3 Structure elucidation of isolated compounds

Table 8: Compounds isolated from *M. lucida*

Compound	Mass of sample obtained (mg)	Yield (%)	Melting point (°C)	TLC visibility of sample spot
1	67.7	0.147	134 – 136	Purple with vanillin spray
2	5.40	0.012	200 – 204	Purple with vanillin spray
3	5.00	0.011	126 – 135	Purple with vanillin spray
4	3.80	0.008	216 – 220	Bright orange UV (365 nm)
5	1.50	0.003	200 – 206	Bright orange UV (365 nm)
6	1.30	0.003	204 – 210	Bright orange UV (365 nm)

Different compounds (**Table 8**) were isolated from the different fractions of the crude extract. The first three compounds (compounds **1**–**3**) were not clearly visible in TLC analyses under UV and were only visible when sprayed with vanillin–sulphuric acid reagent. These were characterised as terpenoids. Two of these terpenoids were of the iridoid family (compound **1** and **2**) and compounds from sample **3** were characterised as steroids. Terpenoids normally give dark purple spots when sprayed with vanillin–sulphuric acid solution (Gorgoi et al, 2014).

Compounds **4**, **5** and **6** were characterised as anthraquinones and all three were clearly visible with a bright orange colour under UV light. This indicated the presence of aromatic rings in the structures of compounds **4** to **6** (Lampman et al, 2010). The presence of conjugation within the structures of compounds **4** to **6** meant that these compounds absorbed within the visible region of the electromagnetic spectrum (Lampman et al, 2010) and were visible on TLC plates and silica columns.

The structures of the isolated compounds were elucidated by interpreting their ESI-MS, IR- as well as NMR- spectral data (^{1}H, ^{13}C, DEPT 135, COSY, HMBC, HSQC and NOESY).

3.3.1 Structure elucidation of compounds 1 and 2

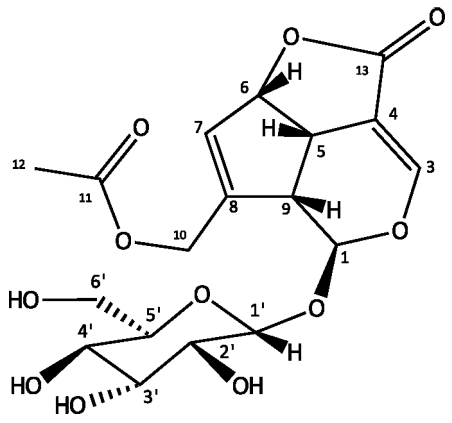

Figure 20 Proposed structure of compound 1 (asperuloside)

Compound **1** (**Fig 20**) was isolated as light grey amorphous powder of melting point 128 – 130 °C and optical rotation (α), of the order of -3.35°.

HR-ESI-MS of compound **1** (**Appendix 4.1**) detected in the positive mode at *m/z* = 415.1250 [M+H$^+$] (molecular formula: $C_{18}H_{22}O_{11}$), 396.1077 [$C_{18}H_{22}O_{11} - H_2O$]. The molecular weight of $C_{18}H_{22}O_{11}$ was 414.3598 g / mol. The unsaturation index of compound **1** was eight.

Percentage composition (using the exact mass of $C_{18}H_{22}O_{11}$ obtained from mass spectrum) for carbon is 52.2057 %, for hydrogen it is 5.3545 % and 42.4985 % for oxygen. The molecular mass determined by mass spectrometry has an accuracy value between ±0.0030 to 0.0306 %.

The IR spectrum of compound **1** (**Appendix 3.1**) displayed strong absorption bands at 3294 (aliphatic OH), 1735(aliphatic C=O), 1698 (aliphatic C=O), 1660 (aliphatic C=C) and 1375–979 cm^{-1} (OH) (Demirezer et al, 2006; Lampman et al, 2010).

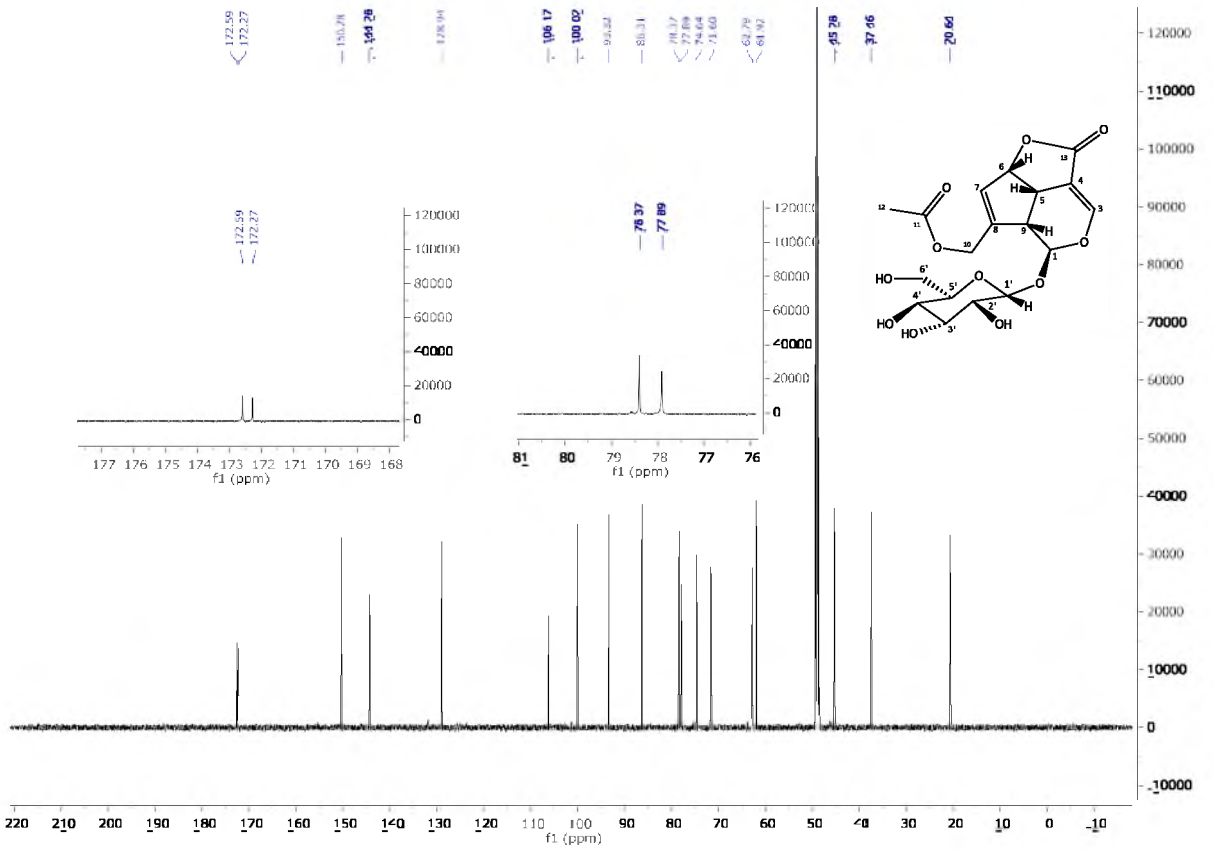

Figure 21 ^{13}C NMR spectrum (in CD_3OD) of compound 1

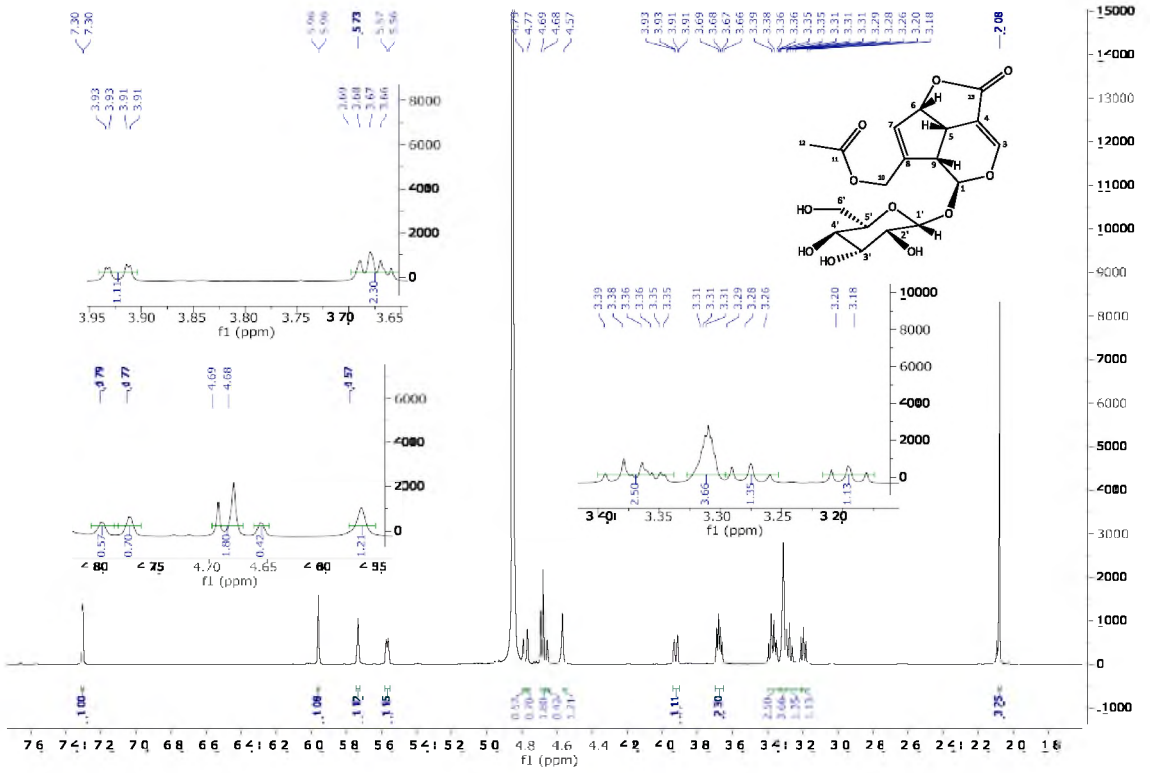

Figure 22 ^{1}H NMR spectrum (in CD_3OD) of compound 1

Table 9: ^{1}H and ^{13}C NMR chemical shift values (in CD_3OD) for compound 1

C	δ_C	HSQC, δ_H (multi, *J* in Hz)	DEPT	HMBC	COSY	NOESY
1	93.3	5.96	CH	C-1, C-4, C-6, C-1'		
3	150.3	7.30 (d, 2.0)	CH	C-2, C-5, C-6, C-13		
4	106.2		C			
5	37.5	3.69 (m)	CH	C-4, C-5, C-8, C-9	3.29, 5.57	5.57
6	86.3	5.57 (d, 6.6)	CH	C-9, C-13	3.69	3.29, 3.69
7	128.9	5.73(s)	CH	C-1, C-6, C-7, C-9, C-10		
8	144.3		C			
9	45.3	3.29(t,9.3)	CH	C-5, C-8, C-9, C-10	3.69	5.57
10	62.7	4.79(dd, 12);4.68(d,7.9)	CH_2	C-1, C-8, C-9, C-10, C-11		4.68;4.79
11	172.3		C			
12	20.6	2.08 (s)	CH_3	C-10, C-11		4.79
13	172.6		C			
1'	100.0	4.69 (d, 6)	CH	C-2	3.21	
2'	74.6	3.21(t, 6;12)	CH	C-1', C-3'	4.69	
3'	77.9	3.36 (m)	CH	C-4'		
4'	71.6	3.28 (m)	CH	C-3', C-5'		
5'	78.4	3.39(m)	CH	C-4'		
6'	61.9	3.93(dd, 11.9; 2.1)	CH_2	C-4', C-5'	3.67	3.67
		3.67 (m)			3.93	3.93

The ^{13}C-NMR (**Fig. 21**) and DEPT 135 NMR spectra (**Appendix 5.1.1 and 5.1.2**) showed the compound to have eighteen carbon atoms, comprising four quaternary carbons at δ106.2 (C-4), 144.3 (C-8), 172.6 (C-13) and 172.3 ppm (C-11), eleven methine (CH) groups, two methylene (CH_2) groups and one methyl (CH_3) group ranging from chemical shifts of 20.6 to 150.3 ppm (**Table 9**) [Bailleul et al, 1977; Demirezer et al, 2006]. The chemical shifts ranging from 62.8 to 100.0 ppm (C-1' to C-6') on the ^{13}C-NMR spectrum indicated the possibility of a six membered cyclic sugar moiety attached to the compound (Demirezer et al, 2006). This was confirmed by the positive result of the Molisch's test (Yisa, 2009).

The chemical shifts ranging from 106.2 to 150.3 ppm (C-3, C-4, C-7 and C-8) on the ^{13}C-NMR spectrum confirmed the presence of the carbon to carbon double bonds (Takeda et al, 2002; Demirezer et al, 2006). The quaternary carbons at δ172.3 and 172.6 ppm were typical of carbonyl carbons in esters (Pretsch et al, 1989; Takeda et al, 2002; Lampman et al, 2010).

On the ^{1}H-NMR spectrum (**Fig. 22**), the methyl group at δ2.05 ppm (C-12, δ20.5 ppm), absorbed more downfield than is normal of a methyl group in a hydrocarbon chain (Pretsch

et al, 1989; Lampman et al, 2010). The behaviour in this case is normally seen in methyl groups of acetyl functional groups (Lampman et al, 2010). The methyl protons are deshielded by the anisotrophic properties of the carbonyl group (Lampman et al, 2010).

The highly deshielded proton signal at δ7.30 ppm, (H-3) was assigned to the proton on the carbon attached to an alkoxy group as well as to the double bond [C=C] (Takeda et al, 2002; Demirezer et al, 2006). This was because of the highly deshielding effect of both the oxygen atom in the alkoxy group as well as the alkene functional group (Lampman et al, 2010). The π electrons of the double bond generated a resonance effect and so caused the proton signal to appear downfield (Lampman et al, 2010). The other proton signals between δ4.68 and 5.96 ppm were assigned to alkoxy groups (Takeda et al, 2002; Demirezer et al, 2006). This included the proton at δ5.96 ppm (H-1), another at δ4.69 ppm (H-1') as well as δ5.57 and δ4.79 ppm (H-6 and H-10 respectively).

Each of the two methylene groups gave two or more signals for each of their protons. One gave two doublets at δ4.79 and 4.68 ppm (H-10). These two protons behaved like diastereotopic hydrogens that were not isochronous (Lampman et al, 2010). They seemed to have split each other and so gave off two doublets. For the other methylene group (H-6') one proton appeared as a doublet of doublets at δ3.93 ppm and the other as a multiplet at δ3.67 ppm. The carbon (C-5') to which they are bonded to is adjacent to a stereocentre (Lampman et al, 2010). This stereocentre has a proton which is splitting the two protons on C-6' which are already splitting each other, hence the doublet of doublets at δ3.71 ppm and the multiplet at δ3.46 ppm (Lampman et al, 2010). The multiplet was probably caused by the interactions of different protons, one on H-5', and the other probably on H-6' and the third from the other proton on the same methylene group on carbon at C-6' (Lampman et al, 2010). The HSQC NMR spectrum (**Appendix 5.1.5**) confirmed that these two pairs of protons were bonded to the carbons at δ61.9 and 62.8 ppm (C-6' and C-10 respectively).

The other protons were assigned to their carbons using the HSQC spectrum as well. The HSQC also indicated that the proton at δ4.57 ppm was probably from a hydroxyl (OH) group as it was not bonded to any carbon atom on the HSQC. The COSY spectrum (**Appendix 5.1.3**) showed the following correlations: at δ3.69 and 5.57, 3.69 and 3.29 ppm, which indicated

that carbon atoms on C-5 and C-6 as well as C-9 and C-5 were bonded together. The correlation between protons at δ3.21 and 4.69 ppm, confirmed the connection between carbon atoms on C-1' and C-2'. The COSY NMR also indicated the correlations between the two protons on carbon atom at C-6'.

Table 10: Correlations of quaternary carbons with protons on different carbons on the HMBC spectrum

Quaternary carbon	Protons which correlates with quaternary carbon
C-4	H-3, H-5, H-9
C-8	H-5, H-6, H-7, H-9, H-10
C-13	H-3, H-6
C-11	H-10, H-12

The HMBC spectrum (**Appendix 5.1.4**) showed that the singlet assigned to the methyl group at δ2.08 ppm (H-12), displayed a strong correlation to carbon atom at C-11, one of the carbonyl carbons. The other carbonyl carbon at δ172.6 ppm (carbon atom at C-13) correlated with protons at δ7.30 ppm (H-3) and 5.57 ppm (H-6). The proton at δ3.69 ppm (H-5) correlated with the carbons at δ106.2 (C-4) and δ45.3 ppm (C-9). It has already been suggested that carbon atom at C-5 is attached to carbon atom at C-6 (from COSY spectrum). These correlations also suggested that carbon atom at C-5 was probably bonded to carbon atom at C-4 and the one at C-9. Still on the HMBC, the proton at δ5.96 ppm (H-1) showed strong correlations to carbons at δ150.3, 37.5 and 100.0 ppm (carbon atoms at C-3, C-5 and C-1' respectively). **Table 9** has more of the correlations indicated by the HMBC spectrum. **Table 10** shows protons which corretates with the quaternary carbon atom. On the NOESY spectrum **(Appendix 5.1.6)** the protons at δ3.29 ppm (H-9); 3.69 (H-5) and 5.57 ppm (H-6) seemed to be close in space. The same applied to the two protons at H-10 of chemical shifts 4.68 and 4.79 ppm.

The proposed structure of compound **1** is like that of asperuloside, an iridoid glycoside, (Glasby, 1982; Takeda et al, 2002). This compound has previously been isolated from *Ferecia apodanthera,* also a Rubiaceae (Bailleul et al, 1977) and from the leaves of *Lasianthus wallichii*, another Rubiaceae (Takeda et al, 2002) as well as from *Galium verum* subsp. *Verum* (Demirezer et al, 2006).

Table 11: **^{13}C-NMR Data of compound 1 and asperuloside (Takeda et al, 2002)**

Carbon	Compound **1** (δ_C)	Asperuloside (δ_C)
1	93.3	93.3
3	150.3	150.3
4	106.2	106.2
5	37.5	37.5
6	86.3	86.3
7	128.9	128.9
8	144.3	144.2
9	45.3	45.2
10	62.7	60.9
11	172.3	172.2
12	20.6	20.7
13	172.6	172.5
1′	100.0	100.0
2′	74.6	74.6
3′	77.9	78.3
4′	71.6	71.5
5′	78.4	77.8
6′	61.9	62.8

Takeda et al (2002) reported spectral data of asperuloside that is similar to the one observed in this study (**Table 11**).

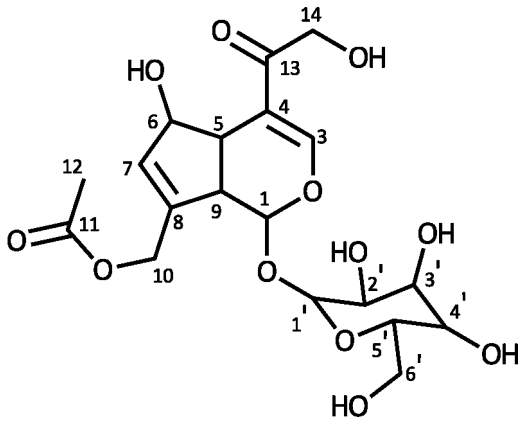

Figure 23 **Proposed structures of compound 2 (asperulosidic acid)**

Compound **2 (Fig. 23)** was isolated as a clear solid. Its melting point was 200 – 204 °C and an optical rotation (α), of the order of +0.02° was measured. ESI-MS **(Appendix 4.2)** detected in the negative mode at *m/z* = 431.1207 [M-H$^+$] (molecular formula: $C_{18}H_{24}O_{12}$), 389.1102 [$C_{18}H_{24}O_{12}$– C_2H_2O]. The molecular weight of compound **2** was 432.3780 g/mol. The unsaturation index of compound **2** was found to be seven.

The IR spectrum of compound **2 (Appendix 3.2)** had strong absorption bands at 3289 (aliphatic OH), 2921 (-CH), 1717(aliphatic C=O), 1640 (aliphatic C=C) and 1246, 1191, 1074, 1060 (C-O), (Lampman et al, 2010; Pretsch et al, 1989).

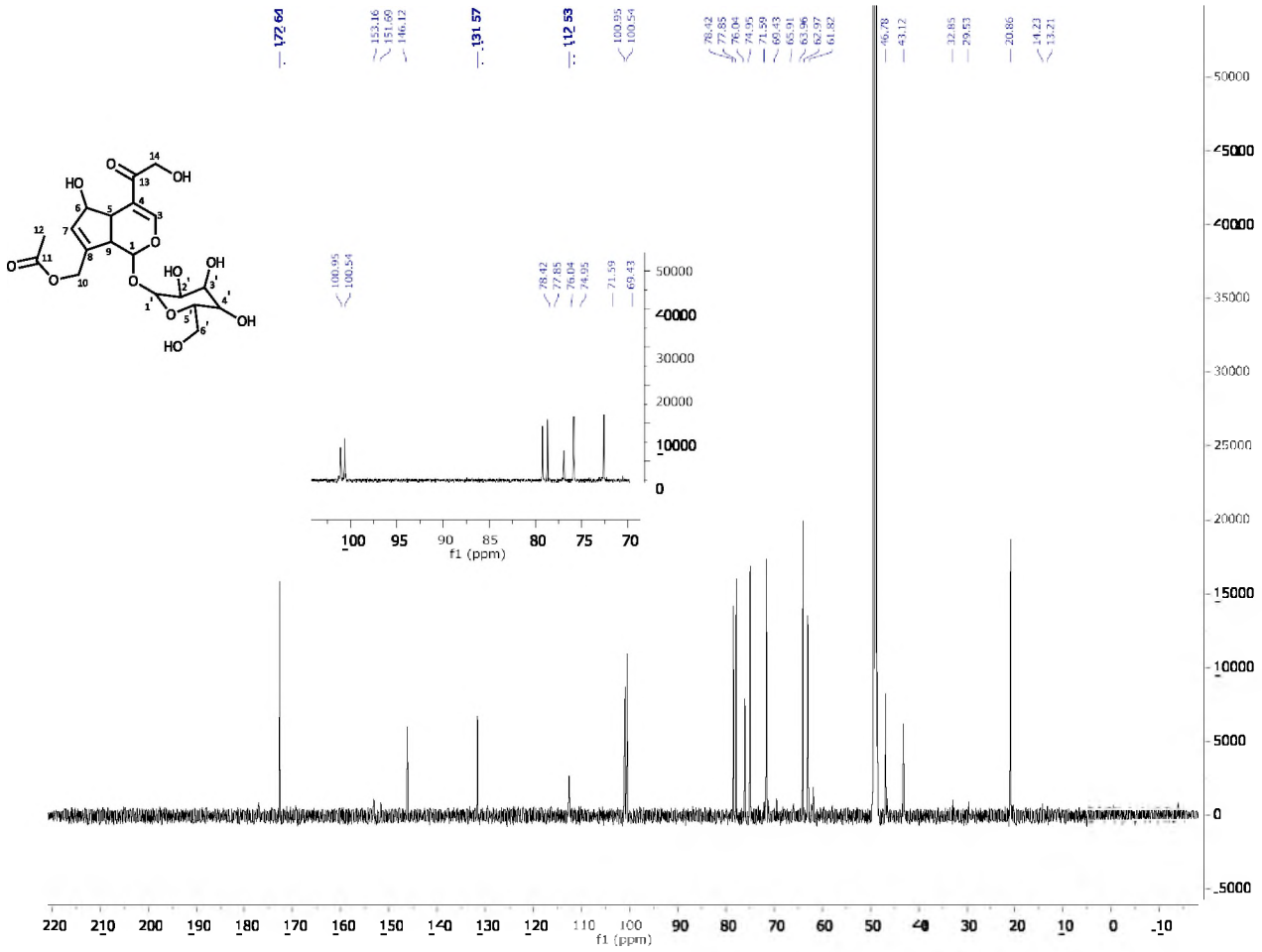

Figure 24: **^{13}C NMR spectrum (in CD_3OD) for compound 2**

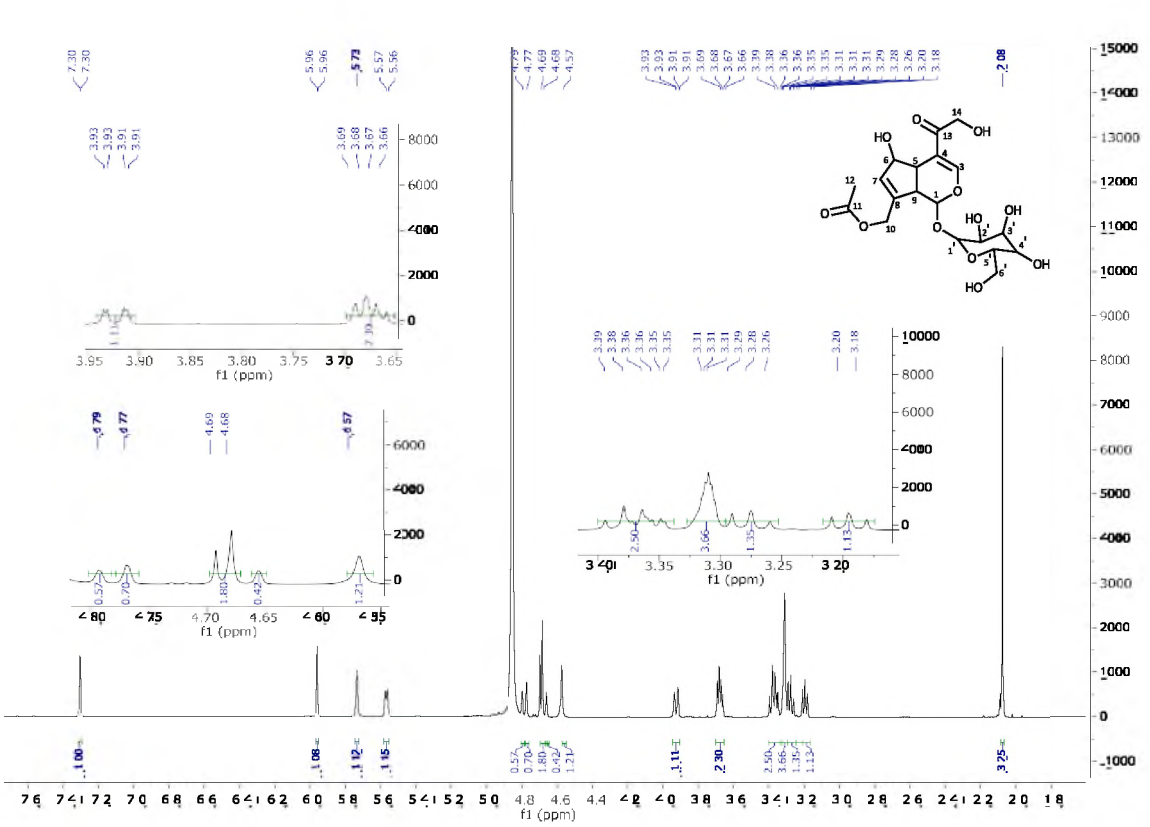

Figure 25 **^{1}H NMR spectrum (in CD_3OD) of compound 2**

Table 12: **^{1}H and ^{13}C NMR chemical shift values (in CD_3OD) for compound 2**

	δ_C	δ_H (multi, J in Hz)	DEPT	HMBC	COSY	NOESY
1	100.5	4.93 (d, 10.8)	CH	C-1'; C-10	2.63	
3	153.1	7.55 (s)	CH	C-5		
4	112.5		C			
5	43.1	3.10 (broad s)	CH		2.63,4.98	
6	76.0	4.98 (m)	CH	C-4; C-5; C-7	3.10	
7	131.5	6.00 (s)	CH			
8	146.1		C			
9	46.7	2.63 (t, 7.8)	CH	C-2; C-7; C-8	3.10, 4.93	
10	63.9	5.01; 4.83 (d, 15)	CH_2	C-1; C-8; C-9; C-11		
11	172.6		C			
12	20.8	2.11 (s)	CH_3	C-11		
13	172.6		C			
1'	100.9	4.74 (d, 7.8)	CH	C-2; C-6'	3.43	
2'	74.9	3.43 (t, 8.6)	CH		4.74	
3'	77.8	3.24 (m)	CH	C-2'; C-4'		
4'	71.5	3.27 (m)	CH	C-1'; C-5'		
5'	78.4	3.30 (m)	CH			
6'	62.9	3.87 (d, 11.5)	CH_2	C-4'; C-5'	3.65	3.65
		3.65 (dd, 11.8; 4.4)			3.87	3.87

The spectral data (IR and NMR [**Fig.24** and **25**; **Table 12**]) for compound **2,** showed the structure of this compound to be similar to that of compound **1** with slight differences. The IR absorptions for both compounds indicated the presence of the same functional groups i.e. hydroxyl and carbonyl groups as well as the aliphatic carbon-carbon double bond. Most of the chemical shifts of carbons and protons in the ^{13}C and ^{1}H NMR spectra for the two compounds were in the same range only that those of compound **2** appeared more downfield than atoms of similar positions in the molecular structure of compound **1**. For example, the carbon atom at C-3 in compound **1** had a chemical shift of 150.2 ppm where as the one on a similar position (C-3) in compound **2** has a chemical shift of 153.1 ppm (**Fig. 24**). The proton at H-3 of compound **1** had a chemical shift of 7.30 ppm where as that on H-3 of compound **2** has a chemical shift of 7.55 ppm (**Fig. 25**).

Both of these compounds, compound **1** and **2**, were elucidated as iridoid glycosides. The major difference between them arose from their aglycon complexes. Apart from the iridoid skeleton being made of two rings, compound **1** had a third ring, a butyrolactone, attached to the iridoid skeleton. Compound **2** has only the original two rings with its carbon atom at C-6 attached to a hydroxyl group and carbon atom at C-13 beraing a carboxylic acid functional group. The carbon atom at C-6 is therefore different in compounds **1** and **2**. The carbon atom at C-6 in compound **1** has a higher chemical shift of 86.3 ppm compared to the chemical shift of 76.0 ppm for the carbon atom on C-6 in compound **2**.

The HMBC (**Appendix 5.2.4**) and HSQC (**Appendix 5.2.5**) correlations confirmed the structure of compound **2** to be as suggested in **Figure 23**. There were correlations between the H-1 with C-1' and C-10. H-6 had a lot of correlations e.g. with C-4, C-5, C-7. The COSY spectrum (**Appendix 5.2.3**) confirmed some of the correlations between protons in compound **2**, for example between H-5 and H-6; H-9 and H-5; H-1' and H-2' as well as the two protons on carbon atom at C-6'. The two protons on C-6' appeared to be in the same environment as indicated by the NOESY spectrum (**Appendix 5.2.6**). Apart from this correlation, the NOESY spectrum indicated fewer interactions of protons within the structure of compound **2** as compared to that of compound **1**.

Table 13: ^{13}C-NMR Data of compound 2 and asperulosidic acid (Demirezer et al, 2006)

Carbon	Compound **2** (δ_C)	Asperulosidic acid (δ_C)
1	100.5	101.1
3	153.1	154.9
4	112.5	109.0
5	43.1	42.6
6	76.0	75.4
7	131.5	131.8
8	146.1	145.9
9	46.7	46.3
10	63.9	63.8
11	172.6	172.5
12	20.8	20.8
13	172.6	172.5
1'	100.9	100.5
2'	74.9	74.9
3'	77.8	78.5
4'	71.5	71.5
5'	78.4	77.8
6'	62.9	63.0

The proposed structure of compound **2** is like that of asperulosidic acid, a hydrolised form of asperuloside (El-Naggar and Beal, 1980; Demirezer et al, 2006). This is also an iridoid glycoside which has previously been isolated from the fruits of *Morinda citrifolia,* a Rubiaceae (Kamiya et al, 2005), as well as from *Galium verum* subsp. *Verum* (Demirezer et al, 2006), *Galium melanantherum,* a Rubiaceae (Tzakou et al, 2007) and from a lot of other families like the Ericaceae, Globulariaceae and Hammamelidaceae (El-Naggar and Beal, 1980). Demirezer et al (2006) reported spectral data of asperuloside that is similar to the one observed in this study (**Table 13**). This information helped to asign the chemical shift values to the different carbon atoms in compound **2**.

3.3.2 Structure elucidation of compounds in sample 3

Sample **3** was purified to a whitish grey amorphous powder of melting point 126 -130 $^{\circ}$C. It gave a positive result to the Liebermann-Burchard's test for terpenes.

HR-ESI-MS of sample **3 (Appendix 4.3**) detected several compounds (**Fig. 26**) in the positive mode, one at *m/z* = 413.2660 [M+H$^+$] (stigmasterol, molecular formula: $C_{29}H_{48}O$), another

one at *m/z* = 415.2130 [M+H$^+$] (β-sitosterol, molecular formula: $C_{29}H_{50}O$), another, a possibility of two compounds at *m/z* = 427.3597 [M+H$^+$] (lanosterol and cycloartenol both of molecular formula: $C_{30}H_{50}O$) and *m/z* = 401.3349 [M+H$^+$] (campesterol, molecular formula: $C_{28}H_{48}O$). The fragments at *m/z* = 397.3820; 395.3673; 409.2184 and 383.3659 could be due to loss of water from the molecular ions of stigmasterol, β-sitosterol, lanosterol or cycloartenol and campesterol respectively (Ohyama et al, 2009; Charturvedula and Prakash, 2012).

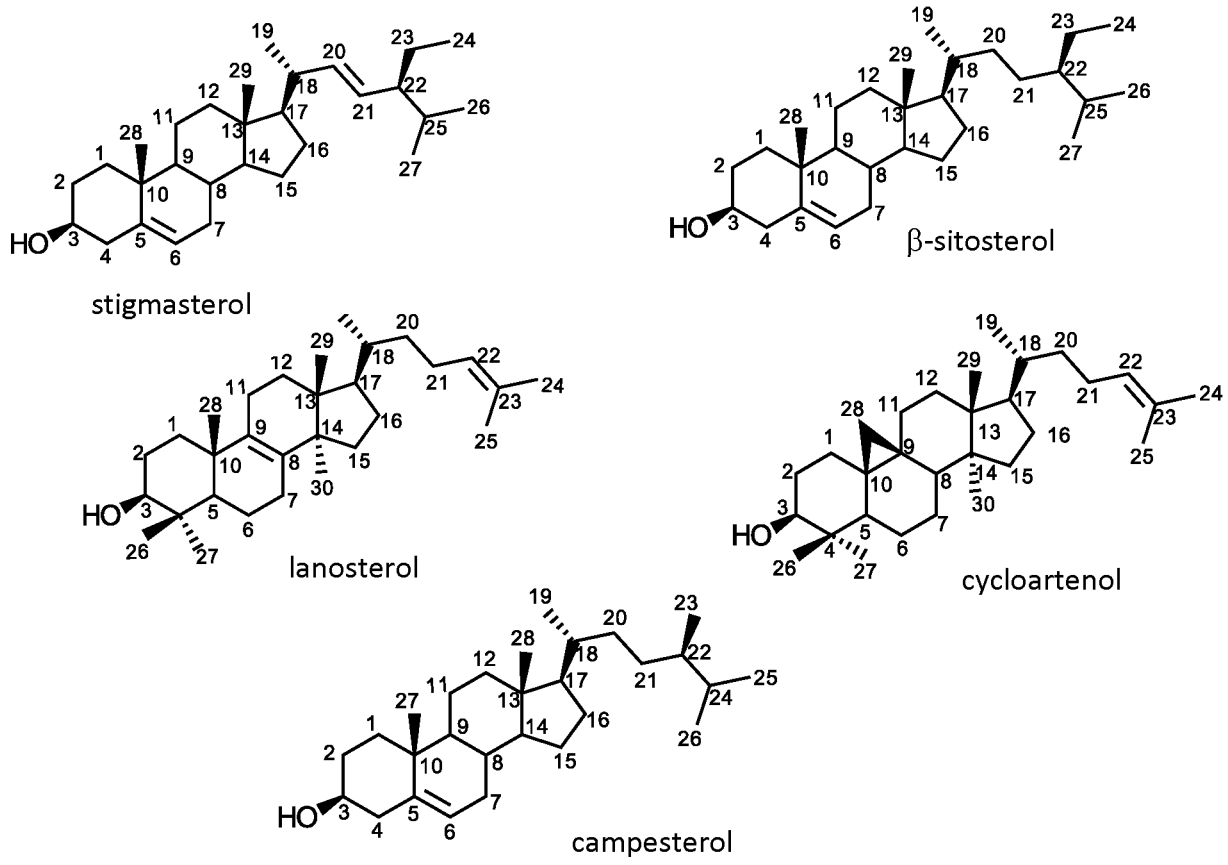

Figure 26: Proposed structures of the terpenoids found in sample 3

The calculated molecular weight (in g/mol) of stigmasterol is 412.7020, that of β-sitosterol is 414.7180, lanosterol and cycloartenol has 426.7290 where as campesterol has 400.6910. The IR spectrum (**Appendix 3.3**) shows absorption bands at 3308 (aliphatic OH), 2800 (-CH), 1643 (aliphatic C=C), 1462 (CH_2), 1367 (CH_3) and 1052 cm^{-1} (C-O) (Lampman et al, 2010; Pretsch et al, 1989).

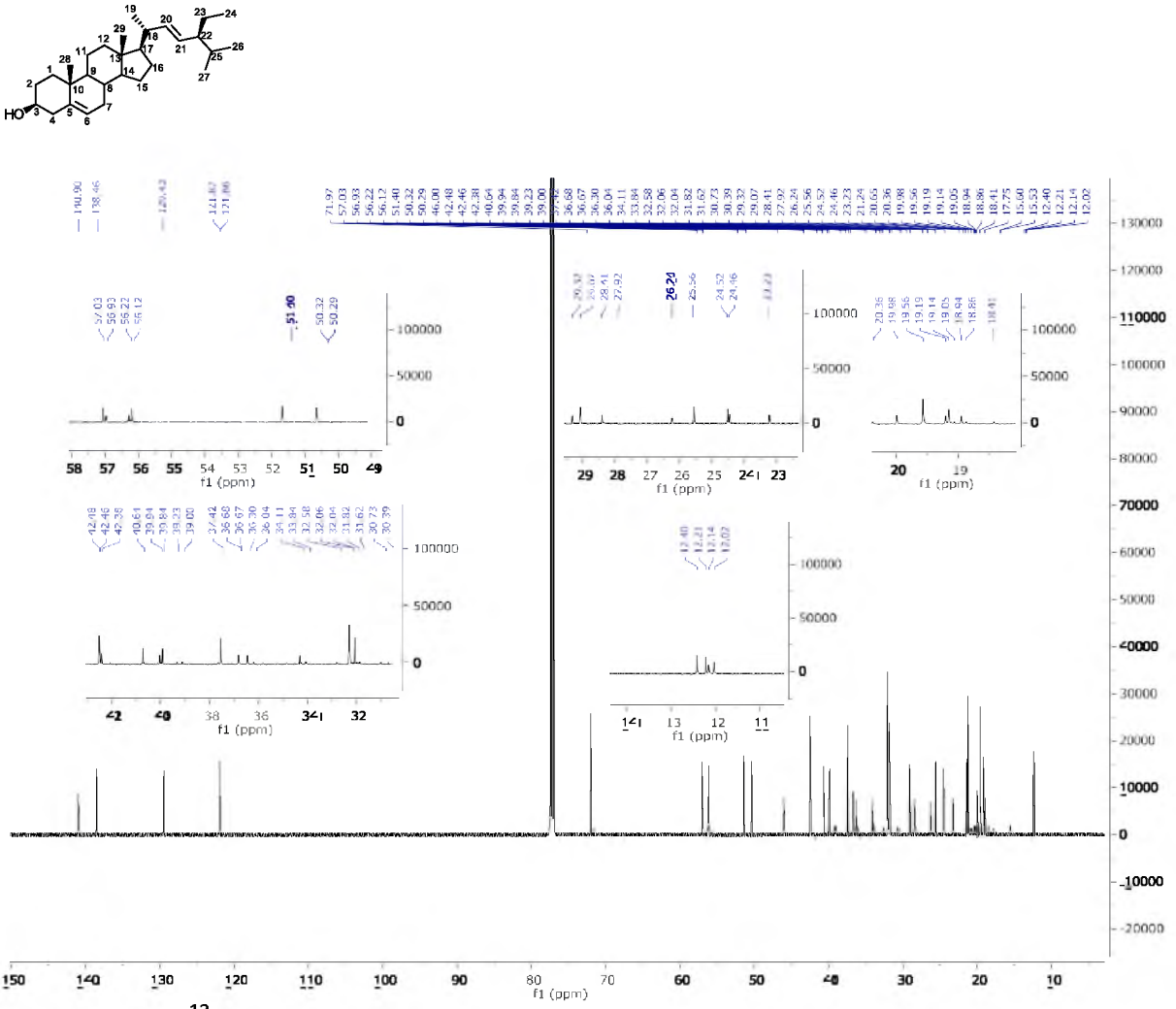

Figure 27: ^{13}**C- NMR spectrum (in $CDCl_3$) of sample 3**

The ^{13}C-NMR (**Fig. 27, Table 16**) indicated the presence of more than forty carbon atoms. It was not possible to work out the exact number due to overlap of signals from the different compounds on one chemical shift. More than six of these carbon atoms were quartenary carbons and more than thirteen were methylene ones (DEPT 135 NMR spectra **Appendix 5.3.1** and **5.3.2**). The ^{13}C chemical shifts above 120 ppm suggested the presence of double bonds in the structure. A number of carbon atoms had chemical shifts between 30 and 59 ppm, this showed how either highly branched or unsaturated the compound was (Mahato and Kundu, 1994). The carbon atom (C-3) found at chemical shift of 72.0 ppm confirmed the presence of a hydroxyl group attached to it (Mahato and Kundu, 1994; Lampman et al, 2010; Chaturvedula and Prakash, 2012). The presence of this hydroxyl group was also indicated by the ^{1}H-NMR (**Fig. 28** and **Table 14**) which showed a deshielded proton at

chemical shift of 3.55 ppm (Mahato and Kundu, 1994; Chaturvedula and Prakash, 2012). The presence of methyl groups with chemical shifts between 10 and 20 ppm was confirmed by the ^{1}H-NMR and HSQC (**Appendix 5.3.5**). HSQC spectra showed that some of the carbon atoms did not have correlations to the protons in the compound, for example the carbon atoms with chemical shifts of 56.9 and 56.2 ppm. This could be due to the fact that the sample had a mixture of compounds some in greater quantities than others. The signals of the more concentrated compound could easily have been identified than the dilute ones.

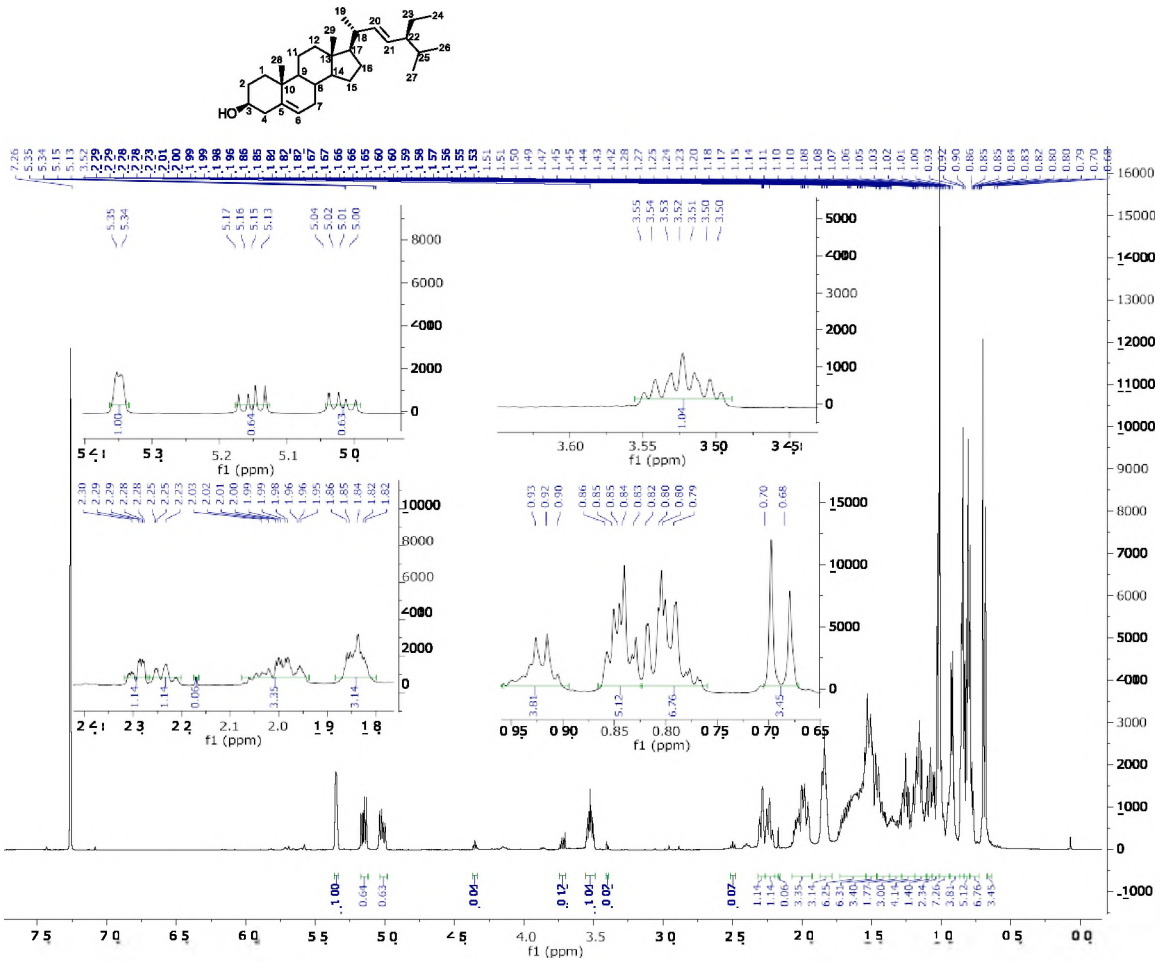

Figure 28: ^{1}**H-NMR spectrum (in $CDCl_3$) of sample 3**

Table 14 has NMR data for stigmasterol. The COSY NMR spectrum **(Appendix 5.3.3)** showed correlations between H-1 and H-2 as well as between H-2 and the proton on the hydroxyl bearing carbon (C-3). The interactions of protons on the NOESY (**Appendix 5.3.6**) and protons to carbons on the HMBC (**Appendix 5.3.4**) spectra are also indicated in **Table 14.**

Table 14: **^{1}H and ^{13}C NMR chemical shift values (in $CDCl_3$) for sample 3**

C	δ_C	HSQC: δ_H (m,J(HZ))	DEPT	HMBC	COSY	NOESY
1	37.4	1.38(m); 1.17(m)	CH_2	C-2; C-19	1.50	
2	31.8	1.50(m); 1.25(m)	CH_2	C-1; C-3	1.17; 3.52	
3	72.0	3.52(m)	CH		1.50; 2.31	
4	42.4	2.31(d, 13); 2.25(d,24.3)	CH_2	C-2; C-3; C-5; C-6	3.52	
5	140.9		C			
6	121.8	5.35	CH		2.02	
7	29.1	2.02; 1.86(m)	CH_2	C-5; C-8	1.53; 5.35	1.53; 1.05
8	32.0	1.53(m)	CH	C-7; C-9	1.86	0.93; 1.86
9	50.3	0.93(m)	CH	C-8; C-10; C-14		1.53
10	36.7		C			
11	21.2	1.58; 1.43(m)	CH_2	C-9; C-12		
12	39.9	1.20; 1.14 (m)	CH_2	C-11; C-13		
13	42.5		C			
14	57.0	1.05(m)	CH	C-8; C-13; C-15		1.86
15	25.6	1.68(m); 1.55(m)	CH_2	C-13		1.97
16	28.4	1.97(m); 1.50(m)	CH_2	C-17; C-18	1.08	1.68
17	56.1	1.08(m)	CH	C-13; C-16; C-18	1.97	
18	40.6	1.35(m)	CH	C-16; C-17		
19	21.4	0.86 (m)	CH_3	C-18; C-20		
20	138.5	5.04(m)	CH	C-21		
21	129.4	5.17(m)	CH			
22	46.0	0.93(m)	CH	C-21		
23	23.2	1.27(m)	CH_2	C-22; C-24		
24	12.4	0.83 (td, 7.2; 3.4)	CH_3	C-22; C-23		
25	29.3	1.28(m)	CH	C-22		
26	20.0	0.82 (d, 1.3)	CH_3	C-22; C-25		
27	19.6	0.80 (d)	CH_3	C-22; C-25		
28	19.1	1.01 (s)	CH_3	C-1; C-5; C-9; C-10		
29	12.2	0.84	CH_3	C-12; C-13		

Stigmasterol and β-sitosterol have been isolated from many plants including *Rubus suavissimus* (Chaturvedula and Prakash, 2012) and *Ageratum conyzoides* (Kamboj and Saluja, 2011). Lanosterol (Ohyama et al, 2009), cycloartenol (Corey et al, 1993) and campesterol (Ohyama et al, 2009) have also been isolated before. These compounds are a group of sterols found in eukaryotic organisms (Suzuki et al, 2006; Vincken et al, 2007; Ohyama et al, 2009).

Where as stigmasterol and β-sitosterol have been previously isolated from M. lucida (Nweze, 2012), this seem to be the first report on the isolation of lanosterol, cycloartenol and campesterol from *M. lucida*.

Table 15: **^{13}C-NMR Data of sample 3 and stigmasterol (Chaturvedula and Prakash, 2012)**

Carbon	Sample 3(δ_C)	Stigmasterol (δ_C)
1	37.4	37.6
2	31.8	32.1
3	72.0	72.1
4	42.4	42.4
5	140.9	141.1
6	121.8	121.8
7	29.1	31.8
8	32.0	31.8
9	50.3	50.2
10	36.7	36.6
11	21.2	21.5
12	39.9	39.9
13	42.5	42.4
14	57.0	56.8
15	25.6	24.4
16	28.4	29.3
17	56.1	56.2
18	40.6	40.6
19	21.4	21.7
20	138.5	138.7
21	129.4	129.6
22	46.0	46.1
23	23.2	25.4
24	12.4	12.1
25	29.3	29.6
26	20.0	20.2
27	19.6	19.8
28	19.1	18.9
29	12.2	12.2

Chaturvedula and Prakash (2012) reported spectral data of stigmasterol that is similar to the one observed in this study (**Table 15**). This information helped to asign the chemical shift values to the different carbon atoms in sample **3**. As Luhata and Munkombwe (2015) pointed out, it was difficult to separate these steroids which appeared as a single spot on the TLC plate. The presence of these compounds in this sample could also be the reason why a low melting point was obtained instead of the normal melting point of stigmasterol of 174 – 176 °C (Chaturvedula and Prakash, 2012). Cycloartenol and campesterol have also been isolated from many plants for example from the Brassicaceae family (Kolesnikova et al, 2006; Suzuki et al, 2006; Vincken et al, 2007; Ohyama et al, 2009) where as lanosterol was

once thought to be synthesised in animals only (Kolesnikova et al, 2006; Suzuki et al, 2006; Ohyama et al, 2009) but has now been isolated from the Brassicaceae family (e.g. from *Arabidopsis thaliana*) as well as from plants of the Euphorbiaceae family (Kolesnikova et al, 2006; Suzuki et al, 2006; Ohyama et al, 2009).

3.3.3 Structure elucidation of compounds 4, 5 and 6

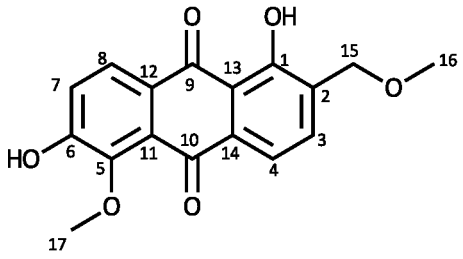

5,15-O-dimethylmorindol

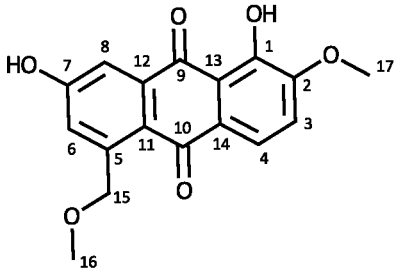

1,7-dihydroxy-2-methoxy-5-(methoxymethyl)anthraquinone

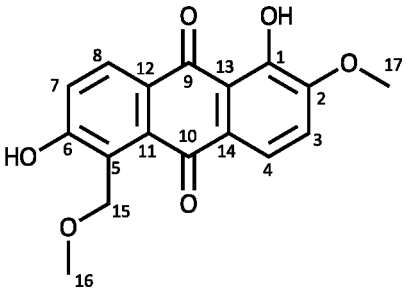

1,6-dihydroxy-2-methoxy-5-(methoxymethyl)anthraquino

Figure 29: Proposed structures of compound 4 (5,15-O-dimethylmorindol), compound 5 (1,7-dihydroxy-2-methoxy-5-(methoxymethyl)anthraquinone) and compound 6 (1,6-dihydroxy-2-methoxy-5-(methoxymethyl)anthraquinone)

Compound **4** (**Fig. 29**) was isolated as orange/yellow amorphous powder of melting point 216–220 °C. Compouns **5** and **6** (**Fig. 29**) were isolated as light yellow amorphous powder of melting points 200–207 °C and 204–210 °C, respectively.

HR-ESI-MS of compound **4 (Appendix 4.4)** was detected in the positive mode at *m/z* = 315.0856 [M+H$^+$] (molecular formula: $C_{17}H_{14}O_6$); 283.0599 ($C_{17}H_{14}O_6$ – OCH_3 and H).

HR-ESI-MS for compound **5** (**Appendix 4.5**) was detected in the negative mode at *m/z* = 313.0704 [M-H$^+$] (molecular formula: $C_{17}H_{14}O_6$); 293.1745 ($C_{17}H_{14}O_6$ – H_2O and 2H); 284.0681 ($C_{17}H_{14}O_6$ – CH_2O).

HR-ESI-MS for compound **6** (**Appendix 4.6**) was detected in the positive mode at *m/z* = 315.0856 [M+H$^+$] (molecular formula: $C_{17}H_{14}O_6$); 282.0520 ($C_{17}H_{14}O_6$ – OCH_3 and H). All three compounds had a molecular weight of 314.2930 g / mol.

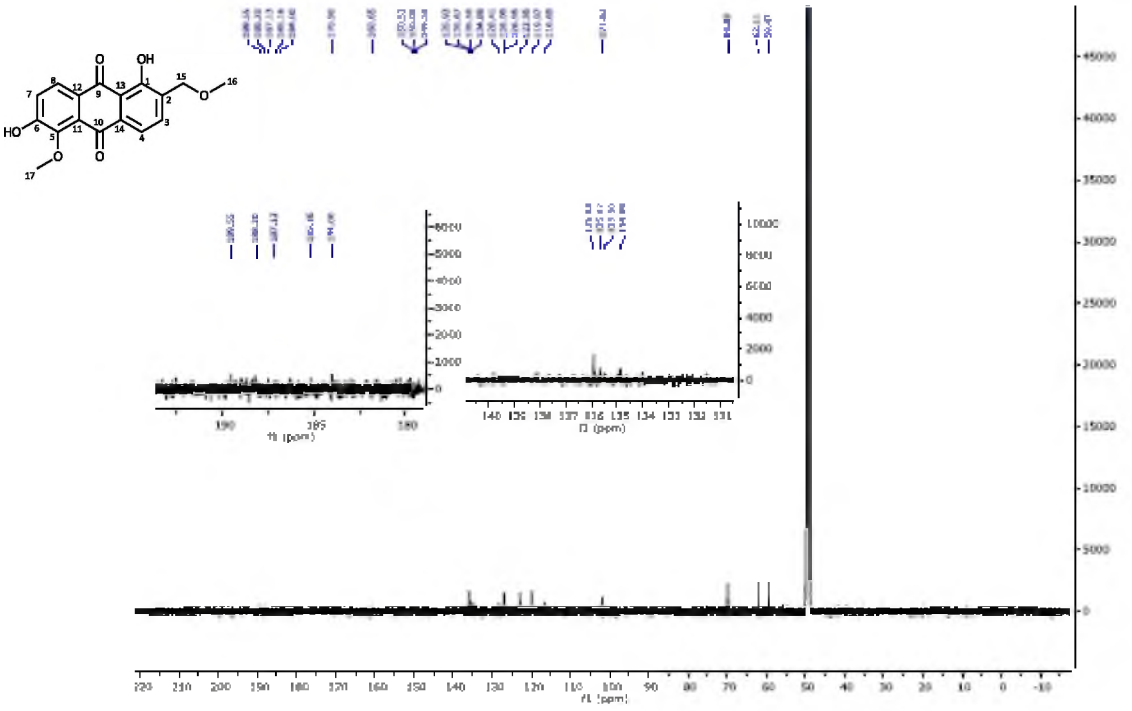

Figure 30: ^{13}C-NMR spectrum (in CD_3OD) of compound 4

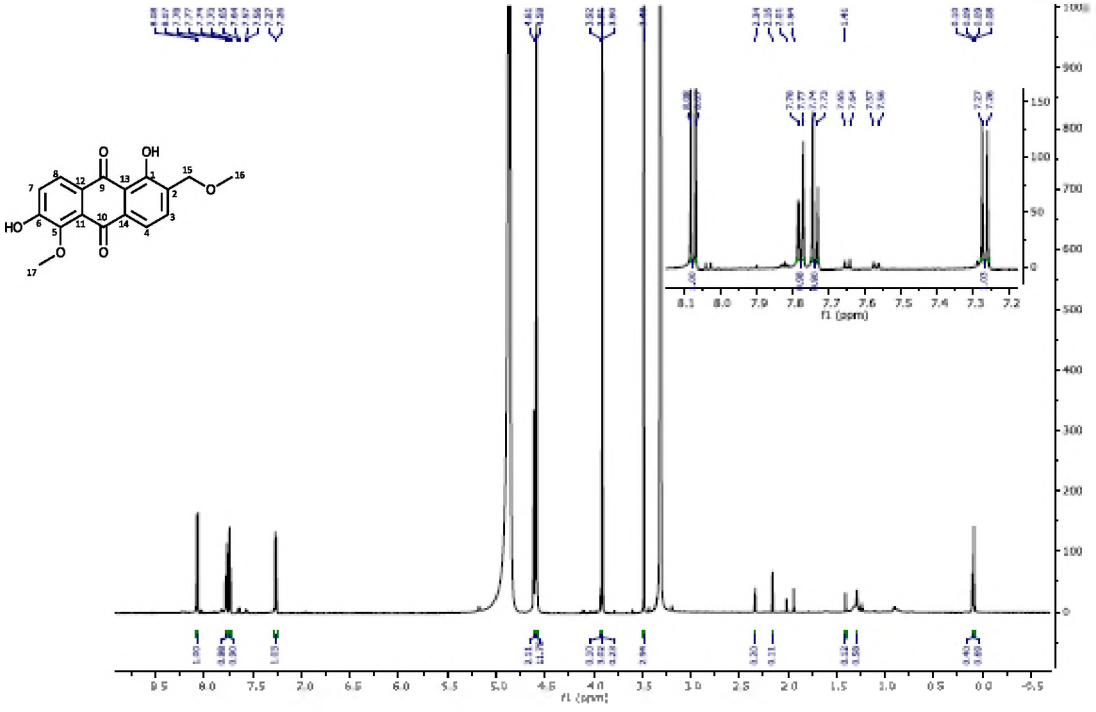

Figure 31: ^{1}H-NMR spectrum (in CD_3OD) of compound 4

Table 16: ^{1}H and ^{13}C NMR data (in CD_3OD)) for compound 4

	δ_C	δ_H (multi, *J* in Hz)	DEPT	HMBC	COSY
1	161.3		C		
2	135.7		C		
3	135.9	7.74(d, 7.8)	CH	C-14	7.78
4	120.0	7.78 (d, 7.8)	CH	C-2; C-10	7.74
5	148.0		C		
6	157.9		C		
7	123.0	7.27 (d, 8.6)	CH	C-8	7.27
8	127.00	8.08 (d, 8.6)	CH	C-7; C-9	8.08
9	189.4		C		
10	183.5		C		
11	125.0		C		
12	127.6		C		
13	115.4		C		
14	134.9		C		
15	69.8	4.61 (s)	CH_2	C-2; C-16	
16	59.5	3.48 (s)	CH_3	C-15	
17	62.1	3.92 (s)	CH_3	C-5	

The IR spectrum for compound **4 (Appendix 3.4)**, compound **5 (Appendix 3.5)** and compound **6 (Appendix 3.6)** had strong absorption bands around 3378 (OH, phenols), 1666-1629 (C=O), 1566-1360 (aromatic C=C) and 1277 -958 cm^{-1} (C-O) [Adesogan, 1973; Kamiya et al, 2005; Lampman et al, 2010]. The unsaturation index for all compounds was eleven.

The ^{13}C-NMR spectrum of compound **4** (**Fig. 30**) indicated the presence of seventeen carbon atoms. Two of these were carbonyl carbons with signals at δ183.5 and 189.4 ppm and eight were quartenary carbons (DEPT 135 NMR spectra**; Appendix 5.4.1 and 5.4.2; Table 16**) [Kamiya et al, 2005; Lampman et al, 2010]. The ^{13}C-NMR spectrum also showed that the compound was aromatic due to the presence of the signals between δ114 and 160 ppm (Kamiya et al, 2005; Lampman et al, 2010). The other carbon signals appeared between δ59 and 69 ppm (**Table 16**) suggesting the vicinity of those carbons to electronegative heteroatoms (Kamiya et al, 2005; Lampman et al, 2010). The DEPT NMR spectrum showed that the carbon at 69.8 ppm was a methylene group.

The ^{1}H-NMR (**Fig. 31**) and HSQC (**Appendix 5.4.5**) spectra confirmed that the carbons at C-3, C-4, C-7 and C-8 had the methine groups (giving a total of four methine groups) and that

there were two methyl groups on C-16 and C-17. The protons on the methine groups appeared downfield with chemical shifts ranging from 7.27 to 8.08 ppm. These were highly deshielded protons typical of those found in an aromatic compound (Kamiya et al, 2005; Lampman et al, 2010). The methyl protons on H-16 and H-17 (δ3.48 and 3.92 respectively) confirmed the presence of heteroatoms (oxygen) in their environment (Pretsch et al, 1989; Lampman et al, 2010). The methylene and methyl signals appeared as singlets on the ^{1}H-NMR spectrum indicating that these protons were not close to each other (Pretsch et al, 1989; Lampman et al, 2010).

Table 17: ^{13}C-NMR Data of compound 4 and 5,15-O-dimethylmorindol (Kamiya et al, 2005)

Carbon	ML4 (δ_C)	5,15-O-dimethylmorindol (δ_C)
1	161.3	159.48
2	135.7	133.94
3	135.9	134.46
4	120.0	118.98
5	148.0	146.89
6	157.9	156.07
7	123.0	120.09
8	127.00	125.57
9	189.4	187.78
10	183.5	181.91
11	125.0	125.81
12	127.6	126.96
13	115.4	114.89
14	134.9	133.27
15	69.8	68.56
16	59.5	58.89
17	62.1	62.36

The COSY NMR spectrum (**Appendix 5.4.3**) showed the presence of ortho-coupled protons on the first and third rings (**Fig. 29**) of compound **4** (Pretsch et al, 1989; Kamiya et al, 2005; Lampman et al, 2010). The H-7 correlated with H-8 and H-3 correlated with H-4 on the COSY spectrum. All of these protons appeared as doublets (with a coupling constant, *J* = 7.8 Hz for H-3 and H-4; *J* = 8.6 for H-7 and H-8) confirming their positions on the structure of the compound. The HMBC NMR spectrum showed that H-4 correlated with the carbonyl carbon (C-10) and that H-8 correlated with the other carbonyl carbon (C-9). This spectrum also

indicated that H-16 and H-17 (the methyl protons) correlated with C-15 and C-5 respectively (**Table 16**). The absence of correlations between the protons on the structure of compound **4** on the NOESY NMR spectrum **(Appendix 5.4.6)** indicated that the protons were not close in space as the compound has a planar (or flat) structure .

Compound **4** was identified as 5,15-O-dimethylmorindol, an anthraquinone (Kamiya et al, 2005), previously isolated from the fruits of *Morinda citrifolia* (Kamiya et al, 2005) [**Table 17**].

The structures of compounds **5** and **6** had an anthraquinone skeleton similar to compound **4 (Fig. 29)**. They also possessed the same groups attached to the first and third rings of their compounds, the difference was in the arrangement of these groups. Compounds **5** and **6** were both thought to be aromatic carboxylic acids because of signal at δ13.01 ppm on their ^{1}H-NMR spectra due to the acidic proton on the carboxylic functional groups. It was realised that this was not the case but that compounds **5** and **6** could have a peri-hydroxyl group. This is a hydroxyl group positioned next to the carbonyl group on either the first or the third ring or on both rings of the anthraquinone (Schripsema and Dagnino, 1996). A hydrogen bond forms between the hydrogen on the hydroxyl group and the carbonyl group (**Fig. 32**) (Schripsema and Dagnino, 1996). This proton gives a signal between 12 and 14 ppm on the ^{1}H-NMR (Schripsema and Dagnino, 1996).

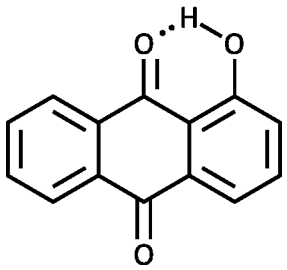

Figure 32: Hydrogen bond between carbonyl group and hydrogen atom on peri-hydroxyl group

The ^{13}C-NMR and ^{1}H-NMR spectra as well as the spectra data for compound **5** are presented in **figures 33**, **34** and **Table 18** respectively. The difference between compound **5** and the other two anthraquinones, compound **4** and compound **6**, was the singlet displayed at δ7.79 ppm which integrated for two protons on the ^{1}H-NMR spectrum (**Fig. 34**). The HSQC NMR

spectrum **(Appendix 5.5.5)** indicated this singlet to belong to two protons on separate carbons but absorbing on the same chemical shift (i.e. this was not a methylene group).

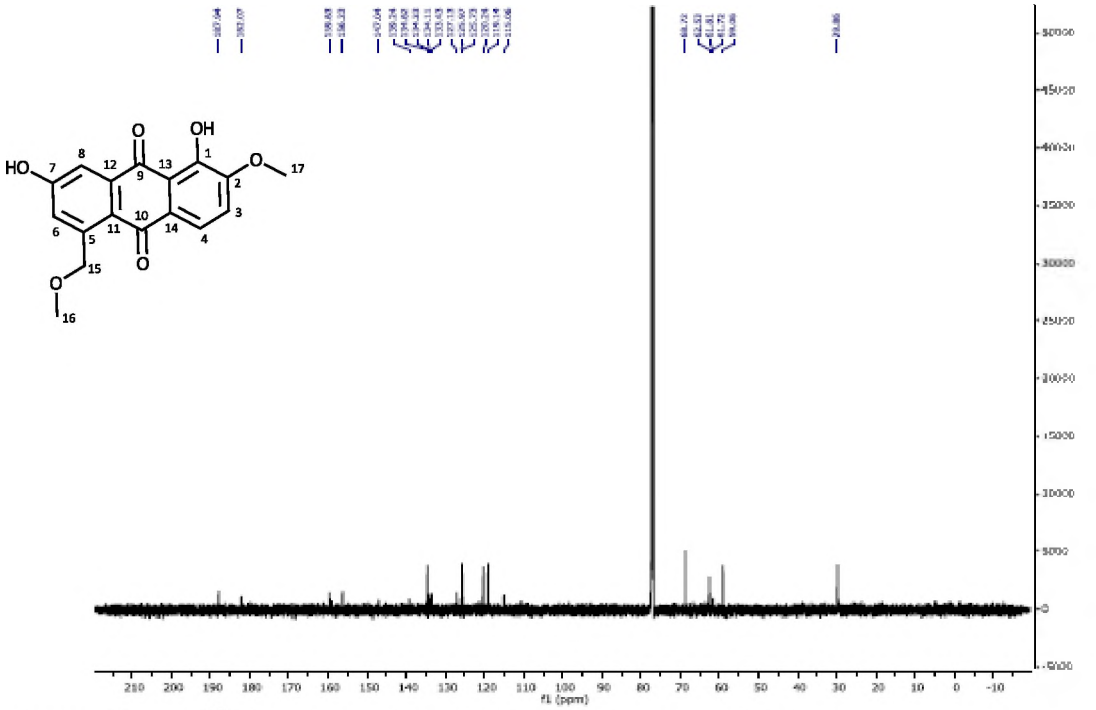

Figure 33: ^{13}**C-NMR spectrum (in $CDCl_3$) of compound 5**

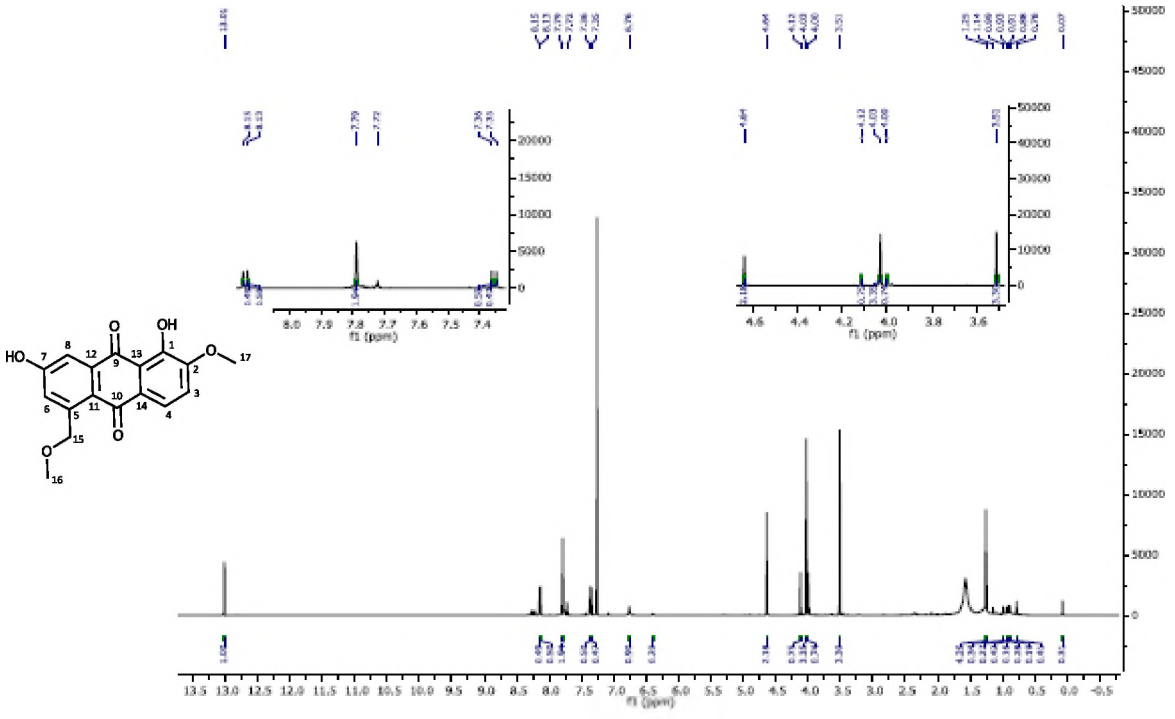

Figure 34: ^{1}**H-NMR spectrum (in $CDCl_3$) of compound 5**

Table 18: **^{1}H and ^{13}C NMR chemical shift values for compound 5**

	δ_C	δ_H (multi, *J* in Hz)	DEPT	HMBC	COSY	NOESY
1	156.2		C			
2	147.0		C			
3	120.2	7.36 (d, 8.5)	CH	C-1; C-2; C-4	8.15	8.15
4	125.7	8.15 (d, 8.5)	CH	C-10	7.36	7.36
5	134.1		C			
6	134.6	7.79 (s)	CH	C-7		
7	159.6		C			
8	119.1	7.79 (s)	CH	C-7; C-9		
9	182.1		C			
10	187.9		C			
11	134.2		C			
12	133.4		C			
13	115.1		C			
14	127.1		C			
15	68.7	4.64 (s)	CH_2	C-5/6; C-16		
16	59.1	3.51 (s)	CH_3	C-15		
17	62.5	4.03 (s)	CH_3			

The third ring had ortho-coupled protons. According to DEPT NMR spectrum (**Appendix 5.5.1 and 5.5.2**), there was only one methylene group at δ4.64 ppm (δ_C68.7 ppm). COSY (**Appendix 5.5.3**) and NOESY (**Appendix 5.5.6**) NMR spectra indicated correlations between H-3 and H-4 which was confirmed by the presence of doublets (H-3 and H-4 both with *J* = 8.5 Hz). Both HMBC (**Appendix 5.5.4**) and HSQC (**Appendix 5.5.5**) were used to arrange the substituents on the first and third rings of this compound.

From the presented data, compound **5** was tentatively identified as 1,7-dihydroxy-2-methoxy-5-(methoxymethyl)anthraquinone and seem not to have been identified before (i.e it is probably a new compound). More of this sample need to be isolated again to confirm this identification. The quantity of the sample isolated in this experiment was small (1.50 mg) and not pure hence the poor NMR spectra.

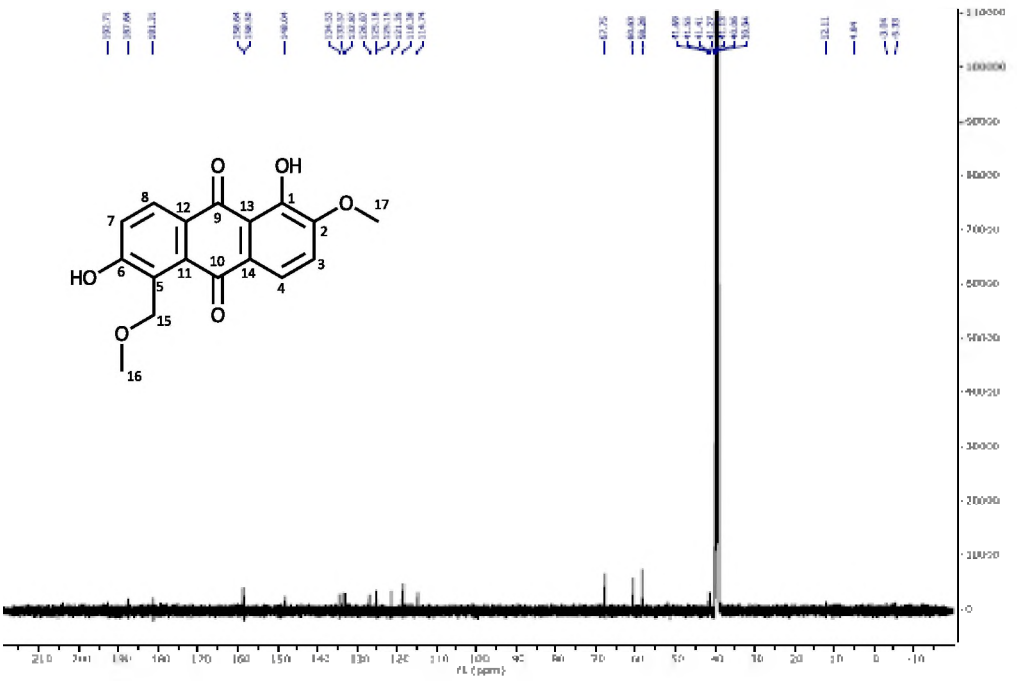

Figure 35: ^{13}C-NMR spectrum [in $(CD_3)_2SO$]of compound 6

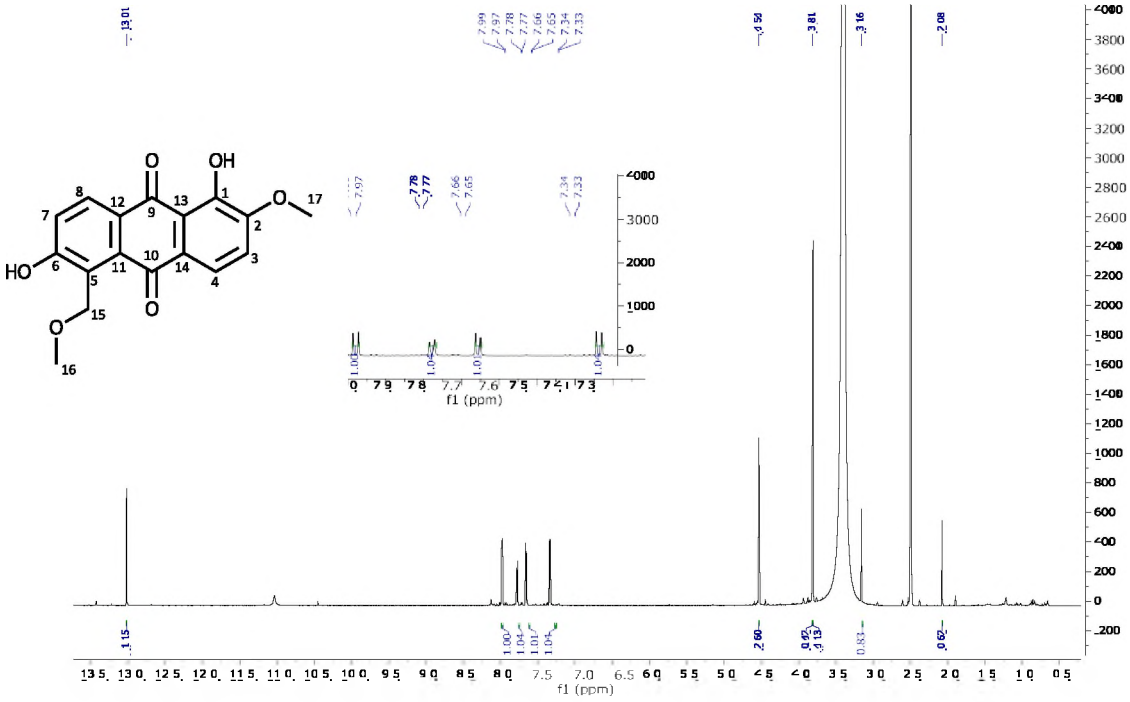

Figure 36: ^{1}H-NMR spectrum [in $(CD_3)_2SO$]of compound 6

For compound **6**, the four pairs of doublets on the ^{1}H-NMR (**Fig. 36**) for the methine groups on the first and third rings indicated the existence of ortho-coupled protons on both rings (*J*

= 8.6 for H-3 and *J* = 8.5 for H-4; *J* = 7.8 for both H-7 and H-8). This was confirmed by the correlations observed on the COSY NMR spectrum (**Appendix 5.6.3**). The H-3 correlated with H-4 where as H-7 correlated with H-8 (**Table 19**). NOESY NMR spectrum (**Appendix 5.6.6**) also indicated the correlation of H-3 and H-4. The ^{13}C (**Fig. 35**) and HMBC (**Appendix 5.5.4**) NMR spectra confirmed the presence of 17 carbon atoms (**Table 19**) just like in compounds **4** and **5**. DEPT 135 (**Appendix 5.6.1 and 5.6.2**) and HSQC (**Appendix 5.6.5**) NMR spectra indicated the presence of one methylene and two methyl groups. HMBC (**Appendix 5.6.4**) of compound **6** indicated a strong colleration between C-2, the carbon bearing the methoxy group and H-3. There was a weak signal for the correlation between H-7 and H-8 to C-5, the carbon bearing the methoxy group.

Table 19: ^{1}H and ^{13}C NMR chemical shift values [in $(CD_3)_2SO$]for compound 6

	δ_C	δ_H (multi, *J* in Hz)	DEPT	HMBC	COSY
1	158.5		C		
2	148.0		C		
3	121.3	7.35 (d, 8.6)	CH	C-2	7.99
4	125.1	7.99 (d, 8.5)	CH	C-10	7.35
5	134.5		C		
6	158.6		C		
7	118.4	7.67 (d, 7.8)	CH	C-5	7.79
8	133.6	7.79 (d, 7.8)	CH	C-6	7.67
9	181.3		C		
10	187.6		C		
11	132.9		C		
12	125.2		C		
13	114.7		C		
14	126.9		C		
15	67.74	4.54 (s)	CH_2	C-5; C-6; C-11; C-16	
16	58.26	3.39 (s)	CH_3	C-15	
17	60.61	3.81 (s)	CH_3		
		13.02 (s)	OH	C-2; C-18	

From the presented data, compound **6** was tentatively identified as 1,6-dihydroxy-2-methoxy-5-(methoxymethyl)anthraquinone and seem not to have been identified before (i.e it is probably a new compound). Just like compound **5**, more quantity of the sample needs to be obtained and analysed further to identify the compound as such. The amount isolated in this experiment was 1.30 mg and not pure.

3.4 Docked results for ubiquinone, atovaquone and compound 4

Atovaquone inhibits the activities of the protein cytochrome bc_1 by mimicking ubiquinone (**Fig 37**), a naturally occurring molecule which is sometimes called coenzyme Q (Baggish and Hill, 2002). The structure of this ubiquinone is similar to that of compound **4** and atovaquone (**Fig. 37**) as they all have a naphthoquinone ring (Baggish and Hill, 2002; Kessl et al, 2007).

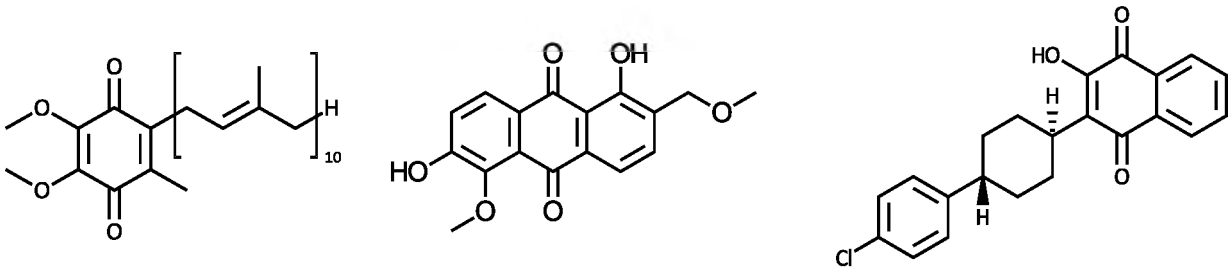

a **b (K_i = 2.07 mM)** **c (K_i = 302.37 µM)**

Figure 37: Molecular structures of (a) ubiquinone (b) compound 4 (c) atovaquone

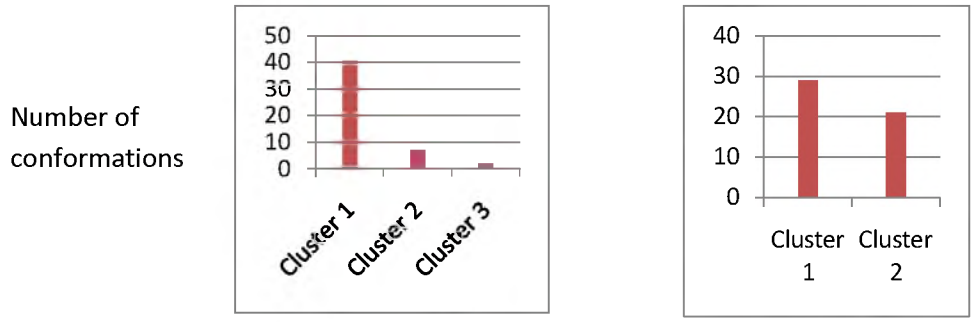

a **b**

Figure 38: Results of docking showing number of distinct conformations in 50 runs for (a) compound 4 (b) atovaquone

The docking results of compound **4** (in cytochrome bc_1) gave different comformations in three clusters from the fifty runs (**Fig. 38a**). The best docked conformation was one of the forty-one conformations in cluster one with the lowest binding energy value of -3.66 Kcal/mol and an estimated inhibition constant (K_i) of 2.07 mM. The results of docked atovaquone gave two clusters (**Fig. 38b**). The best conformation was one of the twenty-nine conformations which had the lowest binding energy of -4.80 Kcal/mol and a K_i value of 302.37 µM. Ubiquinone gave forty-nine distinct conformational clusters with the lowest binding energy value of +644. 34 Kcal/mol. The docking results indicate that compound **4**,

just like atovaquone, can bind within the active site of the protein (**Figures 39 and 40**). The resolution for protein in all docking experiments was 2.00 Å.

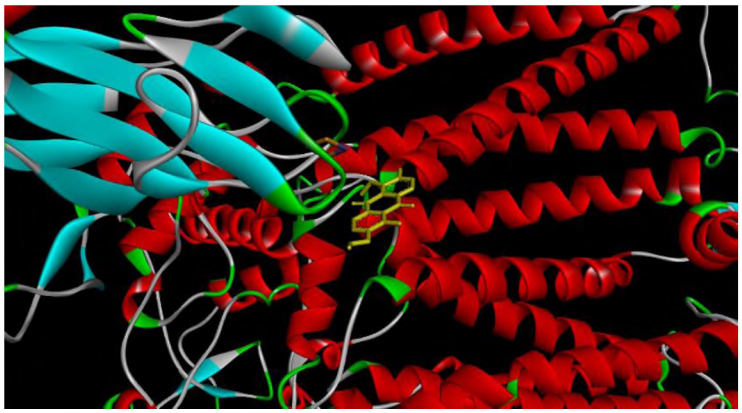

Figure 39: **The structure of compound 4 (the stick model in green) in the binding pocket of cytochrome bc1**

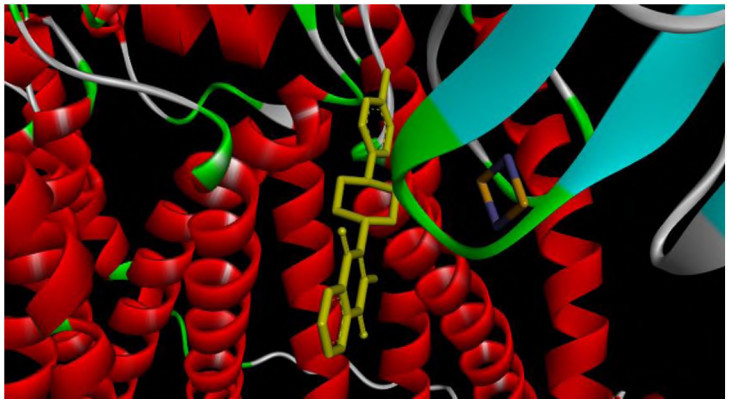

Figure 40: **The structure of atovaquone (the stick model in green) in the binding pocket of cytochrome bc1**

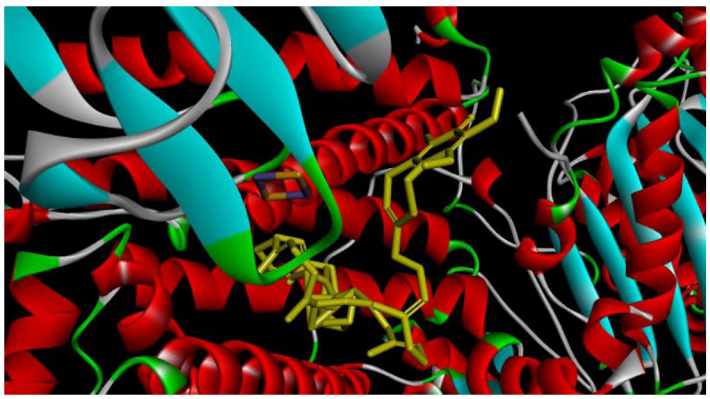

Figure 41: **The structure of ubiquinone (the stick model in green) in the binding pocket of cytochrome bc1**

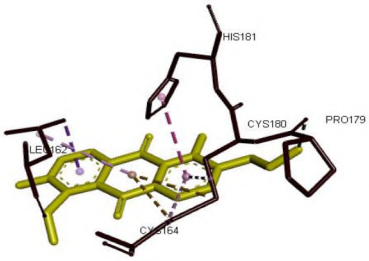

Figure 42: **The structure of compound 4 (in green) in the binding pocket of cytochrome bc1 showing its interactions with amino acid residues of protein. The hydrogen bonds are indicated using broken lines.**

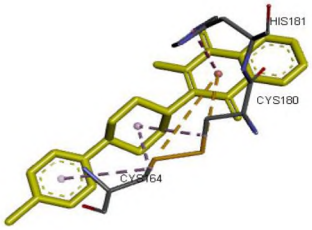

Figure 43: **The structure of atovaquone (in green) in the binding pocket of cytochrome bc1 showing its interactions with amino acid residues of protein. The hydrogen bonds are indicated using broken lines.**

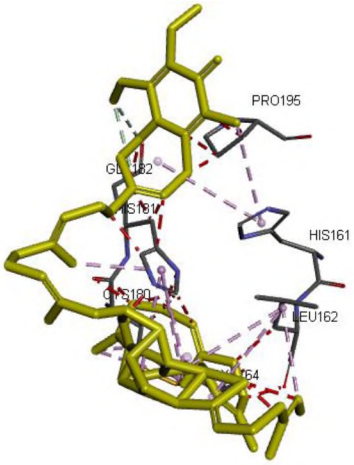

Figure 44: **The structure of ubiquinone (in green) in the binding pocket of cytochrome bc1 showing its interactions with amino acid residues of protein. The hydrogen bonds are indicated using broken lines.**

Figures 39, **40** and **41** show the conformations of the ligands with the lowest binding energy within the binding pocket of the protein. The interactions of the ligands with protein residues are displayed in **Figures 42, 43** and **44**. Both of these compounds formed a hydrogen bond with amino acid His181 of the Rieske iron-sulfur protein (section 1.4, **Fig. 9**) as reported by Kessl et al (2007).

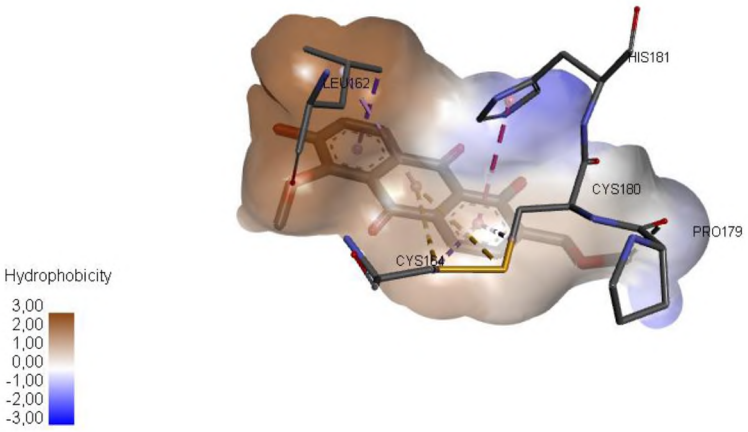

Figure 45: **The structure of compound 4 in the binding pocket of cytochrome bc1 displaying the hydrophobic state of the receptor surface.**

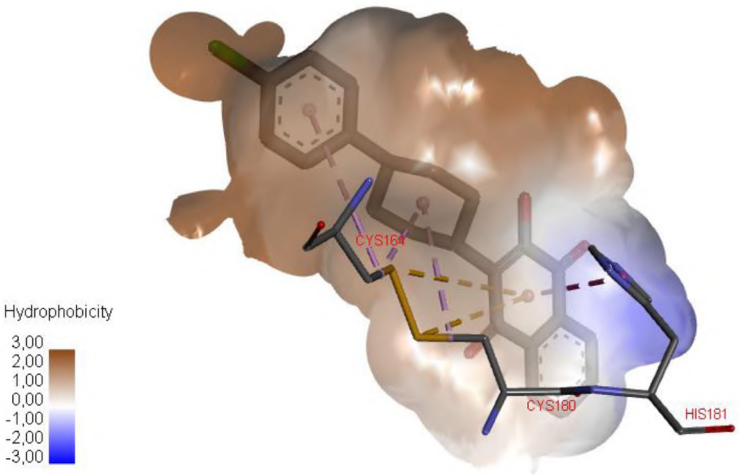

Figure 46: **The structure of atovaquone in the binding pocket of cytochrome bc1 displaying the hydrophobic state of the receptor surface.**

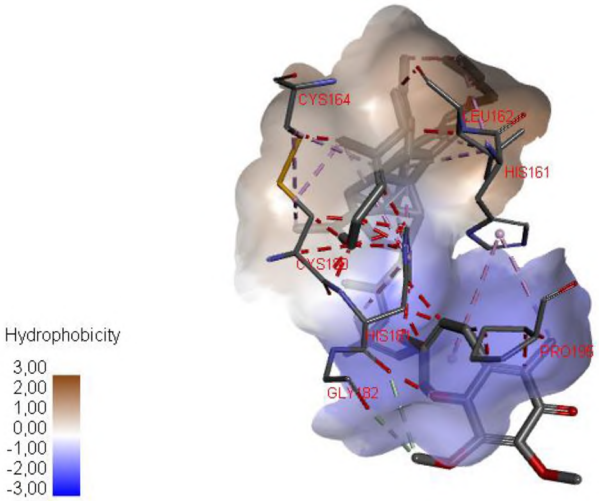

Figure 47: The structure of ubiquinone in the binding pocket of cytochrome bc1 displaying the hydrophobic state of the receptor surface.

Compound **4** showed little activity against *P. falcipalum* using the *in vitro* antimalarial assay. Since compound **4** can bind within the active site of the target molecule, modifying its structure could improve its activity. Docking studies help with identifying parts of the ligand that need to be modified (Pinheiro et al, 2003). For example, **Figures 45**, **46** and **47** show how the different ligands change the surface of the protein. Nearly three quarters of atovaquone induces a hydrophobic property on the receptor's surface. The cause of this effect by atovaquone could be investigated and applied on the drug being designed, for example compound **4**, so that the changes would help the designed drug to improve its binding ability.

This was rigid docking which did not take into account the environment surrounding the target molecule within the pathogen. The interactions observed between the ligands and the protein in the model might not be the same as in flexible docking as well as *in vivo* or *in vitro* experiments. This can be seen from the results of docking ubiquinone to cytochrome bc_1. The lowest binding energy for this docking experiment was +644.34 Kcal/mol, a large amount compared to -3.66 Kcal/mol (for ML4) and -4.80 Kcal/mol (for atovaquone) and yet, in nature, a compound similar to this one is able to function properly.

4. CONCLUSION

The main objective of this study was to assess the antimalarial activity of the crude extract, fractions and isolated compounds of *M. lucida* as well as to characterise and identify the isolated compounds.

The following compounds, comprising of two iridoids (asperuloside and asperulosidic acid), five terpenoids (stigmasterol, β-sitosterol, campesterol, lanosterol and / or cycloartenol) and three anthraquinones [5,15-O-dimethylmorindol, 1,7-dihydroxy-2-methoxy-5-(methoxymethyl)anthraquinone and 1,6-dihydroxy-2-methoxy-5-(methoxymethyl) anthraquinone] were isolated and characterised using spectroscopic techniques of FT-IR, ^{1}H, ^{13}C, DEPT-135, HMBC, HSQC, COSY, NOESY and HR-ESI-MS. All of the compounds have been isolated from different plants before with the exception of 1,7-dihydroxy-2-methoxy-5-(methoxymethyl)anthraquinone and 1,6-dihydroxy-2-methoxy-5-(methoxymethyl) anthraquinone which were tentatively assigned their structures due to insufficient data. To the best of our knowledge, this is the first report on the identification of all of the mentioned compounds, with the exception of stigmasterol and β-sitosterol, from *M. lucida*.

Molecular docking was performed on one of the isolated anthraquinones (5,15-O-dimethylmorindol) to check if it can bind to cytochrome bc_1, a known target for atovaquone. This compound interacted with the same amino acids including His181 of the Rieske iron-sulfur protein as atovaquone, a well known antimalarial agent, interacted with on cytochrome bc_1 indicating a possible similar mode of action. The lowest binding energy for atovaquone was -4.80 Kcal/mol whereas that of 5,15-O-dimethylmorindol was -3.66 Kcal/mol.

The crude extract of *Morinda lucida* suppressed the growth of *Plasmodium falciparum* by 100 % where as some fractions reduced the malaria parasite viability by approximately 50 % at 100 µg/mL. Cell viability for the crude extract in the cell toxicity assay remained at 100 %. An IC_{50} done on the crude sample gave a value of 25 µg/mL. Each of the six compounds tested had very little activity. Their activities were increased when samples of the different compounds were mixed. One of these mixtures (which had 16 µL of 20 µM asperulosidic

acid and 8 µL of 20 µM of sample containing the terpenoids as well as 8 µL of 20 µM of each of compounds 4, 5 and 6) reduced malaria viability to about 22 % at 20 µM and gave an IC_{50} value of 17 µM. Antibacterial assays were also carried out on the crude extract and some fractions. Fractions 2 and 3, the first two fractions obtained from the crude extract, were relatively active (MIC values ranging between 125-1000 µg/mL) against *M. cattarhalis* and *E. faecalis*. Fraction 2 was also the most active on *S. typhimurium* and *S. aureus* (MIC value of 1000 µg/mL) compared with the other fractions. This same fraction also showed some activity against *M. tuberculosis* with MIC_{90} and MIC_{99} values of 40.9 and 46.3 µg/mL respectively in a GPF assay.

This study confirms the ethnomedicinal use of *M. lucida* for the treatment of malaria. More studies need to be done to extract, isolate and investigate the compounds that are responsible for the antimalarial properties of this plant as well as to find out if synergism plays a role in the antimalarial activity of the isolated compounds. Synergetic antimalarials are in great need these times when monotherapy is quickly being overtaken by parasite resistance to drugs.

5. REFERENCES

Abraham, D.J.; Rotella, D.P. (Ed). (2010). Burger's Medicinal Chemistry, Drug Discovery and Development, Vol.7. pp. 603, John Wiley & Sons, Inc.,Publication.

Abrahams, G.L.; Kumar, A.; Savvi, S.; Hung, A.W.; Wen, S.; Abell, C.; Barry, C.E. 3rd; Sherman, D.R.; Boshoff, H.I, Mizrahi, V. (2012). Pathway-selective sensitization of *Mycobacterium tuberculosis* for target-based whole-cell screening. Chemistry and Biology, Vol. 19 (7), pp. 844–854 . doi: 10.1016/j.chembiol.2012.05.020.

Adesoga, E. K. (1973). Anthraquinones and anthraquinols from *Morinda lucida*. Tetrahedron, Vol. 29, pp. 4099–4102.

Adesogan, E. K. (1979). Oruwacin, a new iridoid ferulate from *Morinda lucida*. Phytochemistry, Vol. 18, pp. 175–176.

Adeyemi, T. O. A.; Ogboru, R. O.; Idowu, O. D.; Owoeye, E. A.; Isese, M. O. (2014). Phytochemical screening and health potentials of *Morinda lucida Benth*. International Journal of Innovation and Scientific Research, Vol. 11, pp. 515–519.

Adomi, P. O.; Umukoro, G. E. (2010). Antibacterila activity of aqueous and ethanol crude extracts of the root barks of *Alstonia boonei* and preliminary phytochemical test of *Morinda lucida*. Journal of Medicinal Plants Research, Vol. 4 (8), pp. 644–648.

Addy, B. S.; Owodo, H. T.; Gyapong, R. N. K.; Umeji, C. O.; Mintah, D. N. (2013). Phytochemical Screening and Antimicrobial Study on the leaves of *Morinda lucida* (Rubiaceae). Journal of Natural Sciences Research, Vol. 3 (14), pp. 131–136.

Ashafa, A. O. T.; Olunu, O. O. (2011). Toxicological evaluation of ethanolic root extract of *Morinda lucids* (*L.*) Benth. (Rubiaceae) in male Wistar rats. Journal of Natural Pharmaceuticals, Vol. 2 (2), pp. 108–114.

Askal, H. F.; Khedr, A. S.; Darwish, I. A.; Mahmoud, R. M. (2008). Quantitative thin-layer chromatographic method for determination of amantadine hydrochloride. International journal of biomedical science; Volume 4(2), pp. 155–160.

Baggish, A. L.; Hill, D. R. (2002). Antiparasitic agent atovaquone. Antimicrobial Agents and Chemotherapy, Vol. 46 (5), pp. 1163–1173.

Balogun, E. A.; Akinloye, D. I. (2011). Biochemical effects of methanolic extract of *Morinda*

morindoides and *Morinda lucida* leaves on lipid profile, bilirubin and some marker enzymes. Asian Journal of Medicinal Research, Vol. 1 (1), pp. 12–16.

Bello, I. S.; Oduola, T.; Adeosun, O. G.; Omisore, N. O. A.; Raheem, G. O.; Ademosun, A. A. (2009). Evaluation of antimalarial activity of various fractions of *Morinda lucida* leaf extract and *Alstonia boonei* stem bark. Global Journal of Pharmacology, Vol. 3 (3), pp. 163–165.

Boonphong, S.; Pvangsombat, S.; Baramee, A.; Mahidol, C.; Ruchirawat, S.; Kittakoop, P. (2007). Bioactive compounds from *Bauhinia purpurea* possessing antimalarial, antimycobacterial, antifungal, anti-inflammatory and cytotoxic acticities. Journal of Natural Products, Vol. 70, pp795–801.

Briggs, L. H.; Cain, B. F.; Le Quesne, P. W. (1963). The structure of asperuloside. Tetrahedron Letters, Vol. 2, pp. 69–74.

Busari, M. B.; Ogbadoyi, E. O.; Karibu, A. Y.; Sani, S. (2014). Trypanocidal properties of aqueous leaf extract of *Morinda lucida*. Asian Journal of Biological Sciences, Vol. 7 (6), pp. 262–269.

Careri, M.; Elviri, L.; Mangia, A. (2001). Liquid chromatography – UV determination and liquid chromatography – atmospheric pressure chemical ionisation mass spectrometric characterisation of sitosterol and stigmasterol in soybean oil. Journal of Chromatography A, Vol. 935 (2001), pp. 249–257.

Chaturvedula, V. S. P; Prakash, I. (2012). Isolation of stigmasterol and β-sitosterol from the dichloromethane extract of Rubus suavissimus. International Current Pharmaceutical Journal, Vol. 1 (9), pp. 239–242.

Chukwuemeka, I. M.; Udeozo, I. P.; Odo, M. C.; Oraekwute, E. E.; Ugwu, O. P. C. (2013). Phytochemical analysis of crude ethanol leaf extract of *Morinda lucida*. International Journal of Research and Reviews in Pharmacy and Applied Science, Vol. 3 (4), pp. 470–475.

Collins, L. A.; Torrero, M. N.; Franzblau, S. G. (1998). Green fluorescent protein reporter microplate assay for high-throughput screening of compounds against *Mycobacterium tuberculosis*. Antimicrobial Agents and Chemotherapy, Vol. 42, 344–347.

Cooksey, R.; Crawford, J. T.; Jacobs, W. R.; Shinnick, T. M. (1993). A Rapid method for

screening antimicrobial agents for activities against a strain of *Mycobacterium tuberculosis* expressing firefly luciferase. Antimicrobial Agents and Chemotherapy, Vol. 37 (6), p. 1348–1352.

Corey, E. J.; Matsuda, S. P. T.; Bartel, B. (1993). Isolation of an *Arabidopsis thaliana* gene encoding cycloartenol synthase by functional expression in a yeast mutant lacking lanosterol synthase by the use of a chromatographic screen. Proc. Natl. Acad. Sci., USA, 90, 11628–11632.

Cos, P.; Vlietinck, A. J.; Berghe, D. V.; Maes, L. (2006). Anti-infective potential of natural products: How to develop a stronger in vitro 'proof-of-concept'. Journal of Ethnopharmacology, Vol. 179, pp. 76–82.

Dan, N.; Bhakat, S. (2015). New paradigm of an old target: An update on structural biology and current progress in drug design towards plasmepsin II. European Journal of Medicinal Chemistry, Vol. 95, pp. 324–348.

de Andrade-Neto, V. F.; Goulart, M. O. F.; da Silva Filho, J. F.; da Silva, M. J.; do Carmo F. R. Pinto, M.; Pinto, A. V.; Zalis, M. G.; Carvalho, L. H.; Krettli, A. U. (2004). Antimalarial activity of phenazines from lapachol, b-lapachone and its derivatives against *Plasmodium falciparum in vitro* and *Plasmodium berghei in vivo*. Bioorganic & Medicinal Chemistry Letters, Vol 14, pp. 1145–1149.

Demirezer, L. Ö.; Gürbüz, F.; Güvenal, Z.; Ströch, K.; Zeeck, A. (2006). Iridoids, Flavonoids and Monoterpene Glycosides from *Galium verum* subsp. *Verum.* Turk J. Chem. Vol. 30: 525–534.

De Voss, J.J.; Rutter, K.; Schroeder, B.G.; Su, H.; Zhu, Y.; Barry, C.E. (2000). The salicylate-derived mycobactin siderophores of *Mycobacterium tuberculosis* are essential for growth in macrophages. 3rd. *Proc Natl Acad Sci U.S A*. Vol. 97 (3), 1252–1257.

Dewick, P. M. (2002). Medicinal natural products, a biosynthetic approach. 2nd Ed., John Wiley & Sons, Ltd. West Sussex, United Kingdom.

Dike, P. I.; Olawole, O. O.; Adebiyi, E. F. (2012). Ethnobotanical survey for potential antimalarial plants in South-Western Nigeria. Journal of Ethnopharmacology, Vol. 144, pp. 618–626.

Dinio, T.; Gorka, A. P.; McGinniss, a.; Roepe, P. D.; Morgan, J. B. (2012). Investigating the

activity of quinine analogues vs. chloroquine resistant *Plasmodium falciparum*. Bioorg Med Chem., Vol. 20 (10), pp. 3292–3297.

Edeoga, H. O.; Okwu, D. E.; Mbaebie, B. O. (2005). Phytochemical constituents of some Nigerian medicinal plants. African Journal of Biotechnology, Vol. 4 (7), pp. 685–688.

El-Naggar, L.; Beal, J. L. (1980). Iridoids. A review. Journal of Natural Products, Vol. 43 (6), pp. 649–707.

Eloff, J. N. (1998). A sensitive and quick microplate method to determine the minimal inhibitory concentration of plant extracts for bacteria. Planta Medica, Vol. 64, pp. 711–713.

Ettari, r.; Bova, F., Zappala, M.; Grasso, S.; Micale, N. (2010). Falcipain-2 inhibitors. Medicinal Research Review, 30 (1), 136–167.

Evans, W. C. (2002). Trease and Evans Pharmacognosy. 15th Ed., SAUNDERS, Elsevier Ltd.

Fogel, G. B.; Cheung, M.; Pittman, E.; Hecht, D. (2008). In silico screening against wild-type and mutant *Plasmodium falciparum* dihydrofolate reductase. Journal of Molecular Graphics and Modelling, Vol. 26, pp. 1145–1152.

Ginsburg, H.; Famin, O.; Zhang, J.; Krugliak, M. (1998). Inhibition of glutathione-dependent degradation of **heme** by chloroquine and amodiaquine as a possible basis for their antimalarial mode of action. Biochemical Pharmacology, Vol. 56, pp. 1305–1313.

Glasby, J. S. (1982). Encyclopaedia of the terpenoids. John Wiley and Sons Ltd., Vol. 1 and 2.

Gorgoi, J.; Nakhuru, K. S.; Policegoudra, R. S.; Chattopadhyay, P.; Rai, A. K.; Veer, V. (2014). Isolation and characterisation of bioactive components from *Mirabilis jalapa* L. Radix. Journal of Traditional and Complementary Medicine, Vol. Xxx, pp. 1–7.

Golenser, J.; Waknine, J. H.; Krugliak, M.; Hunt, N. H.; Grau, G. E. (2006). Current perspectives on the mechanism of action of artemisinins. International Journal of Parasitology, Vol. 36, 1427–1441.

Gomes, A.; Saha, A.; Chartterjee, I.; Chakravarty, A. K. (2007). Viper and cobra venom neutralisation by β-sitosterol and stigmasterol isolated from the root extract of *Pluchea indica* Less. (Asteraceae). Phytomedicine, Vol. 14, pp. 637–643.

Gottlieb, H. E.; Kotlyar, V.; Nudelman, A. (1997). NMR chemical shifts of common laboratory solvents as trace impurities. Journal of Organic Chemistry, Vol. 62, pp. 7512–7515.

Hellmann, J. K.; Münter, S.; Wink, M.; Frischknecht, F. (2010). Synergistic and additive

effects of epigallocatechin gallate and digitonin on *Plasmodium* sporozoite survival and motility. Plos One, Vol. 5 (1), pp. 1–7.

Hirata, T.; Kobayashi, T.; Wada, A.; Ueda, T.; Fujikawa, T.; Miyashita, H.; Ikeda, T.; Tsukamoto, S.; Nohara, T. (2011). Anti-obesity compounds in green leaves of *Eucommia ulmoides.* Bioorganic & Medicinal Chemistry Letters, V0l. 21, pp. 1786–1791.

Hrycyna, C. A.; Summers, R. L.; Lehane, A. M.; Pires, M. M.; Namanja, H.; Bohn, K.; Kuriakose, J.; Ferdig, M.; Henrich, P. P.; Fidock, D. A.; Kirk, K.; Chmielewski, J.; Martin, R. E. (2014). Quinine dimmers are potent inhibitors of the *Plasmodium falciparum* chloroquine resistance trancporter and are active against quinoline-resistant *P. falciparum*. ACS Chemical Biology, Vol. 9, pp. 722–730.

http://database.prota.org/PROTAhtml/Morindalucida_En.htm, 13 / 04 / 2015

Hunte, C; Koepke, J; Lange, C; Roßmanith, T; Michel, H. (2000). Structure at 2.3 Å resolution of the cytochrome *bc*1 complex from the yeast *Saccharomyces cerevisiae* co-crystallized with an antibody Fv fragment. Structure, Vol. 8 (6), pp. 669–684.

Ishak, N.; Yazan, L. S.; Lajis, N. H. (2010). Nordamnacanthal induced apoptosis and mitotic-G2/M arrest with downregulation of BCL-2 in the human breast cancer cell line (MCF-7). Medical Health Science Journal, Vol. 2, pp. 27–38.

Iwu, M. M. (2014). Handbook of African medicinal plants. 2nd Ed., CRC Press, Tailor and Francis group, FL, U.S.

Kamboj, A.; Saluja, A. K. (2011). Isolation of stigmasterol and β-sitosterol from petroleum ether extract of aerial parts of *Ageratum conyzoides* (Asteraceae). International Journal of Pharmacy and Pharmaceutical Sciences, Vol. 3 (1), pp. 94–96.

Kamiya, K.; Tanaka, Y.; Endang, H.; Umar, M.; Sakate, T. (2005). New Anthraquinone and Iridoid from the Fruits of *Morinda citrifolia.* Chemical and Pharmaceutical Bulletin, Vol. 53(12), pp. 1597–1599.

Kazeem, M. I.; Adamson, O. J.; Ogunwande, I. A. (2013). Modes of inhibition of α-amylase and α-glucosidase by aqueous extract of *Morinda lucida Benth* leaf. Biomedical Research International, Vol. 2013, 6 pages.

Kessl, J. J.; Meshnick, S. R.; Trumpower, B. L. (2007). Modeling the molecular basis of

atovaquone resistance in parasites and pathogenic fungi. Trends in Parasitology, Vol. 23 (10), pp. 494–501.

Keusch, G. T.; Jacewicz, M.; Hirschman, S. Z. (1972). Quantitative microassay in cell culture for enterotoxin of *Shigella dysenteriae*. Journal of Infectious Diseases, Vol. 125, pp. 539–541.

Kolesnikova, M.; Xiong, Q.; Lodeiro, S.; Hua, L.; Matsuda, S. (2006). Lanosterol biosynthesis in plants. Archives of Biochemistry and Biophysics, Vol. 447, pp. 87–95.

Koumaglo, K.; Gbeassor, M.; Nikabu, O.; de Souza, C.; Werner, W. (1992). Effects of three compounds extracted from *Morinda lucida* on on *Plasmodium falciparum.* Planta Medica, Vol. 58 (6), pp. 533–534.

Krishna, S.; Uhlemann, A.; Haynes, R. K. (2004). Artemisinins: mechanisms of action and potential for resistance. Drug Resistance Updates, Vol. 7, pp. 233–244.

Kumar, A.; Paliwal, D.; Saini,D.; Thakur, A; Aggarwal, S.; Kaushik, D. (2014). A comprehensive review on synthetic approach for antimalarial agents. European Journal of Medicinal Chemistry, Vol., 85, pp. 147–178.

Kuwayama, K.; Tsujikawa, K.; Muyaguchi, H.; Kanamori, T.; Iwata-Togawa, Y.; Inoue, H.; Kishi, T.; Tsunoda, N. (2005). Effects of the various preparation procedures of Dragendorff reagent on sensitivity for thin layer chromatography. National Research Institute of Police Science, Vol. 10 (2), pp. 127–133.

Lampman, G. M.; Pavia, D. L.; Kriz, G. S.; Vyvyan, J. R. (2010). Spectroscopy, 4th Ed. Brooks/Cole Cengage Learning.

Lawal, H. O.; Etatuvie, S. O.; Fawehinmi, A. B. (2012). Ethnomedicinal and Pharmacological properties of *Morinda lucida*. Journal of Natural products, Vol. 5, pp. 93–99.

Luhata, L. P.; Munkombwe, N. M. (2015). Isolation and characterisation of stigmasterol and β-sitosterol from *Odontonema strictum* (Acanthaceae). Journal of Innovations in Pharmaceuticals and Biological Sciences, 2(1), 88–95.

Mahato, S. B.; Kundu, A. P. (1994). ^{13}C NMR spectra of pentacyclic triterpernoids – A compilation and some salient features. Phytochemistry, Vol. 37 (6), pp. 1517–1775.

Makler, M. T.; Ries, J. M.; Williams, J. A.; Bancroft, J. E.; Piper, R. C.; Gibbins, B. L.; Hinrichs,

D. J. (1993). Parasite lactate dehydrogenase an assay for *Plasmodium falciparum* drug sensitivity. American Journal of Tropical Medicine and Hygiene, Vol. 48 (6), pp. 739–741.

Manguin, S.; Bangs, M. J.; Pothikasikorn, J.; Chareonviriyaphap, T. (2010). Review on global co-transmission of human *Plasmodium* species and *Wuchereria bancrofti* by Anopheles mosquitoes. Infection, Genetics and Evolution, Vol., 10, pp. 159–177.

Meshnick, S. R. (2002). Artemesinin: mechanisms of action, resistance and toxicity. International Journal of Parasitology, Vol. 32, pp. 1655–1660.

Mir, M. A.; sawhney, S. S.; Jassal, M. M. S. (2013). Qualitative and quantitative analysis of phytochemicals of Taraxacum officinale. Wudpecker Journal of Pharmacy and Pharmacology, Vol. 2 (1), pp. 001–005.

Muthas, D.; Nöteberg, D.; Sabnis, Y. A.; Hamelink, E.; Vrang, L.; Samuelsson, B.; Karlén, A.; Hallberg, A. (2005). Synthesis, biological evaluation, and modelling studies of inhibitors aimed at the malarial proteases plasmepsin I and II. Bioorganic and Medicinal Chemistry, Vol. 13, pp. 5371–5390.

Noedl, H.; Wongsrichanalai, C.; Wernsdorfer, W. H. (2003). Malaria drug-sensitivity testing: new ways, new perspectives. Elsevier, **TRENDS** in Parasitology, Vol. 19 (4).

Nweze, N. E. (2012). *In vitro* anti-trypanosomal activity of *Morinda lucida* leaves. African Journal of Biotechnology, Vol. 11 (7), pp. 1812–1817.

Oduola, T.; Bello, I.; Adeosun, G.; Ademosun, A.; Raheem, G.; Avwioro, G. (2010). Hepatotoxicity and nephrotoxocity evaluation in Wistar albino rats exposed to *Morinda lucida* leaf extract. North American Journal of Medical Sciences, Vol. 2 (5), pp. 230–233.

Odutunga, A. A.; Dairo, J. O.; Minari, J. B.; Bamisaye, F. A. (2010). Anti-diabetic effect of *Morinda lucida* stem bark extracts on alloxan-induced diabetic rats. Research Journal of Pharmacology, Vol. 4 (30, pp. 78–82.

Ogunlana, O. E.; Farombi, O. E. (2008). *Morinda lucida*: Antioxidant and reducing activities of crude methanolic stem bark extract. Advances in Natural and Applied Sciences, Vol. 2(2), pp. 49–54.

Ohyama, K.; Suzuki, M.; Kikuchi, J.; Saito, K.; Muranaka, T. (2009). Dual biosynthetic

pathways to phytosterol via cycloartenol and lanosterol in *Arabidopsis*. PNAS, Vol. 106 (3), pp. 725–730.

Olasehinde, G. I.; Ojurongbe, O.; Adeyeba, A. O.; Fagade, O. E.; Valecha, N.; Ayanda, I. O.; Ajayi, A. A.; Egwari, L. (2014). *In vitro* studies on the sensitivity pattern of *Plasmodium falcipurum* to antimalarial drugs and local herbal extracts. Malaria Journal, Vol. 13 (63), pp 1–7.

Ollinger, J., Bailey, M. A., Moraski, G. C., Casey, A., Florio, S., Alling, T., Miller, M. J., Parish, T. (2013). A dual read-out assay to evaluate the potency of compounds active against *Mycobacterium tuberculosis*. PloS one, Vol. 8 (4), pp 1–9.

Olumayokun, A.; Olajide, s.; Awe, O.; Makinde, M. (1999). Evaluation of the anti-diabetic property of *Morinda lucida* leaves in streptozotonic-diabetic rats. Journal of Pharmacy and Pharmacology, Vol. 51, pp. 1321–1324.

Owolabi, M. S.; Padilla-Camberos, E.; Ogundajo, A. L.; Ogunwande, I. A.; Flamini, G.; Yusuff, O. K.; Allen, K.; Flores-Fernandez, K. I.; Flores-Fernandez, J. M. (2014). Insecticidal activity and chemical composition of the *Morinda lucida* essential oil against pulse beetle *Callosobruchus maculates.* The Scientific World Journal, Vol. 2014, Article ID 784613, 7 pages.

Patra, A.; Jha, S.; Murthy, P. N.; Manik; Sharone, A. (2010). Isolation and characterisation of stigmast-5-en-3β-ol (β-sitosterol) from the leaves of *Hygrophila spinosa* T. Anders. International Journal of Pharma Sciences and Research, 1(2), 95–100.

Pauli, G. F.; Case, R. J.; Inui, T; Wang, Y.; Cho, S.; Fischer, N. H.; Franzblau, S. G. (2005). New perspectives on natural products in TB drug research. Life Sciences, Vol. 78, pp. 485–494.

Perez-Sacau, E.; Esteves-Braun, A.; Ravelo, A. G.; Yapu, D. G.; Turba, A. G. (2005). Antiplasmodial activity of naphthoquinones related to lapachol and ƃ-lapachone. Chemistry and Diversity, Vol. 2, pp. 264–274.

Pinheiro, J. C.; Kiralji, R.; Ferreira, M. M. C. (2003). Artemisinin derivatives with antimalarial activity against *Plasmodium falciparum* designed with the aid of quantum chemical and partial least squares methods. QSAR & Combinatorial Science, Vol. 22, pp. 830–842.

Pretsch, E.; Seibl, J.; Simon, W.; Clerc, T. (1989). Tables of Spectral data for structure

determination of organic compounds, 2nd Ed., Springer-Verlag, Berlin Heidelberg.

Rasoanaivo, P.; Wright, C. W.; Willcox, M. L.; Gilbert, B. (2011). Whole plant extracts versus single compounds for the treatment of malaria: synergy and positive interactions. Malaria Journal, Vol. 10 (Suppl 1):S4.

Rath, G.; Ndozao, M.; Hostettmann, K. (1995). Antifungal anthraquinones from *Morinda lucida*. Pharmaceutical Biology, Vol. 33, (2), pp. 107–114.

Robert, A.; Dechy-Cabaret, O.; Cazelles, J.; Meunier, B. (2002). From mechanistic studies on artemesinin derivatives to new modular antimalarial drugs. Acc. Chem. Res. Vol. 35, pp. 167–174.

Rosenthal, P. J. (1998). Proteases of malaria parasites: new target for chemotherapy. Emerging infectious Diseases, 4 (1), 49–57.

Rosenthal, P. J. (2004). Cystein proteases of malaria parasites. International Journal for Parasitology, Vol. 34, pp. 1489–1499.

Saikia, R.; Talukdar, A. D.; Chetia, P.; Choudhury, M. D. (2013). Preliminary phytochemical investidation and TLC profiling of ethnomedicinally important plant, *Scoparia dulcis* Linnaeus. Pleione, Vol. 7 (2), pp. 366–372.

Sanchez, C. P.; Stein, W. D.; Lanzer, M. (2008). Dissecting the components of quinine accumulation in *Plasmodium falciparum*. Molecular Microbiology, Vol. 67 (5), pp. 1081–1093.

Santos, C. B. R.; Vieira, J. B.; Lobato, C. C.; Hage – Melim, L. I. S.; Souto, R. N. P.; Lima, C. S.; Costa, E. V. M.; Brasil, D. S. B.; Maĉedo, W. J.; Carvalho, J. C. T. (2014). A SAR and QSAR study of new artemisinin compounds with antimalarial activity. Molecules, Vol. 19, pp. 367–399.

Schripsema, J.; Dagnino, D. (1996). Elucidation of the substitution pattern of 9, 10 – anthraquinones through the chemical shifts of peri-hydroxyl protons. Phytochemistry, Vol. 42 (1), pp. 177–184.

Shandilya, A.; Chacko, S.; Jayaram, B.; Ghosh, I. (2013). A plausible mechanism for the antimalarial activity of artemisinin: a computational approach. Scientific Reports, Vol. 3, 2513.

Sharma, R. K.; Younis, Y.; Mugumbate, G.; Njoroge, M.; Gut, J.; Rosenthal, P. J.; Chibale, K.

(2015). Synthesis and structure-activity-relationship studies of thiazolidinediones as antiplasmodial inhibitors of the *Plasmodium falciparum* cystein protease falcipaine-2. European Journal of Medicinal Chemistry, Vol. 90, pp. 507–518.

Siwe Noundou, X. (2012). Isolation and identification of anti-cancer compounds from Alchornear species and their encapsulation into nanostructured drug delivery systems. PhD (Chemistry). [Unpublished]: University of Johannesburg. https://ujdig.space.uj.ac.za (27/11/2015).

Subramani, T.; Yeap, S. K.; Ho, W. Y.; Ho, C. L.; Osman, C. P.; Ismail, N. H.; Afizan, N. M.; Rahman, N. A.; Alitheen, N. B. (2015). Nordamnacanthal potentiates the cytotoxic effects of tamoxifen in human breast cancer cells. Oncology Letters, Vol. 9, pp. 335–340.

Sudhanshu Saxena; Pant, N.; Jain, D.C.; Bhakuni, R. S. (2003). Antimalarial agents from plant sources. Current Science, Vol. 85 (9), pp. 1314–1329.

Suzuki, M.; Xiang, T.; Ohyam, K.; Seki, H.; Saito, K.; Muranaka, T.; Hayashi, H.; Katsube, Y.; Kushiro, T.; Shibuya, M.; Ebizuka, Y. (2006). Lanosterol synthase in dicotyledonous plants. Plany Cell Physiology, Vol. 47 (5), pp. 565–571.

Takahiko Fujikawa et.al. (2012). Asperuloside stimulates metabolic function in rats across several organs under high-fat diet conditions, acting like the major ingredient of *Eucommia* leaves with anti-obesity activity. Journal of Nutritional Science, Vol. 1: 1–11.

Takeda, Y.; Shimidzu, H.; Mizuno, K.; Inouchi, S.; Masuda, T.; Hirata, E.; Shizanto, T.; Aramoto, M.; Otsuka, H. (2002). An Iridoid Glucoside Dimer and a non-glycosidic Iridoid from the leaves of *Lasianthus wallichii*. Chem. Pharm. Bull. 50(10) 1395–1397.

The Collaborative Drug Discovery database. (2016). (Burlingame, C. A. www.collaborativedrug.com).

Titanji, V.; Zofou,; Ngemenya, M. N. (2008). Antimalarial potential of medicinal plants used for the treatment of malaria in Cameroonia folk medicine. African Journal of Traditional Complementary and Alternative Medicine, Vol. 5 (3), pp. 302–321.

Toole, G.; Toole S. (1999). Understanding Biology, 4th Ed. Stanley Thornes (Publishers) Ltd, Cheltenham, UK.

Tzakou, O; Mylonas, P.; Vagias, C.; Petrakis, P. V. (2007). Iridoid glycosides with insecticidal

activity from *Galium melanantherum*. ZnaturForsch, Vol. 62c, pp. 597–602.

Umar, M. B.; Ogbadoyi, E. O.; Ilumi, J. Y.; Salawu, O. A.; Tijani, A. Y.; Hassan, I. M. (2013). Antiplasmodial efficacy of methanolic root and leaf extracts of *Morinda lucida*. Journal of Natural Sciences Research, Vol. 3 (2), pp. 112–123.

Unekwuojo, E. G.; James, O.; Olubunmi, A. R. (2011). Suppressive, curative and prophylactic potentials of *Morinda lucida* (Benth) against erthrocytic stage of mice infective chloroquine sensitive *Plasmodium berghei* NK-65. British Journal of Applied Science & Technology, Vol.1 (3), pp. 131–140.

Van Tyne, D.; Dieye, B.; Valim, C.; Daniels, R. F.; Séne, P. D.; Lukens, A. K.; Ndiaye, M.; Bei, A. K.; Ndiaye, Y. D.; Hamilton, E. J.; Ndir, O.; Mboup, S.; Volkman, S. K.; Wirth, D. F.; Ndiaye, D. (2013). Changes in drug sensitivity and antimalarial drug resistance mutations over time among *Plasmodium falciparum* parasites in Senegal. Malaria Journal, Vol. 12 (1), 441.

Van Wyk, B; Wink, M. (2004). Medicinal plants of the World. 1st Ed., Briza Publications, Pretoria, South Africa.

Viljoen, A.; Mncwangi, N.; Vermaak, I. (2012). Anti-inflammatory iridoids of botanical origin. Current Medicinal Chemistry, Vol. 19, pp. 2104–2127.

Villalobos, T.; Ibarra, R. G.; Acosta, J. (2013). 2D, 3D-QSAR and molecular docking of 4(1H)-quinolones analogues with antimalarial activities. Journal of Molecular Graphics and Modelling, Vol. 46, pp. 105–124.

Vincken, J.; Heng, L.; Groot, A.; Gruppen, H. (2007). Saponins, classification and occurrence in the plant kingdom. Phytochemistry, Vol. 68, pp. 275–297.

Wang, S.; Jacobs-Lorena, M. (2013). Genetic approaches to interfere with malaria transmission by vector mosquitoes. Trends in Biotechnology, Vol. 31, pp. 185–193.

Wankhar, W.; Srinivasan, S.; Rajan, R.; Rathinasamy, S. (2015). Phytochemicals screening and antimicrobial efficacy of *Scoparia dulcis Linn* (Scrophulariaceae) against clinical isolates. Journal of Pharmacognosy and Phytochemistry, Vol. 3 (6), pp. 17–21.

WHO. (2015). World Malaria Report.

Wu, Z.; Wang, J.; Fang, D.; Zhang, G. (2013). Analysis of iridoid glucosides from *Paedeira scandens* using HPLC-ESI-MS/MS. Journal of Comatography B, Vol. 923-924, pp. 54–64.

Yeo, A. E. T.; Edstein, M. D.; Rieckmann, K. H. (1997). Antimalarial activity of the triple combination of proguanil, atovaquone and dapsone. Acta Tropica, Vol. 67, pp. 207–214.

Yisa, J. (2009). Phytochemical analysis and antimicrobial activity of *Scoparia dulcis* and *Nymphaea lotus*. Australian Journal of Basic and Applied Sciences, Vol. 3 (4), pp. 3975–3979.

6. APPENDICES

Appendix 1: Table showing different plants with antimalarial properties

Scienctific and family names of plant (common names included in some cases)	Plant parts used	Active chemicals	Other uses of plant	References
Artemisia annua; *Asteraceae*	Aerial parts	Artemisinin; sesquiterpene lactone	Traditional tonic; febrifuge; antibiotic	Van Wyk et al, 2004
Azadirachta indica; *Meliaceae* (neem)	Leaves, stem bark and roots	Nimbin; nimbidin; nimbinin desacetylnimbin; salannolide (meliacin); nortriterpenoids; flavonoids	Anti-inflammatory; antipyretic	Iwu, 2014
Bauhinia acuminate, *B. purpurea* and *B. rufescens; Leguminosae*	Leaves, stem bark, roots	Flavonoids; terpenoids; phenolic compounds	Stomach disorders; skin diseases	Iwu, 2014; Boonphong et al, 2007
Carica papaya L.; *Caricaceae* (papaya)	Leaves, fruit	Alkaloids (carpaine, isocarpaine, dihydrocarpaine I and II)	Ringworms; hypertension; anthelmintic	Dike et al, 2012; Iwu, 2014
Cinchona pubescens; *Rubiaceae*	Bark	Quinoline alkaloids	Bitter tonic; antiarrhythmic	Evans, 2002; Van Wyk et al, 2004
Cryptolepsis sanguinolenta; *Apocynaceae*	Leaves, stem, roots	Quindoline alkaloid cryptolepine	Antimicrobial; hepatitis; diabetis; upper respiratory tract infection	Iwu, 2014
Diospyros abyssinica and D. Crassiflora; *Ebenaceae*	Roots, stem, aerial parts	Triterpenoids; diquinones, naphthaquinones	Dysentery; jaundice; eye inflammation	Iwu, 2014
Enantia chlorantha; Annonaceae	Stem,	Alkaloids; saponins; flavanoids	Typhoid fever; jaundice; urinary tract infection	Evans, 2002; Iwu, 2014
Liriodendron tulipifera; *Magnoliaceae*	Bark, wood	Alkaloids; lignans; monoterpenes, sesquiterpene lactones	Fever; tonic	Van Wyk et al, 2004
Magnolia grandiflora and *M. officinalis*; *Magnoliaceae*	Leaves, bark	Sesquiterpenes; alkaloids	Rheumatism; antimicrobial against amoeba parasites	Van Wyk et al, 2004
Morinda lucida; Rubiaceae	Leaves, root and stem bark	Iridoid, anthraquinones, anthraquinols	Pains, fevers, jaundice, hypertension, diabetes, dysentery	Iwu, 2014
Polyathia suaveolens; Annonaceae	Stem bark	Alkaloids e.g. isoquinolines	Blackwater fever, anthelmitic, stomach ache	Iwu, 2014
Psidium guajava; *Myrtaceae* (guava)	Leaves	Phenolic compounds (tannins, flavonoids); essential oil; triterpenoids	Anti-diarrhoeal, anti-diabetic; source of vitamin C	Dike et al, 2012; Van Wyk et al, 2004
Sclerocarya birrea; *Anacardiaceae* (marula fruit, daniya)	Bark	Flavonoids; catechins; gallotannins	Anti-diabetic; dysentery; general tonic	Iwu, 2014
Siphonochilus aethiopicus; *Zingiberaceae* (African ginger)	Rhizomes, roots	Sesquiterpene of the furanoid type; curcumin-like compounds	Anti-inflammatory; bronchodilatory	Van Wyk et al, 2004

Appendix 2: Table of solvent systems used to elute columns of fractions

Fraction	Solvent system (ration used)								
2a	Pure hexane	Hexane /EtOAc 3:2	Hexane /EtOAc 2:3	Hexane /EtOAc 1:4	Hexane /EtOAc 1:5	Hexane /EtOAc 1:9	Hexane /EtOAc 1:10	Pure EtOAc	EtOAc /MeOH 20:1
2b	Pure hexane	Hexane /EtOAc 8:1	DCM /MeOH 30:1						
2c	Pure hexane	Hexane /EtOAc 15:1	Hexane /EtOAc 12:1	Hexane /EtOAc 10:1	Hexane /EtOAc 8:1	Hexane /EtOAc 5:1	Hexane /EtOAc 3:1		
3	Pure PE	PE /EtOAc 9:1	PE /EtOAc 4:1	PE /EtOAc 3:1	PE /EtOAc 2:1	PE /EtOAc 1:1	PE /EtOAc 1:2	PE /EtOAc 1:3	EtOAc /MeOH 20:1
4	Pure hexane	Hexane /EtOAc 15:1	Hexane /EtOAc 12:1	Hexane /EtOAc 10:1	Hexane /EtOAc 8:1	Hexane /EtOAc 6:1	Hexane /EtOAc 5:1	Hexane /EtOAc 3:1	Pure EtOAc
5a	Pure hexane	Hexane /EtOAc 15:1	Hexane /EtOAc 12:1	Hexane /EtOAc 10:1	Hexane /EtOAc 8:1	Hexane /EtOAc 5:1	Hexane /EtOAc 1:1	Pure EtOAc	EtOAc /MeOH 20:1
5b	Pure EtOAc	EtOAc /MeOH 10:1	EtOAc /MeOH 10:2	EtOAc /MeOH 10:4	EtOAc /MeOH 10:5	EtOAc /MeOH 10:6	EtOAc /MeOH 10:8	EtOAc /MeOH 1:1	
5c	Pure EtOAc	EtOAc /MeOH 100:1	EtOAc /MeOH 100:2	EtOAc /MeOH 100:3	EtOAc /MeOH 100:1				
5d	Pure DCM	DCM /MeOH (10:1)	DCM /MeOH (8:1)	DCM /MeOH (6:1)	DCM /MeOH (4:1)				

Appendix 3: Infrared Spectra

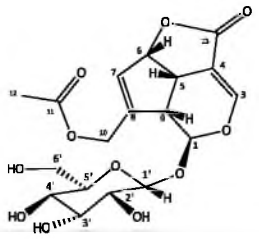

Appendix 3.1: IR of compound 1

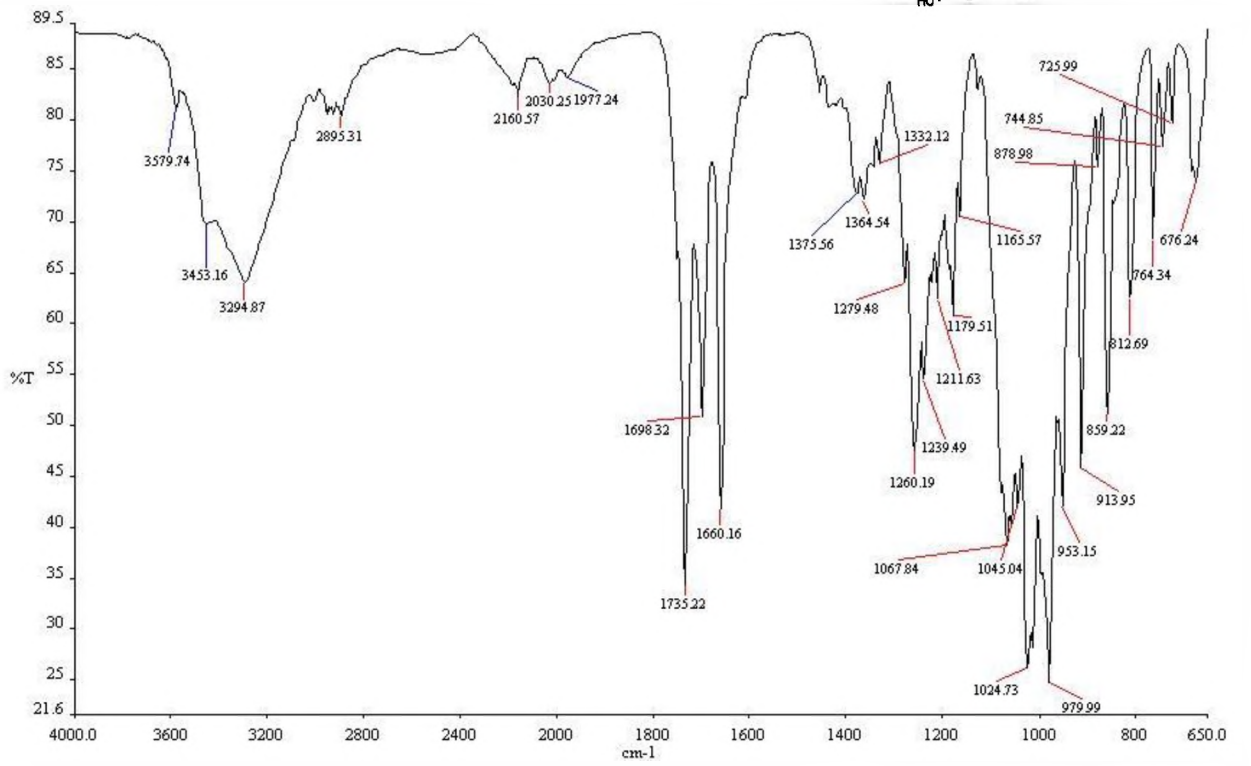

Appendix 3.2: IR of compound 2

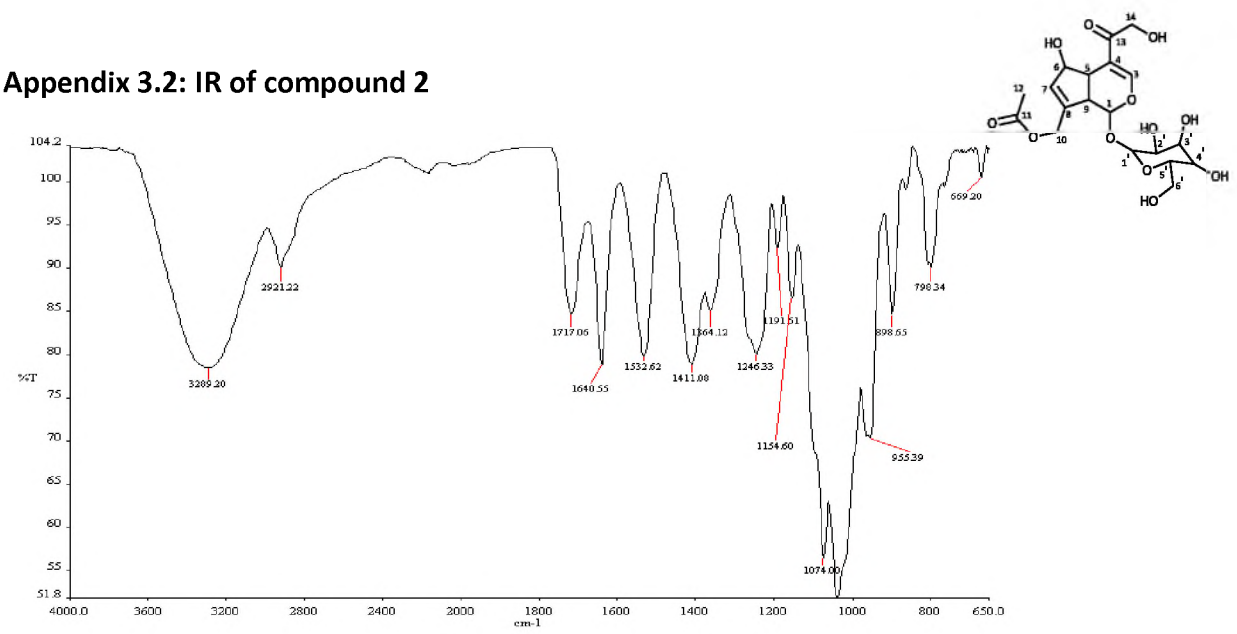

Appendix 3.3: IR of sample 3

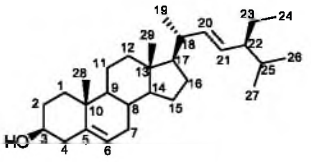

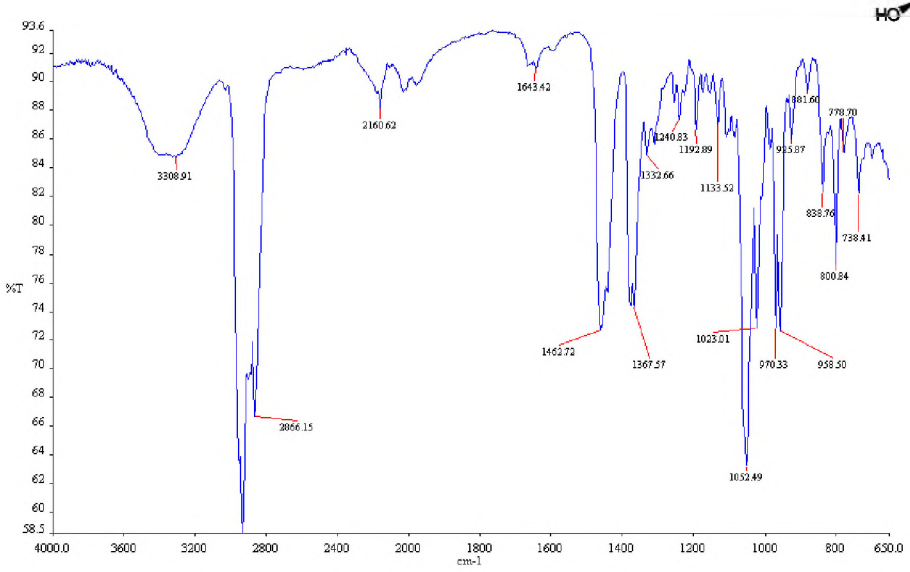

Appendix 3.4: IR of compound 4

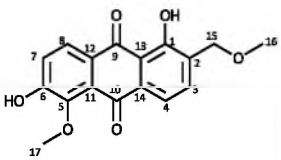

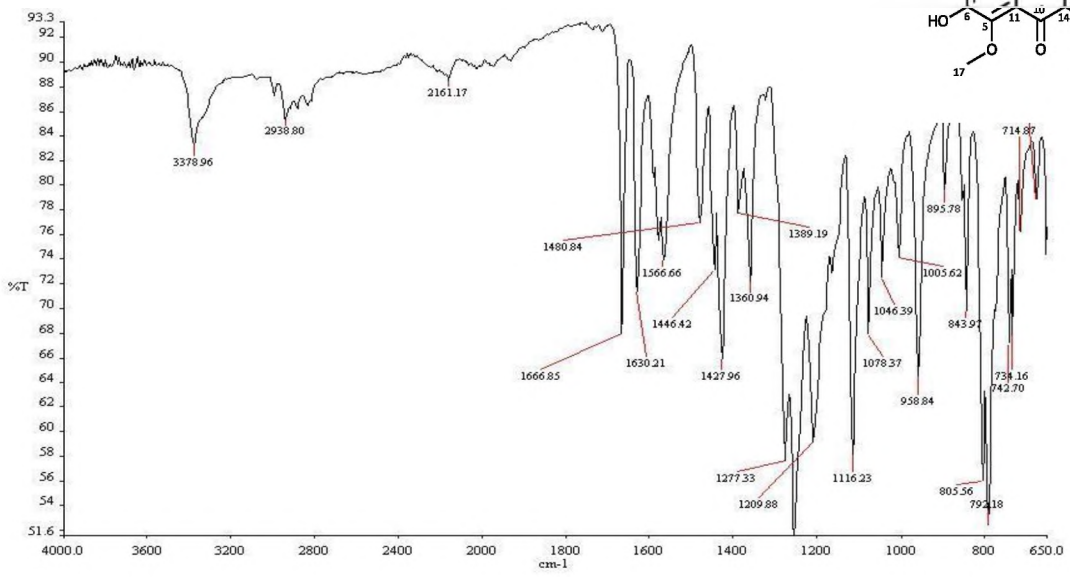

Appendix 3.5: IR of compound 5

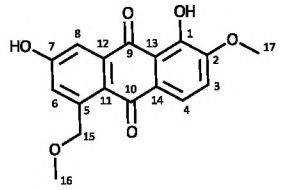

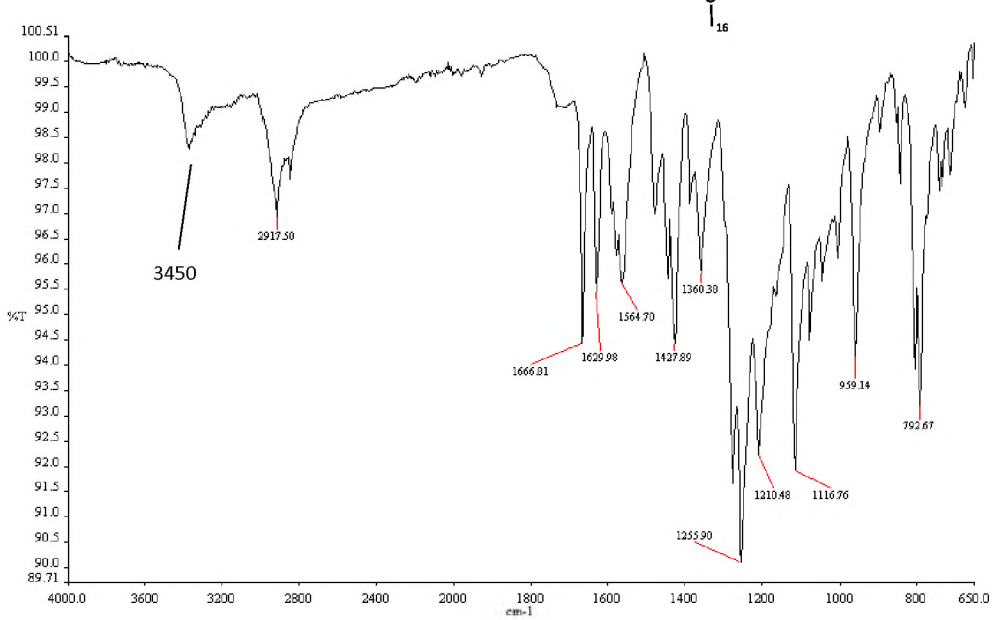

Appendix 3.6: IR of compound 6

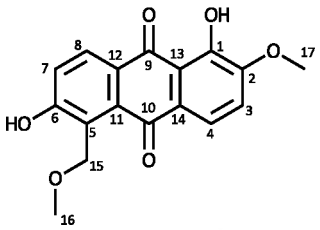

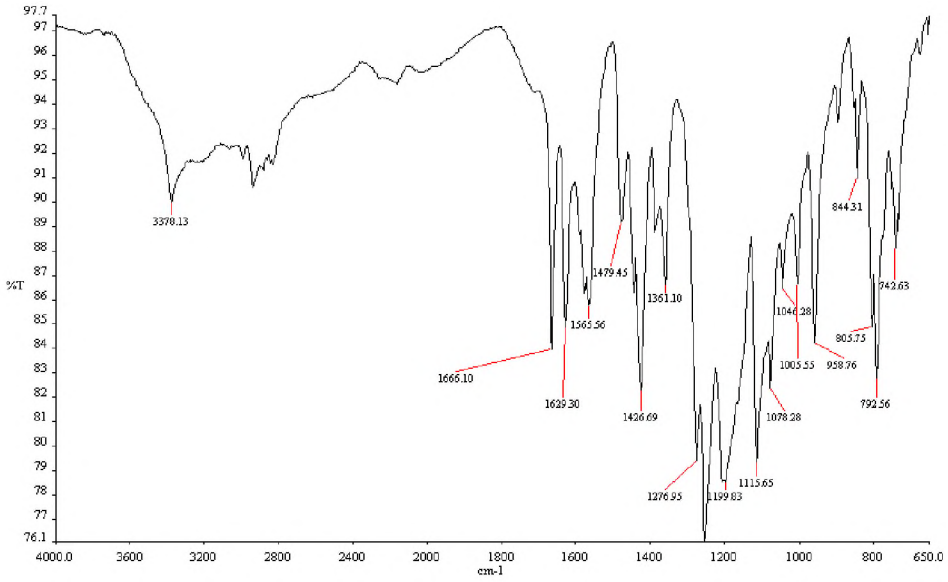

Appendix 4: Mass spectra

Appendix 4.1: MS of compound 1

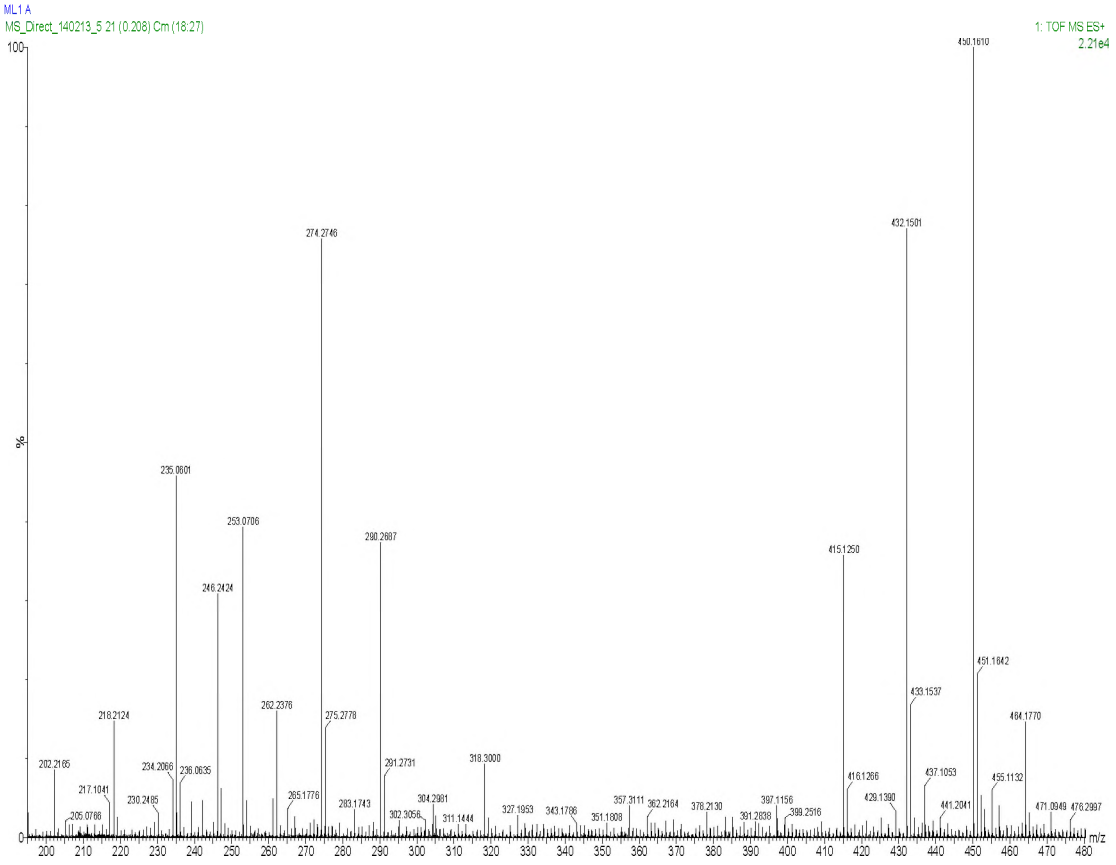

Appendix 4.2: MS of compound 2

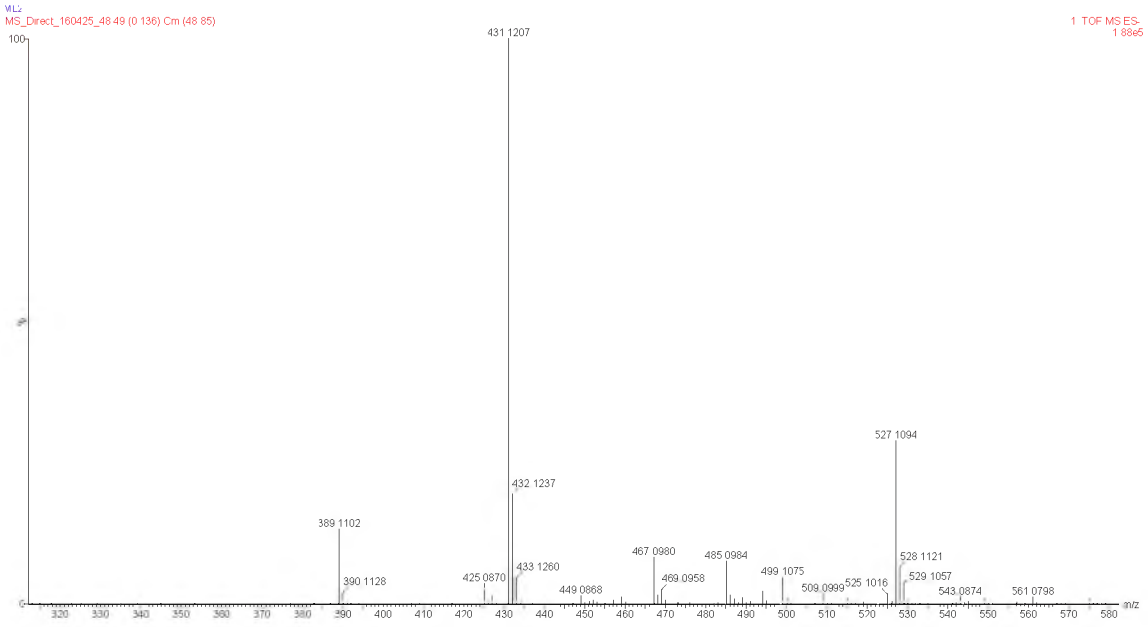

Appendix 4.3: MS of sample 3

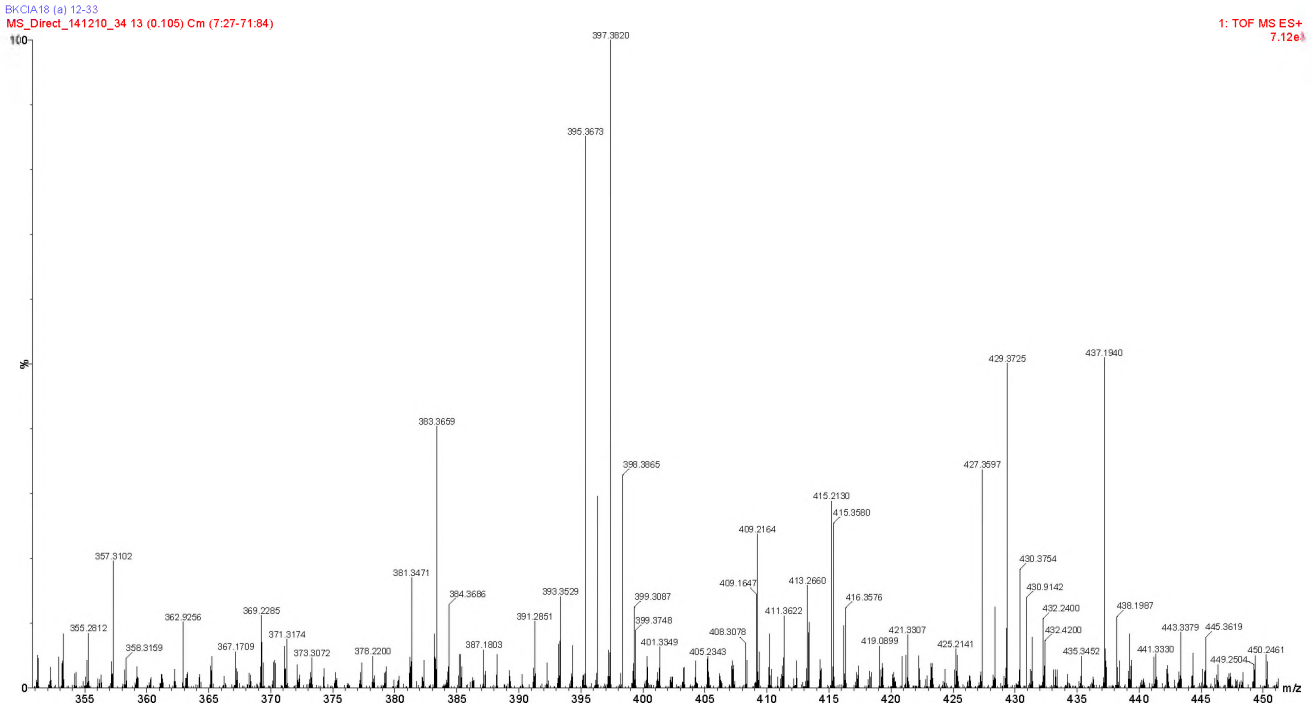

Appendix 4.4: MS of compound 4

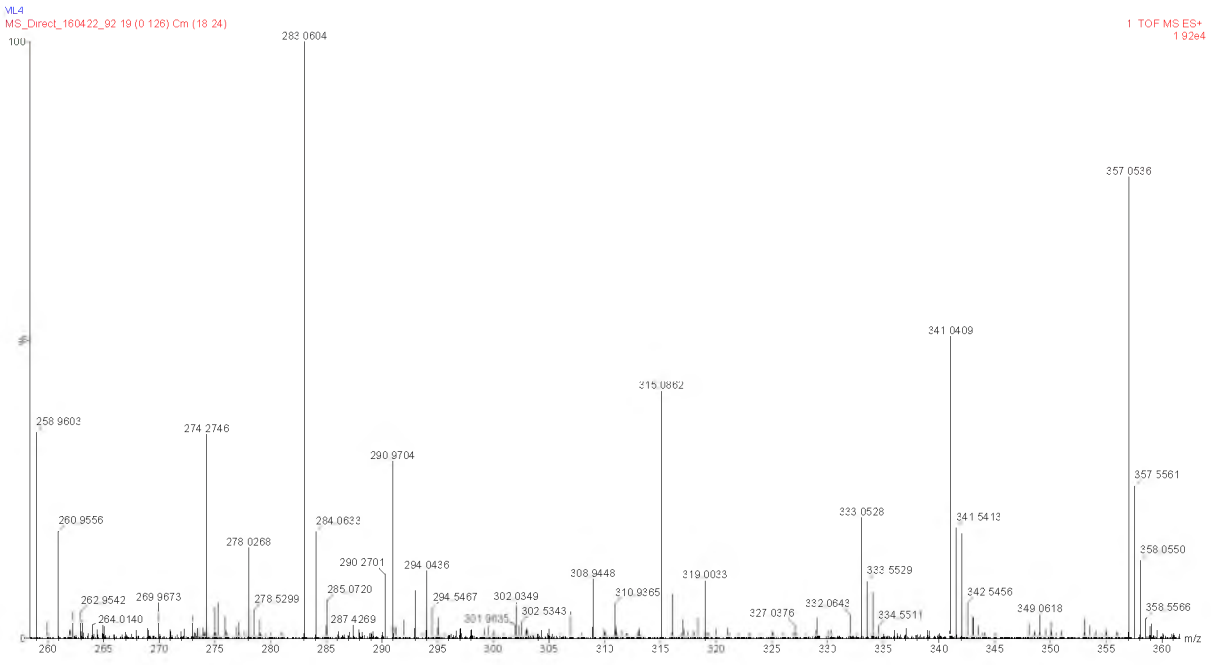

Appendix 4.5: MS of compound 5

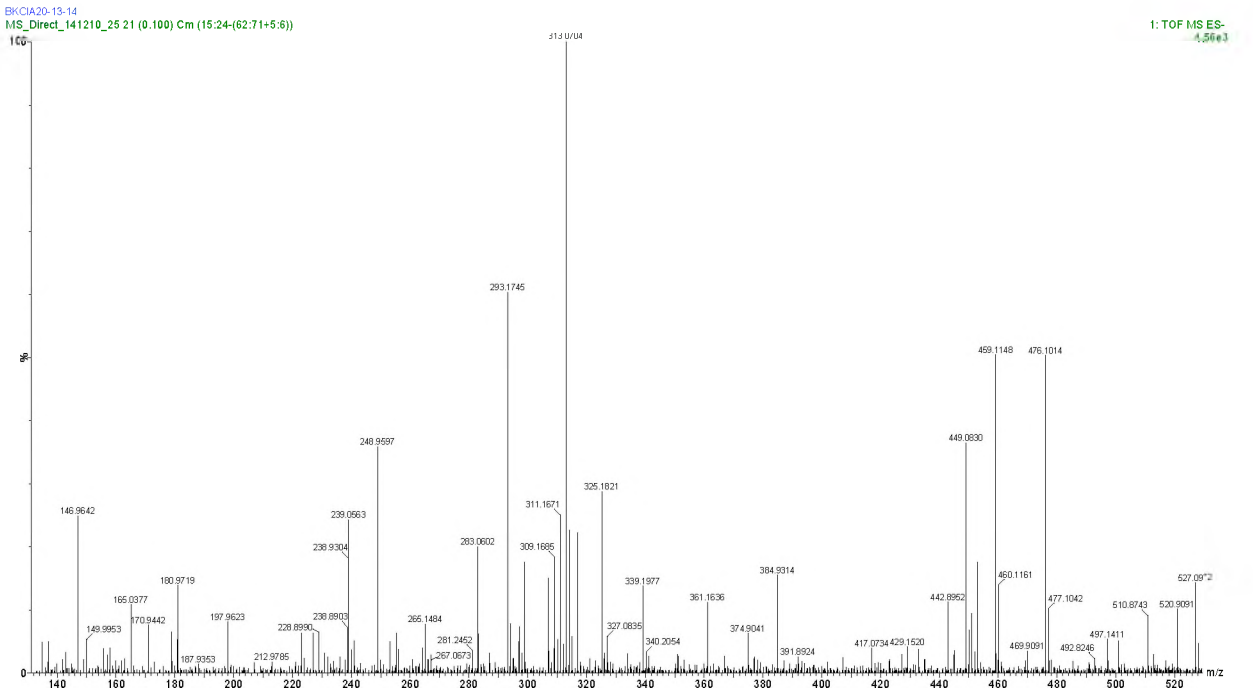

Appendix 4.6: MS of compound 6

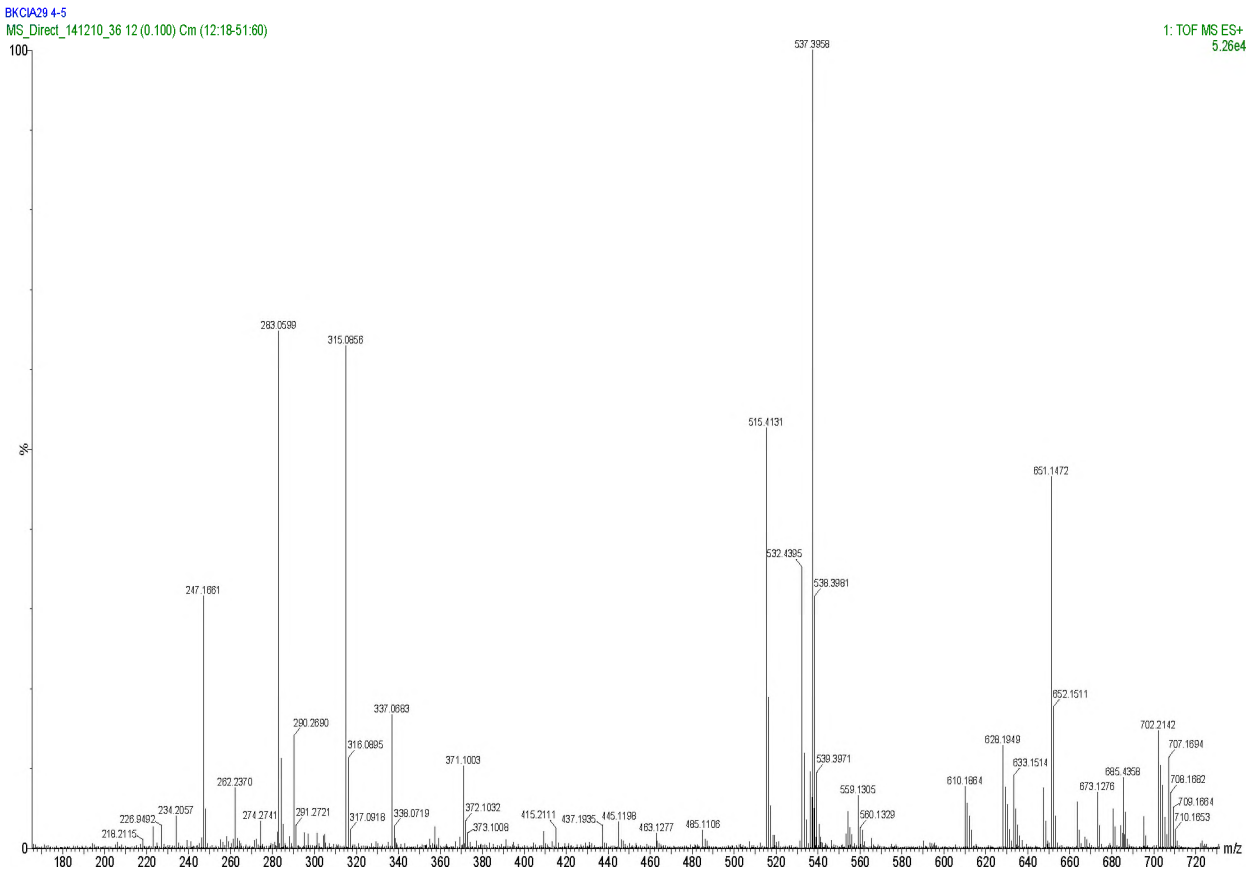

Appendix 5: Nuclear Magnetic Resonance Spectra

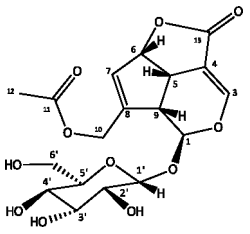

Appendix 5.1 NMR for compound 1

Appendix 5.1.1 DEPT 135 NMR for compound 1

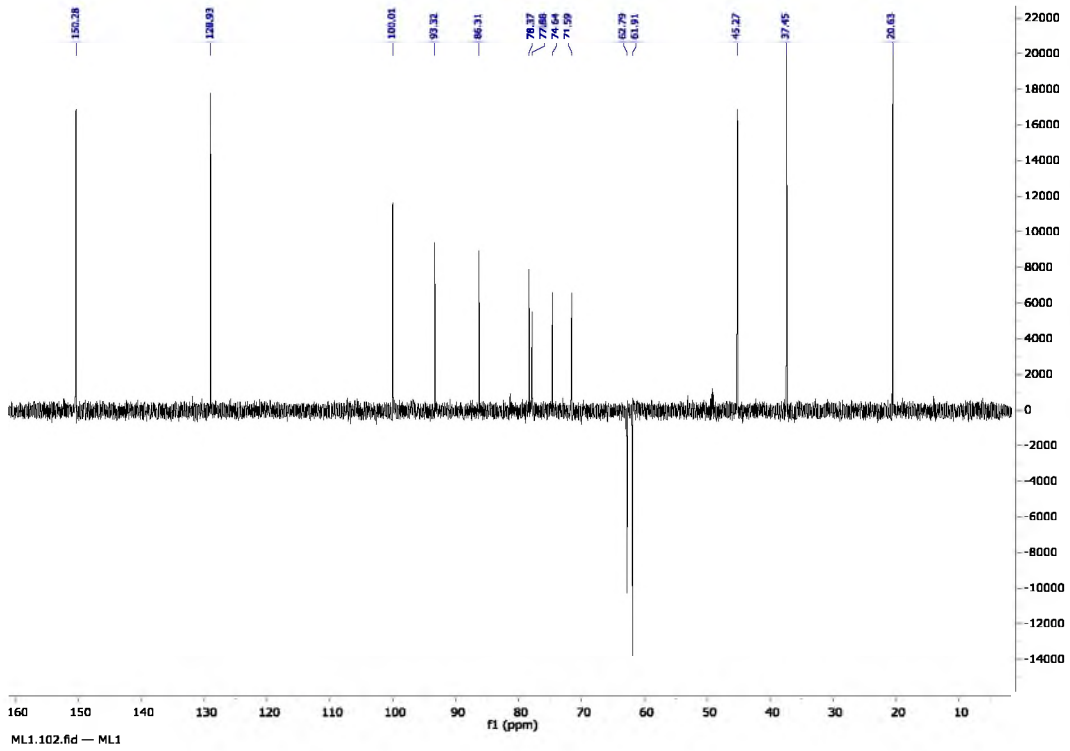

Appendix 5.1.2 ^{13}C & DEPT 135 NMR for compound 1

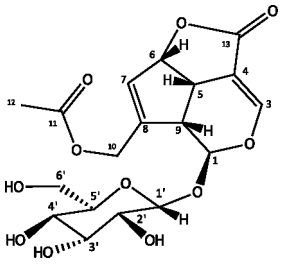

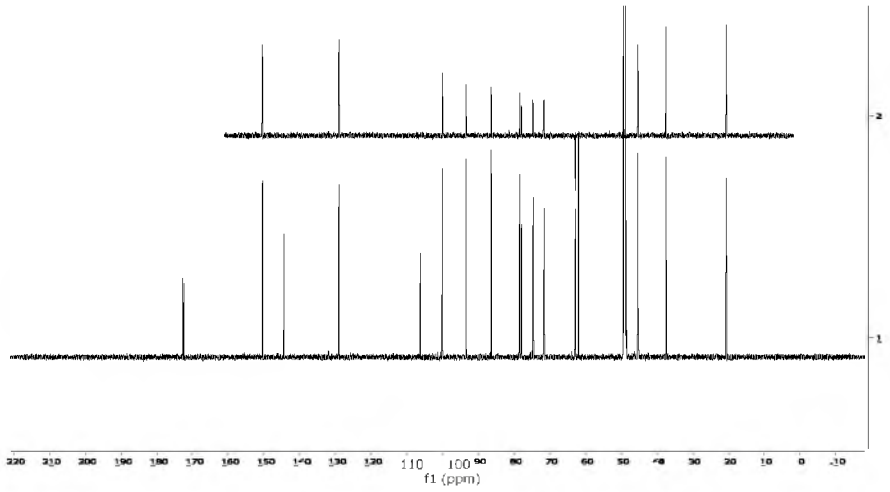

Appendix 5.1.3 COSY NMR for compound 1

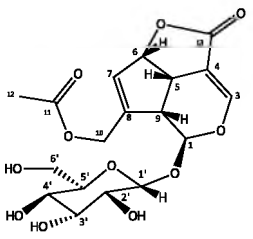

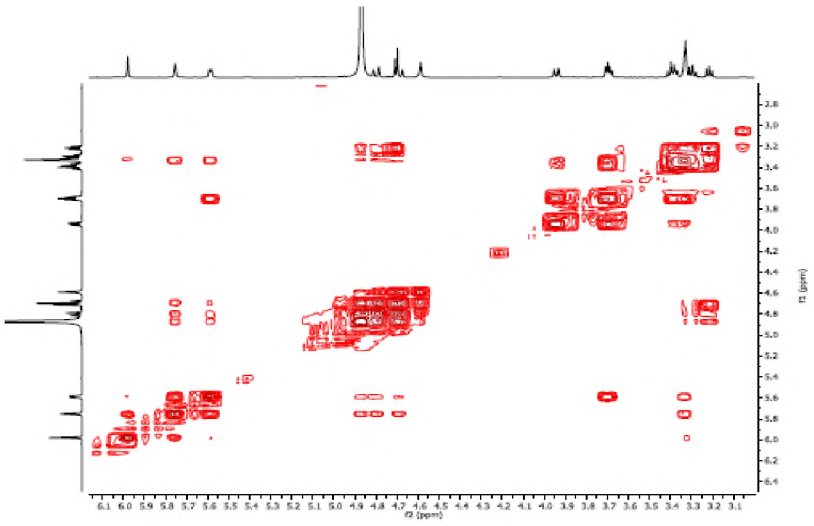

Appendix 5.1.4 HMBC NMR for compound 1

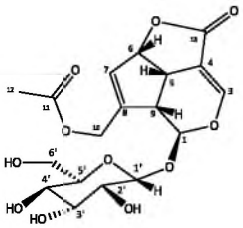

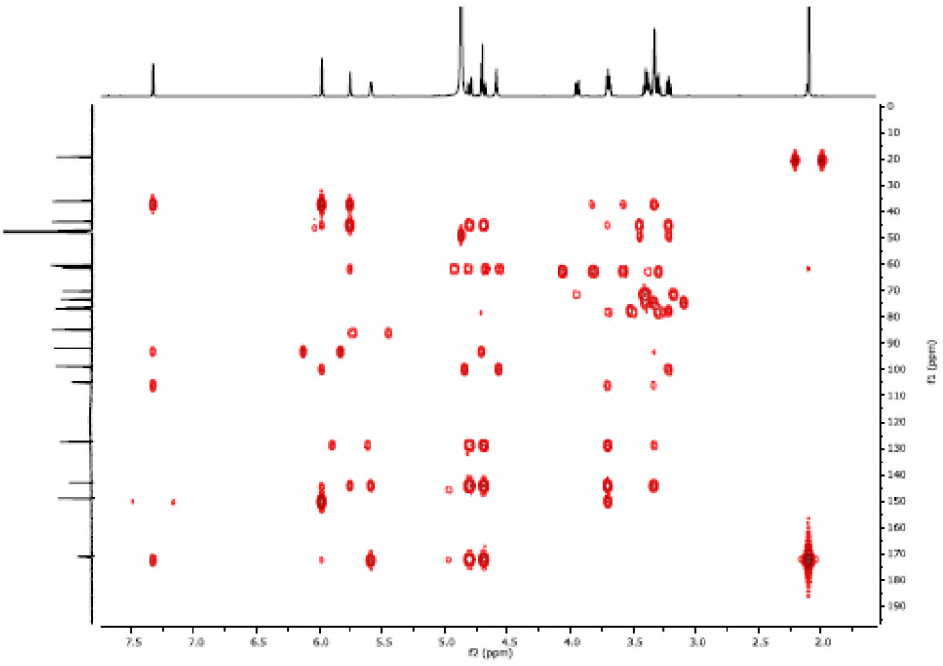

Appendix 5.1.5 HSQC NMR for compound 1

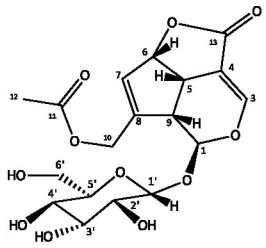

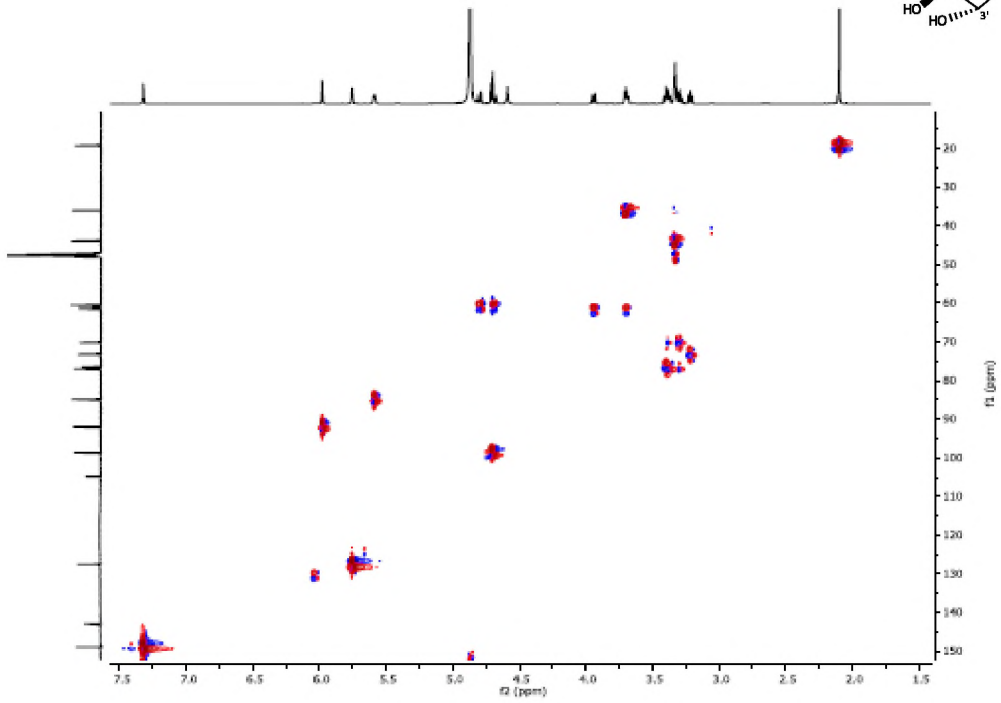

Appendix 5.1.6 NOESY NMR for compound 1

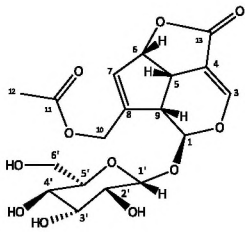

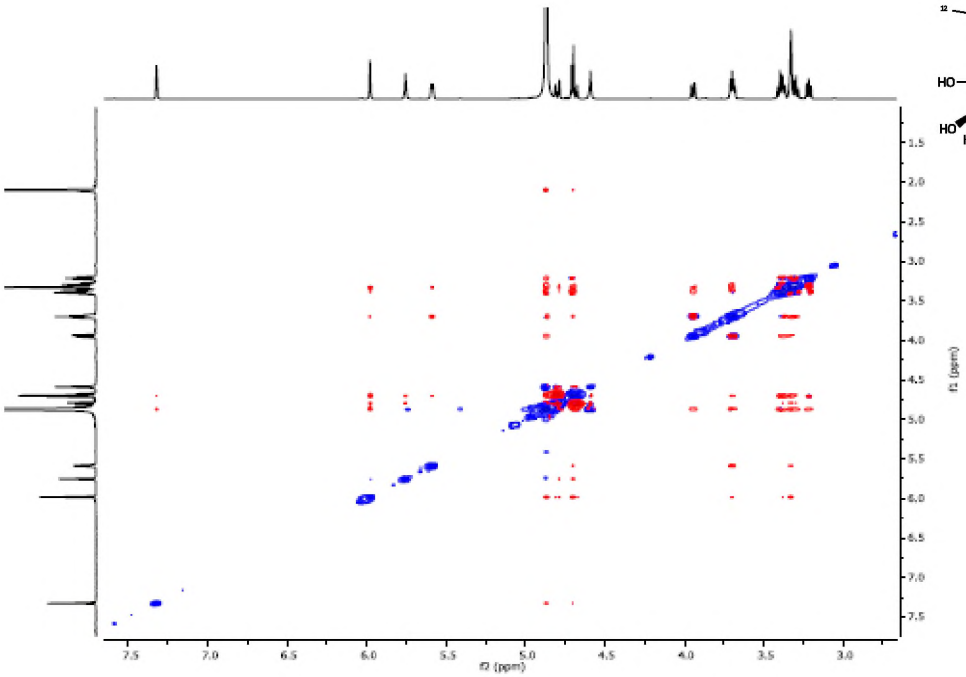

Appendix 5.2 NMR for compound 2

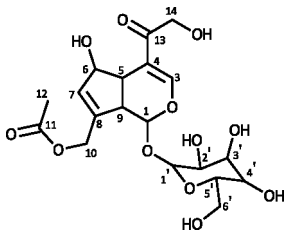

Appendix 5.2.1 DEPT 135 NMR for compound 2

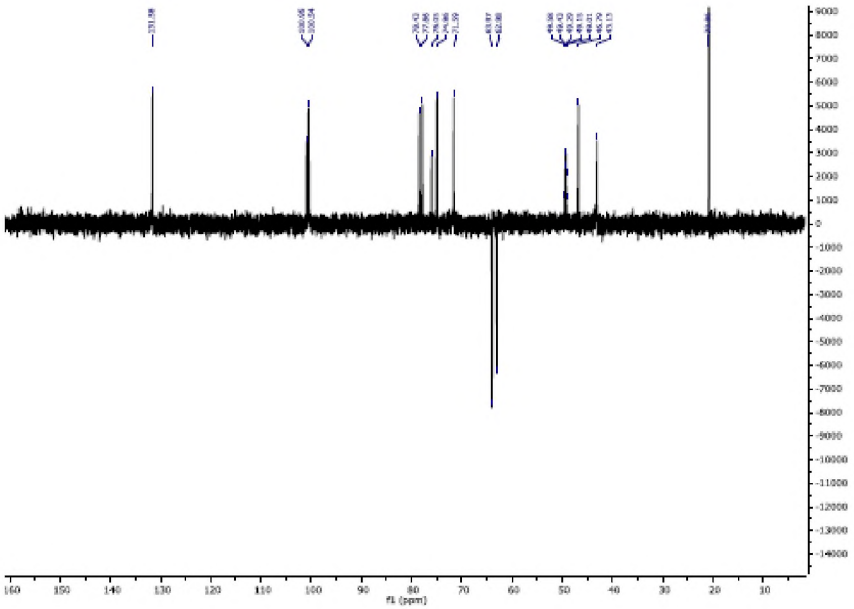

Appendix 5.2.2 ^{13}C & DEPT 135 NMR for compound 2

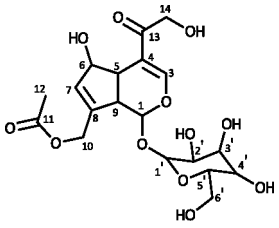

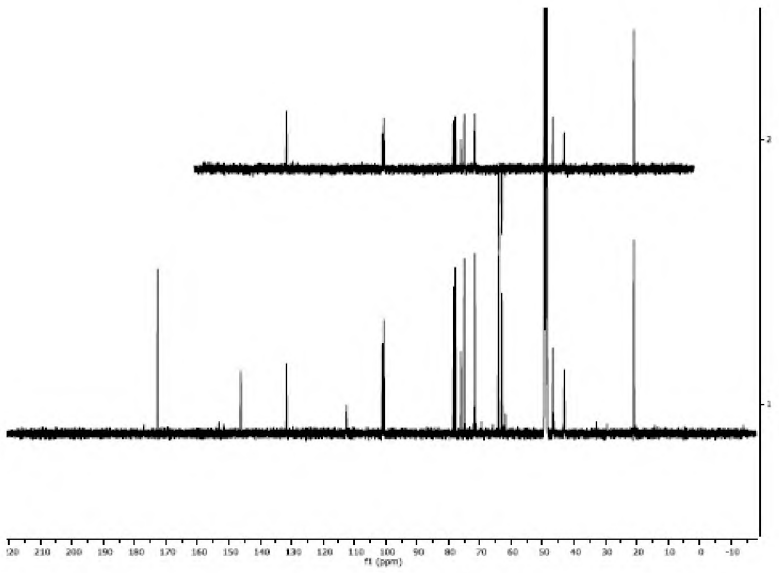

Appendix 5.2.3 **COSY NMR for compound 2**

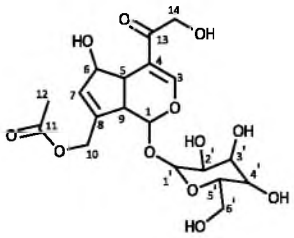

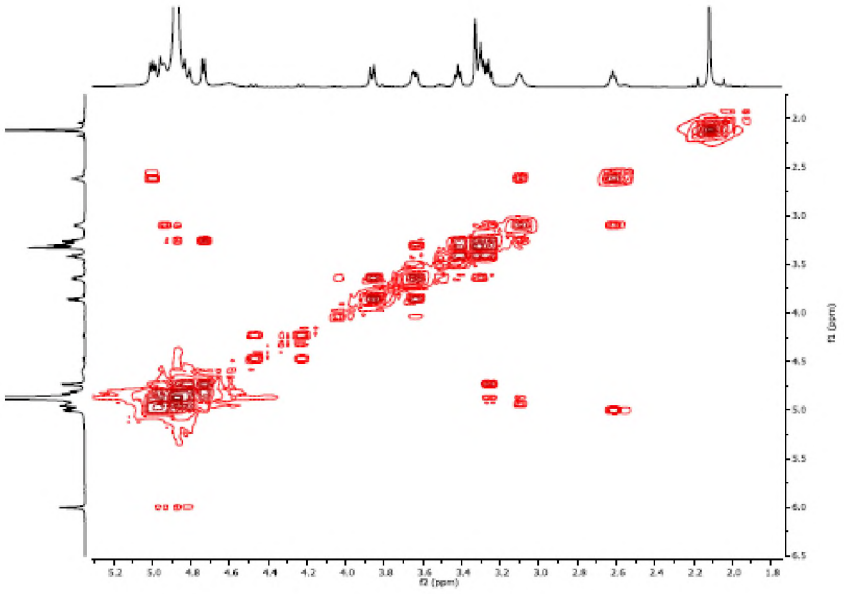

Appendix 5.2.4 **HMBC NMR for compound 2**

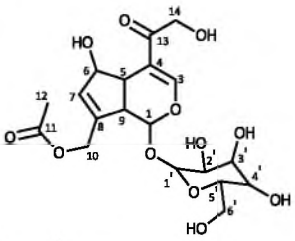

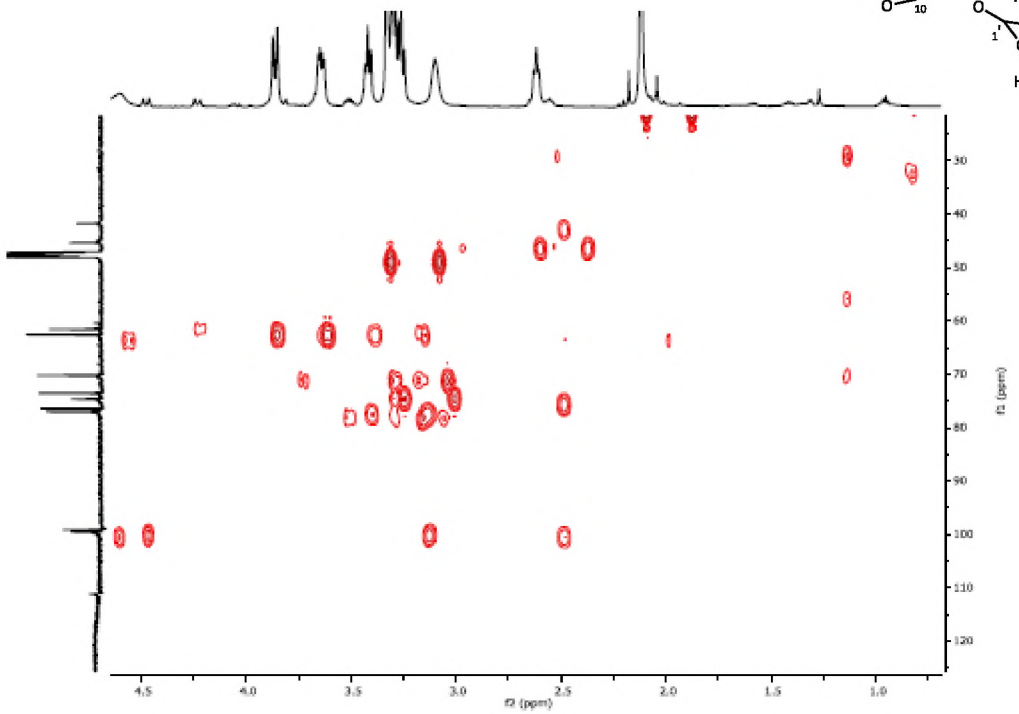

Appendix 5.2.5 **HSQC NMR for compound 2**

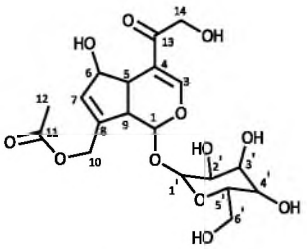

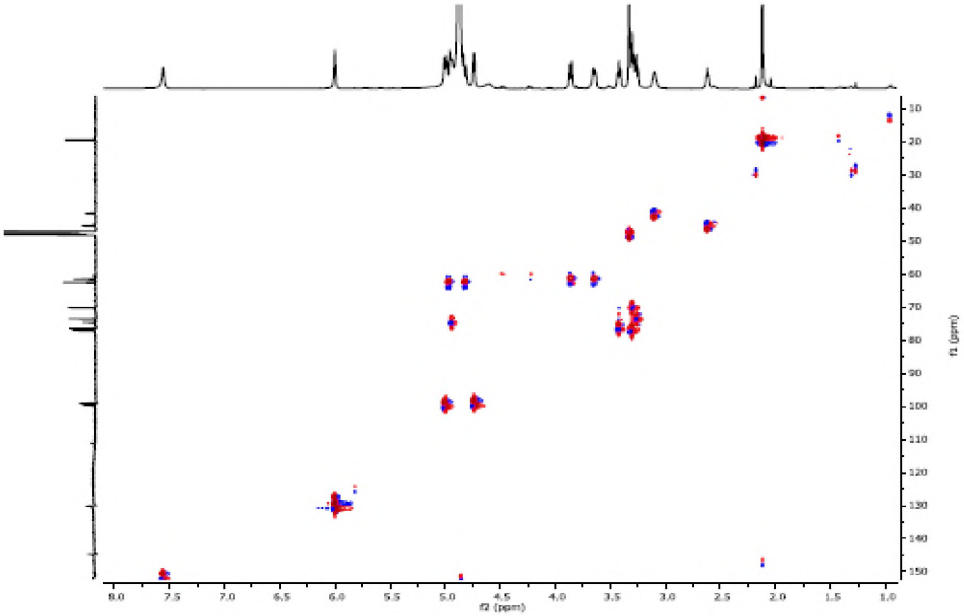

Appendix 5.2.6 **NOESY NMR for compound 2**

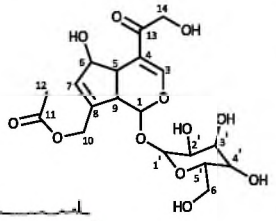

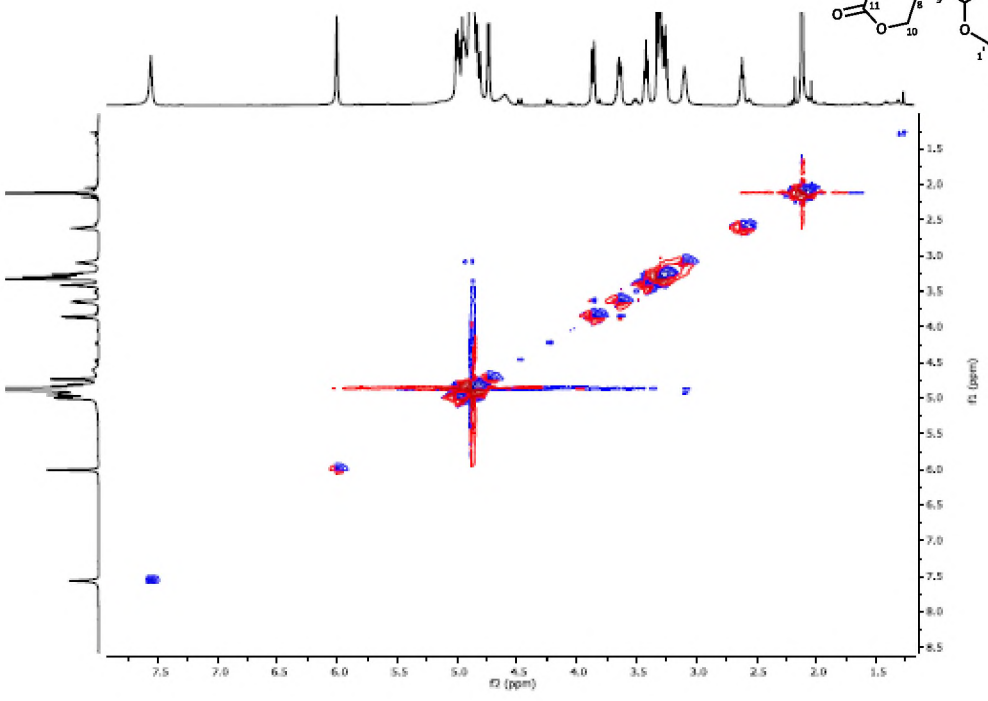

Appendix 5.3 **NMR for sample 3**

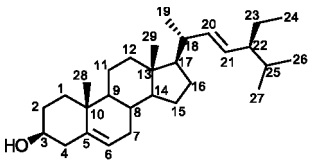

Appendix 5.3.1 **DEPT 135 NMR for sample 3**

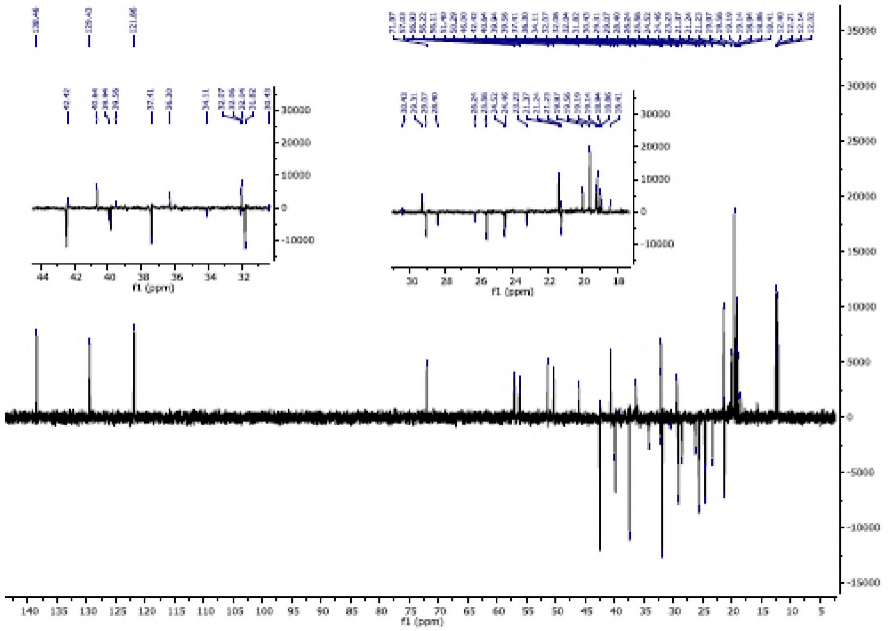

Appendix 5.3.2 **^{13}C & DEPT 135 NMR for sample 3**

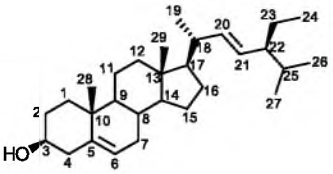

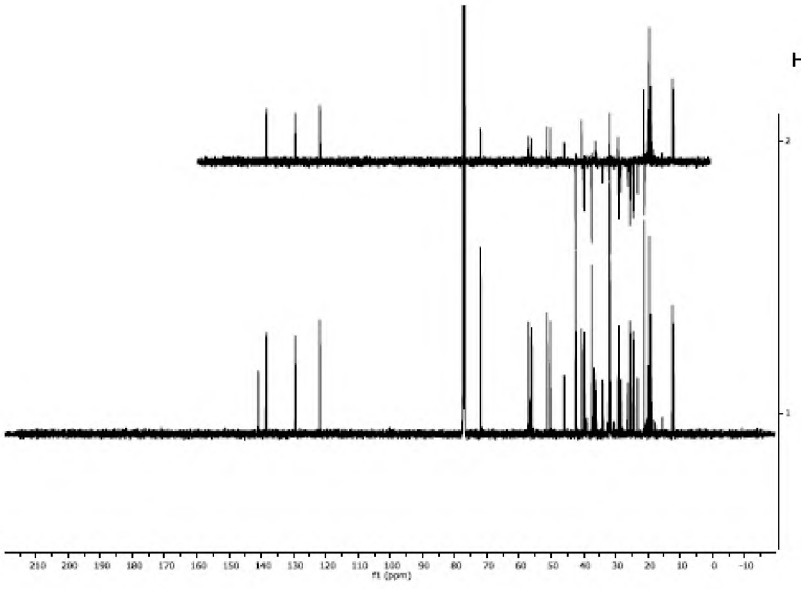

Appendix 5.3.3(a) **COSY NMR for sample 3**

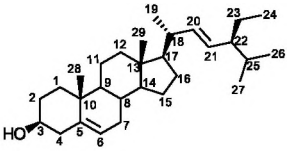

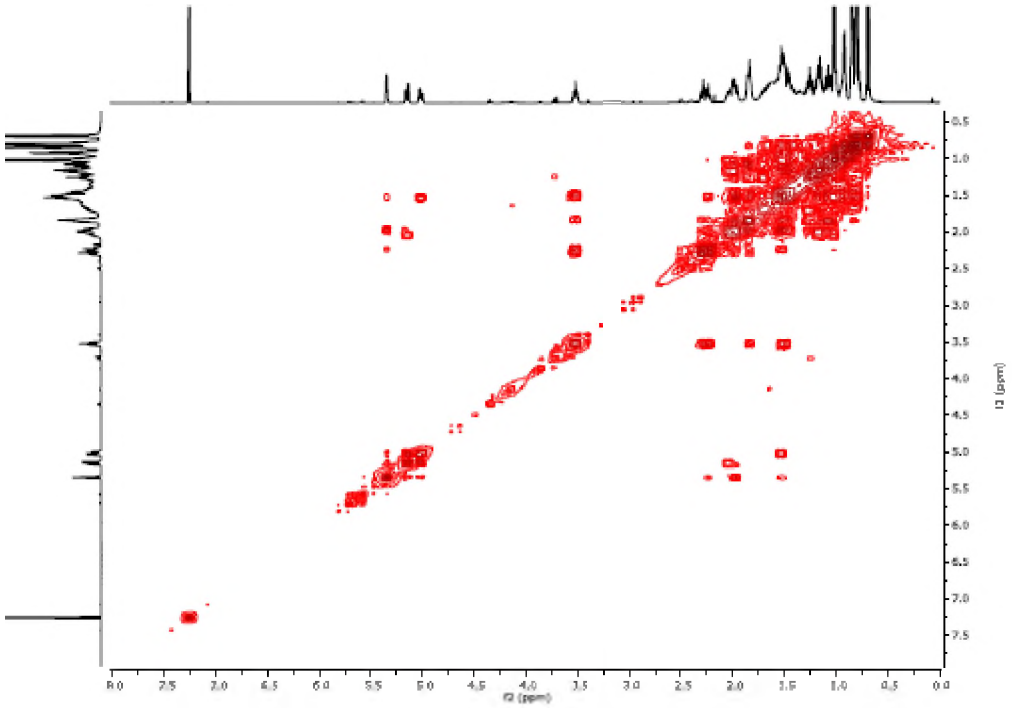

Appendix 5.3.3(b) **COSY NMR for sample 3**

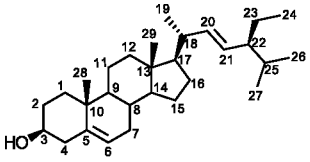

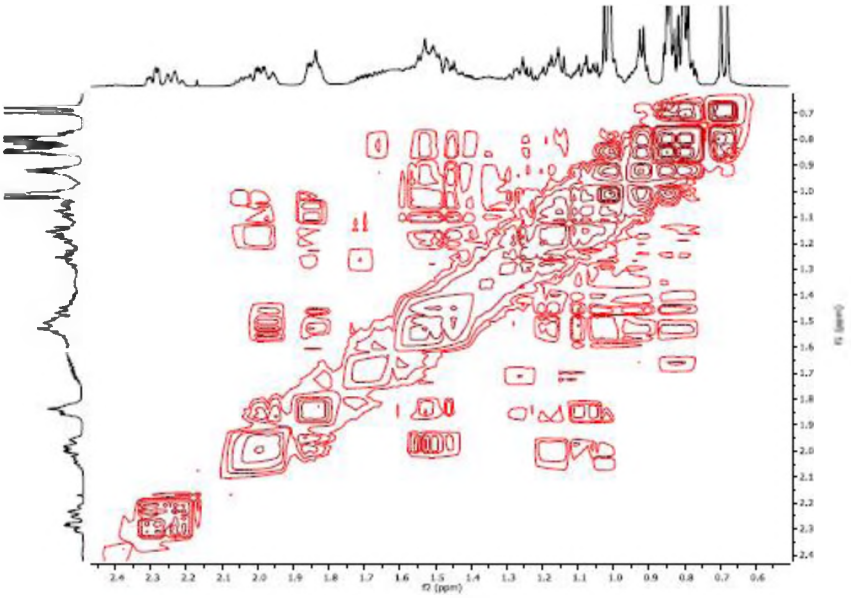

Appendix 5.3.4 HMBC NMR for sample 3

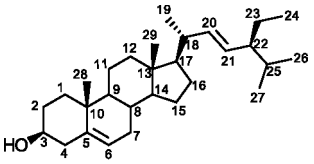

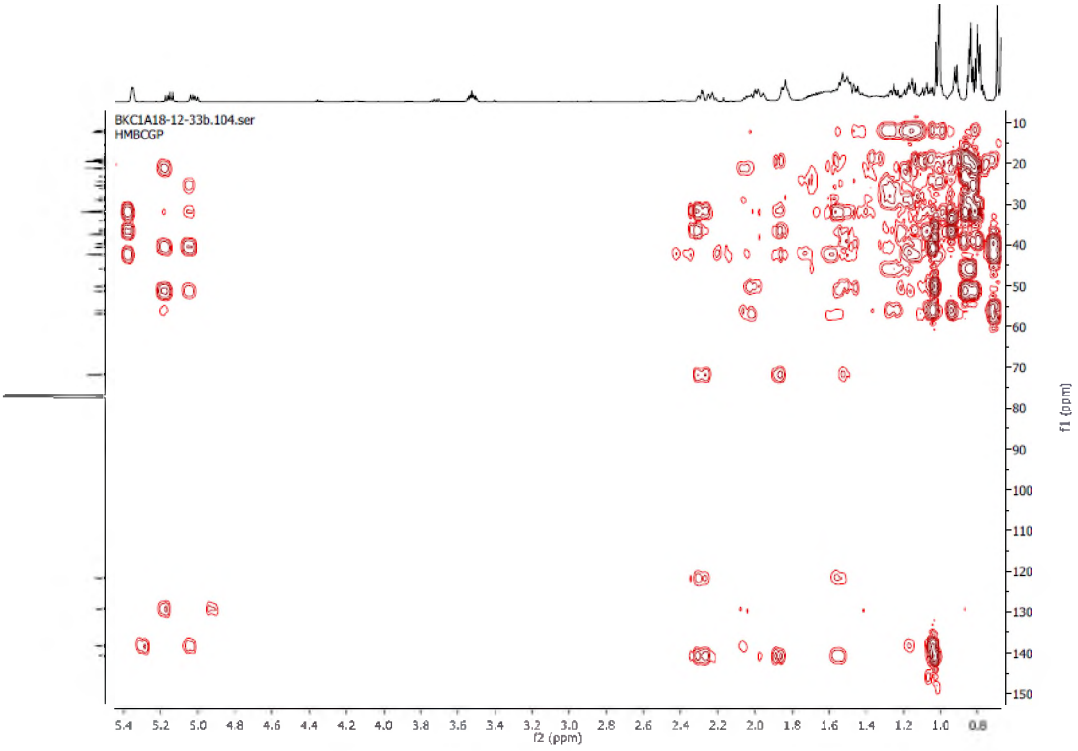

Appendix 5.3.5 HSQC NMR for sample 3

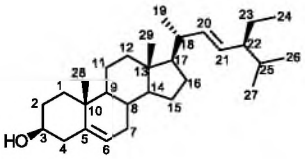

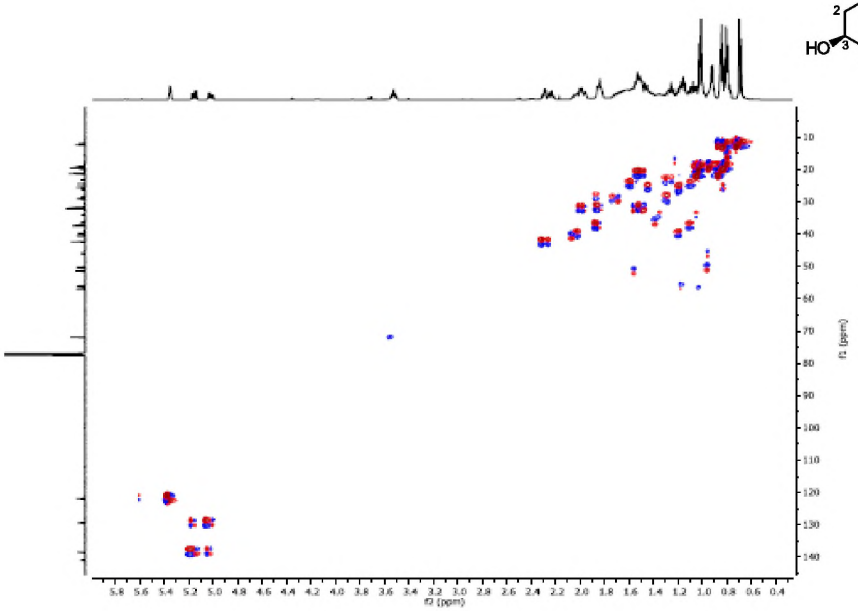

Appendix 5.3.6(a) **NOESY NMR for sample 3**

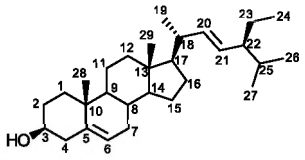

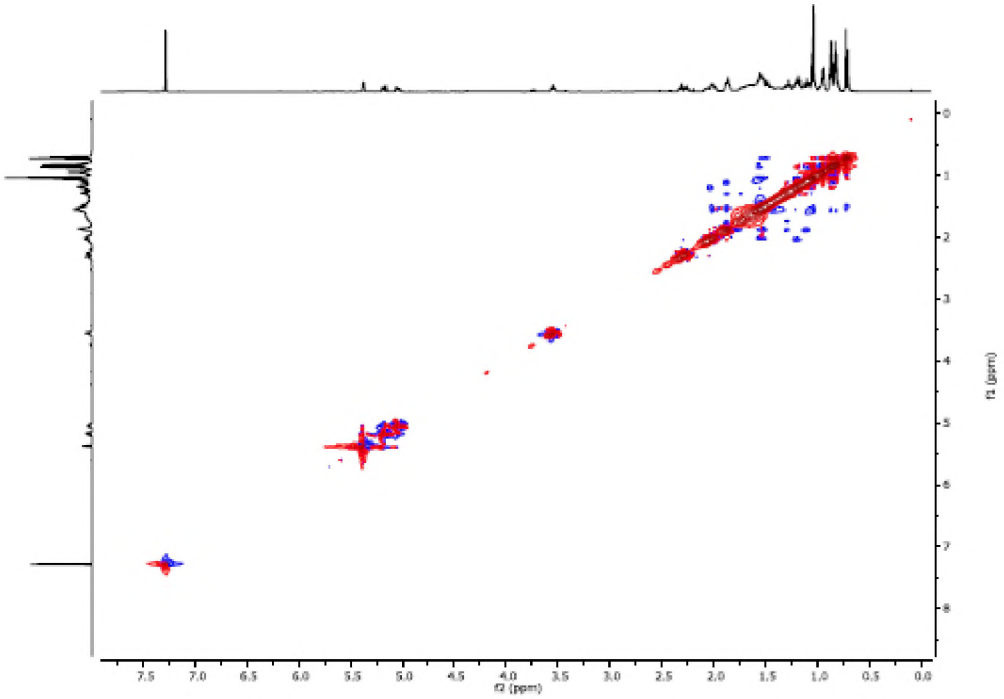

Appendix 5.3.6(b) **NOESY NMR for sample 3**

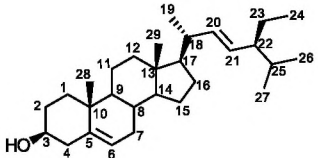

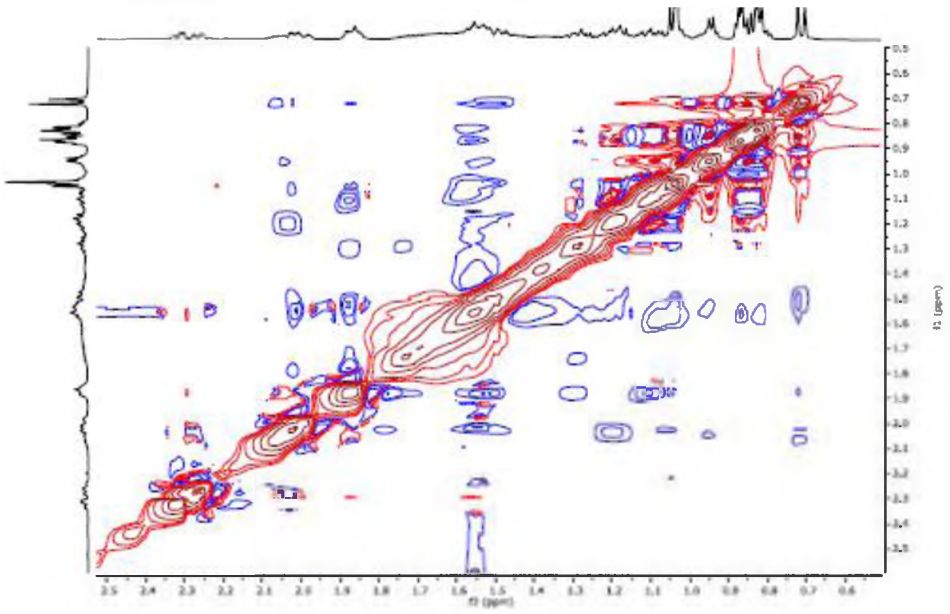

Appendix 5.4 **NMR for compound 4**

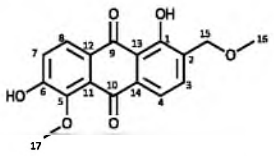

Appendix 5.4.1 **DEPT 135 NMR for compound 4**

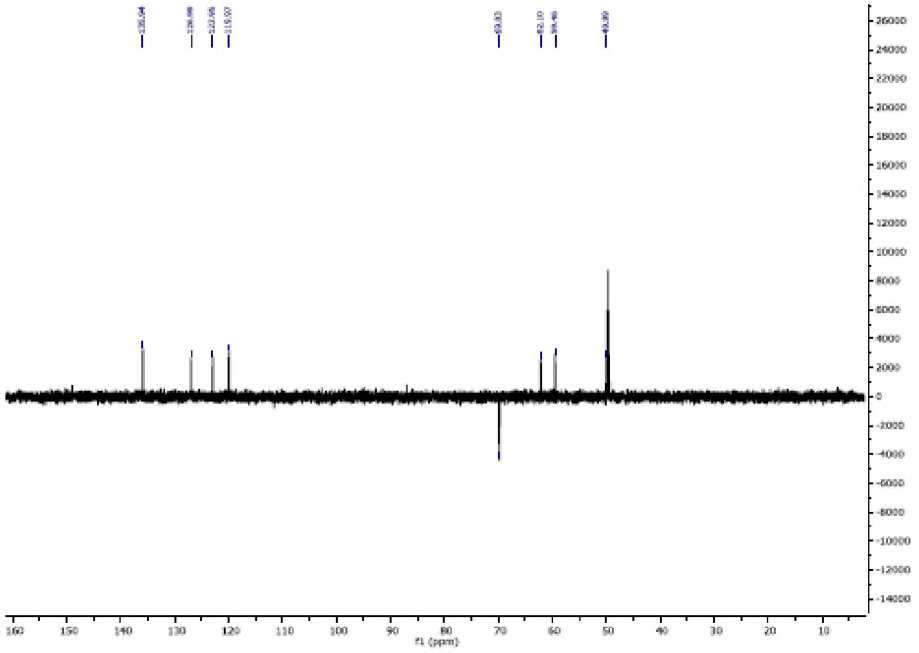

Appendix 5.4.2 **^{13}C & DEPT 135 NMR for compound 4**

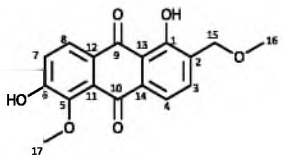

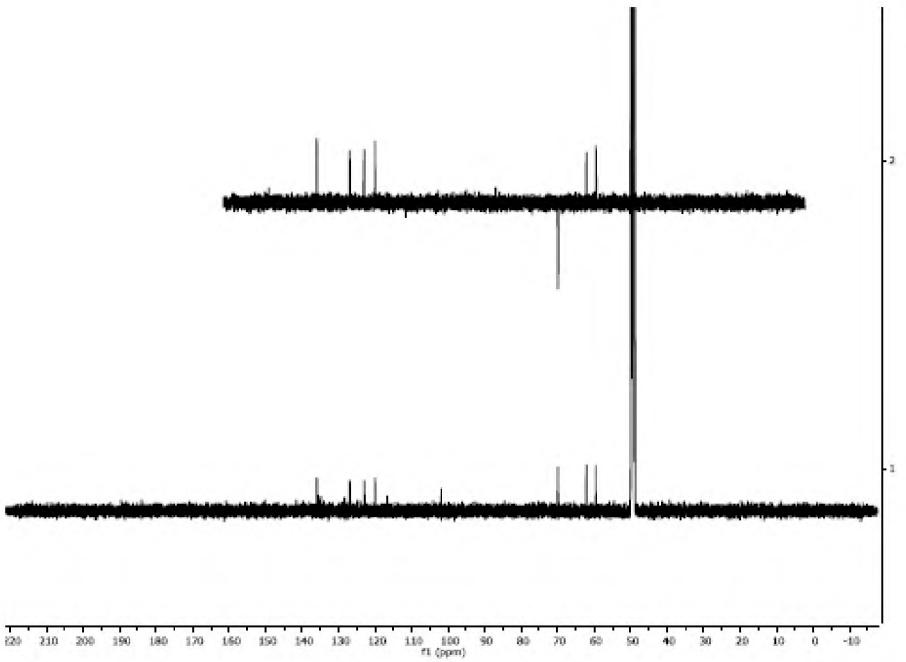

Appendix 5.4.3 **COSY NMR for compound 4**

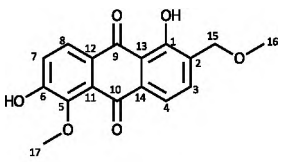

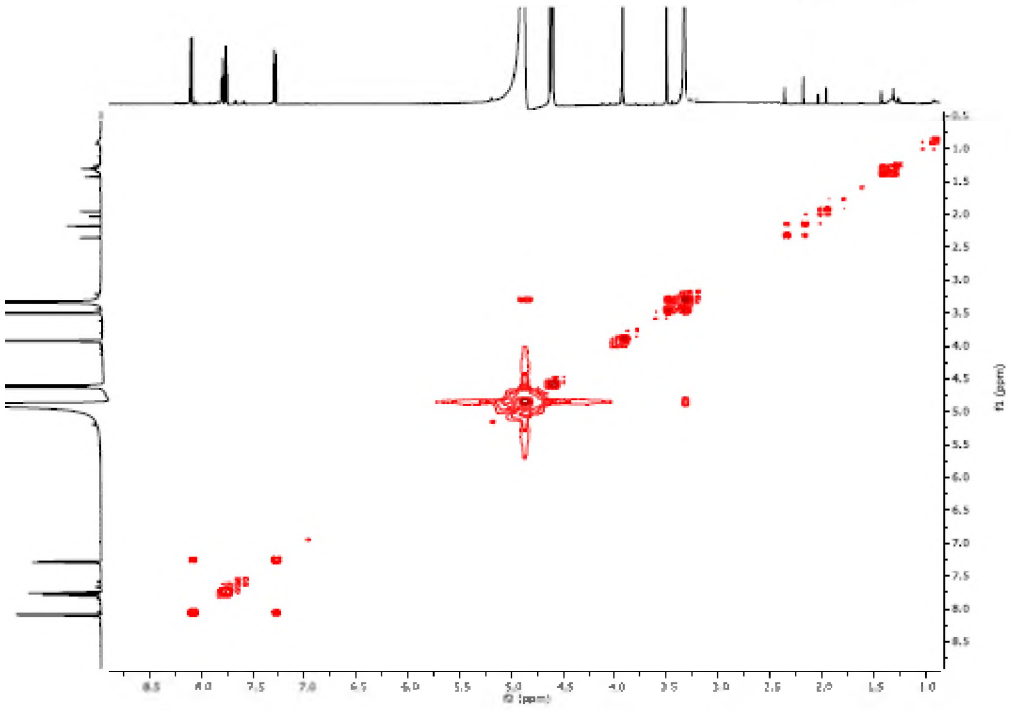

Appendix 5.4.4 **HMBC NMR for compound 4**

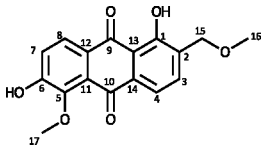

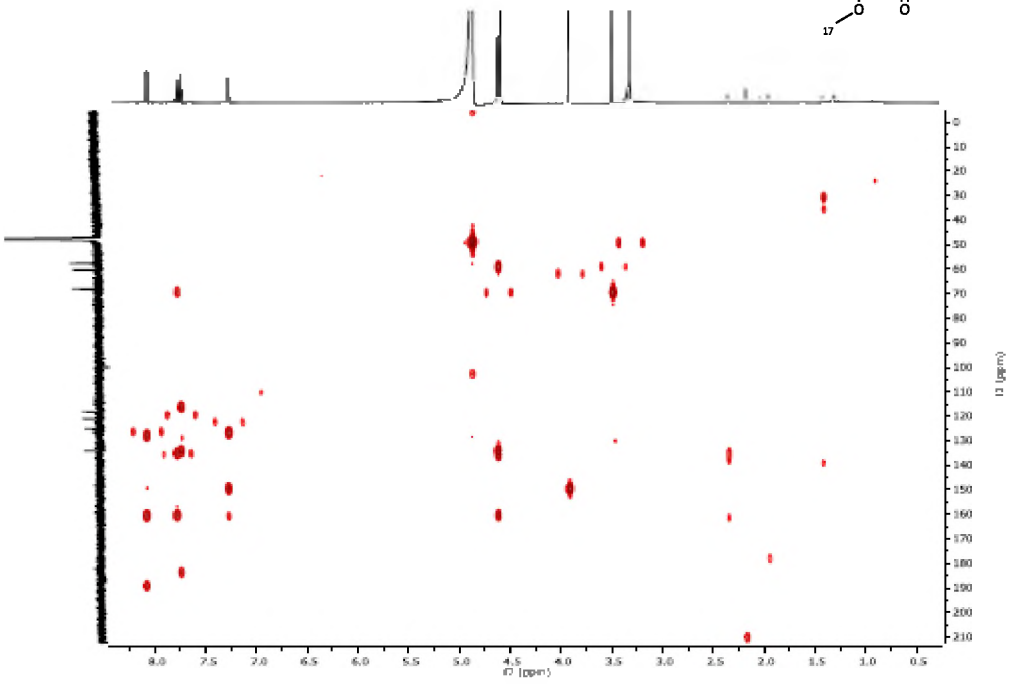

Appendix 5.4.5 **HSQC NMR for compound 4**

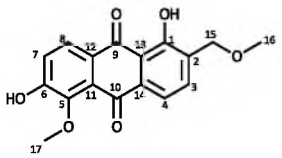

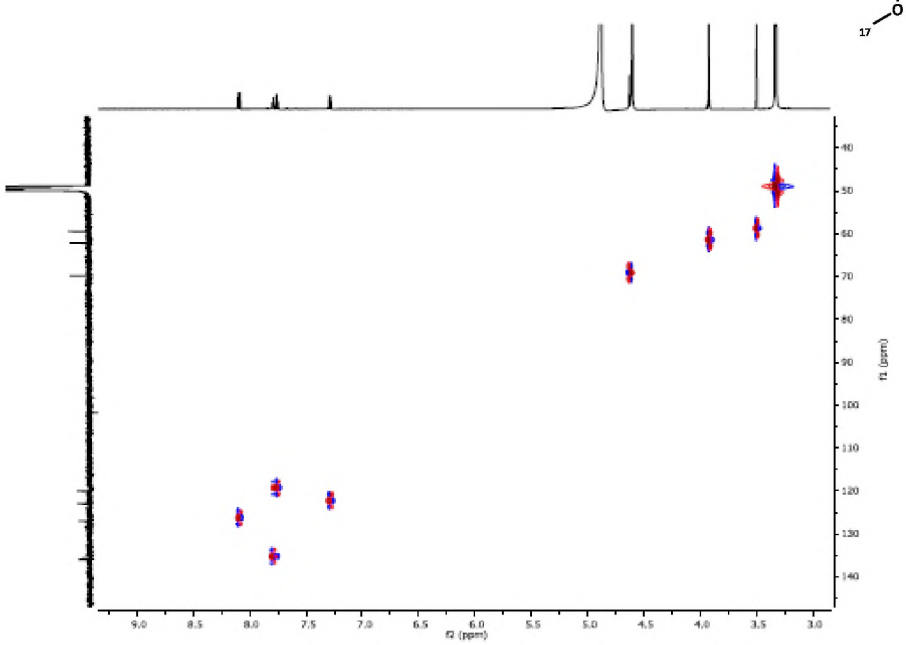

Appendix 5.4.6 **NOESY NMR for compound 4**

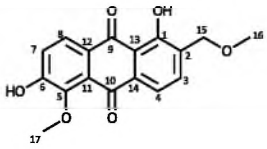

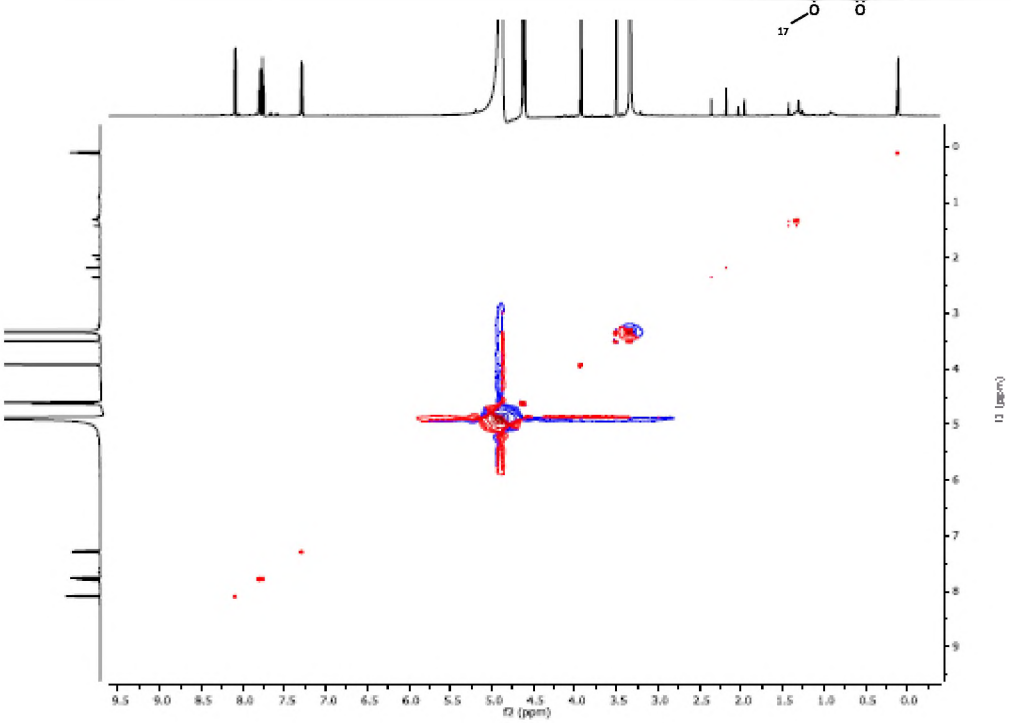

Appendix 5.5 **NMR for compound 5**

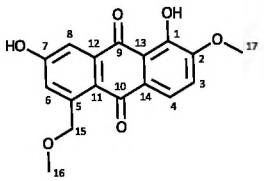

Appendix 5.5.1 **DEPT 135 NMR for compound 5**

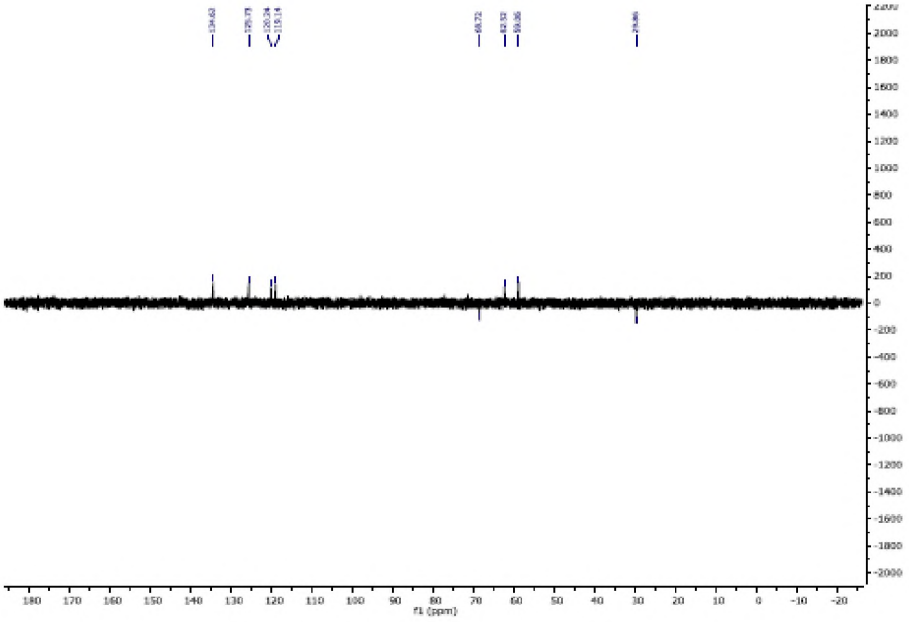

Appendix 5.5.2 **^{13}C & DEPT 135 NMR for compound 5**

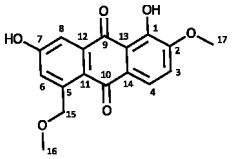

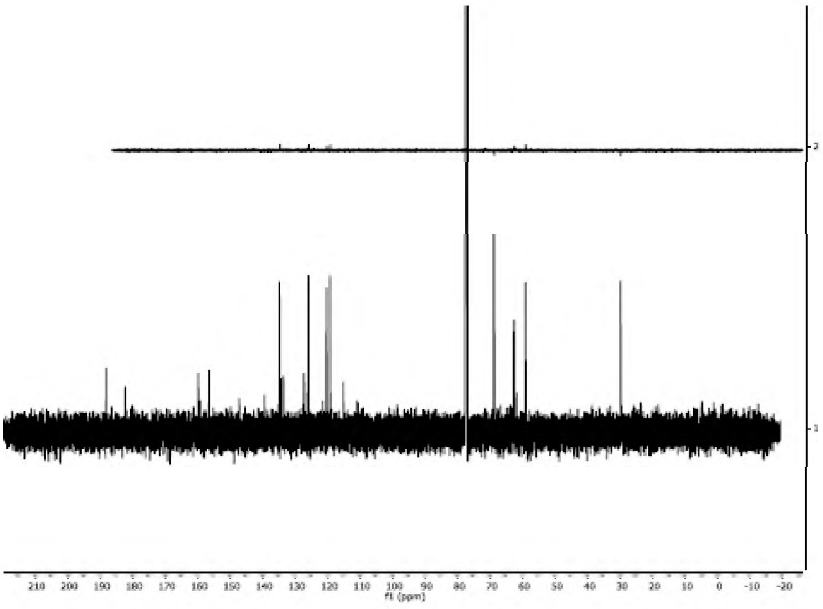

Appendix 5.5.3(a) **COSY NMR for compound 5**

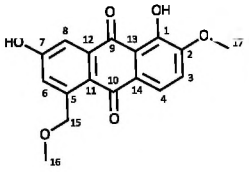

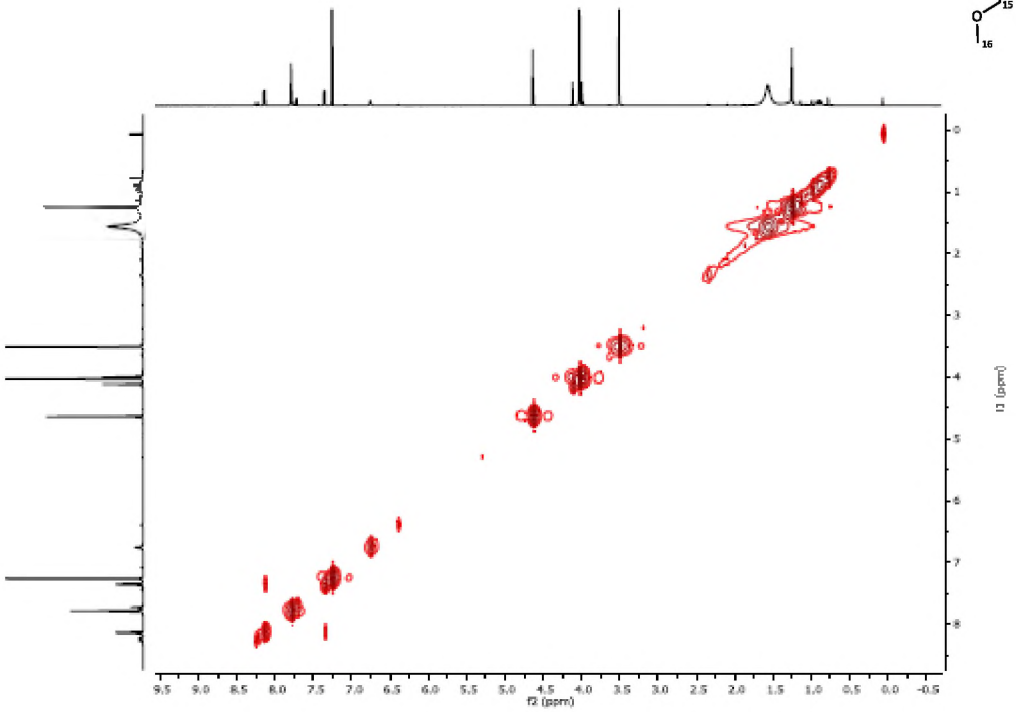

Appendix 5.5.3(b) **COSY NMR for compound 5**

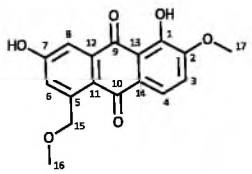

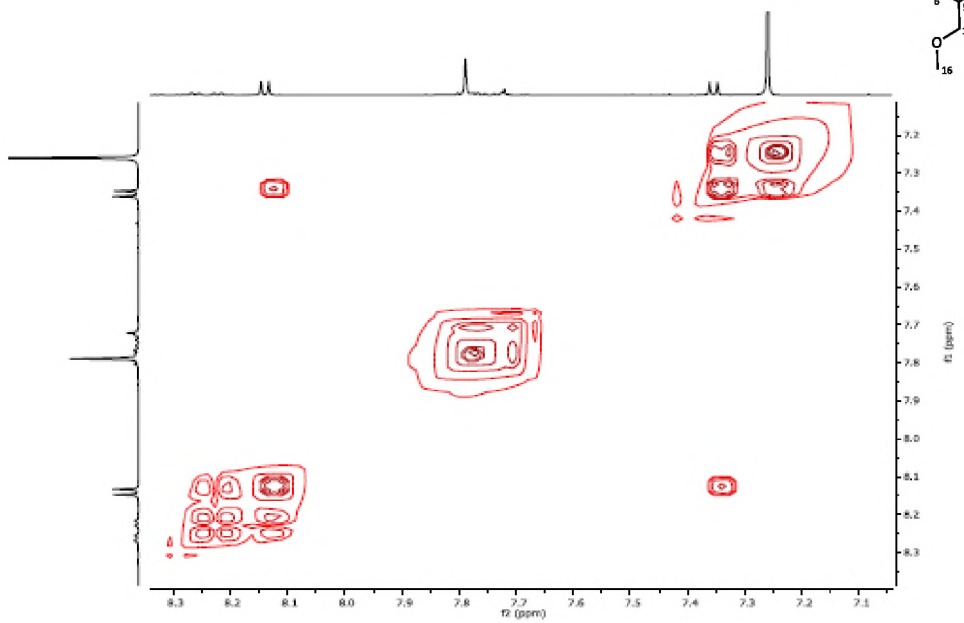

Appendix 5.5.4 **HMBC NMR for compound 5**

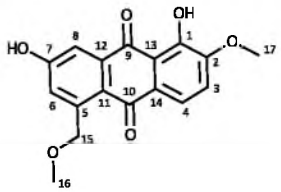

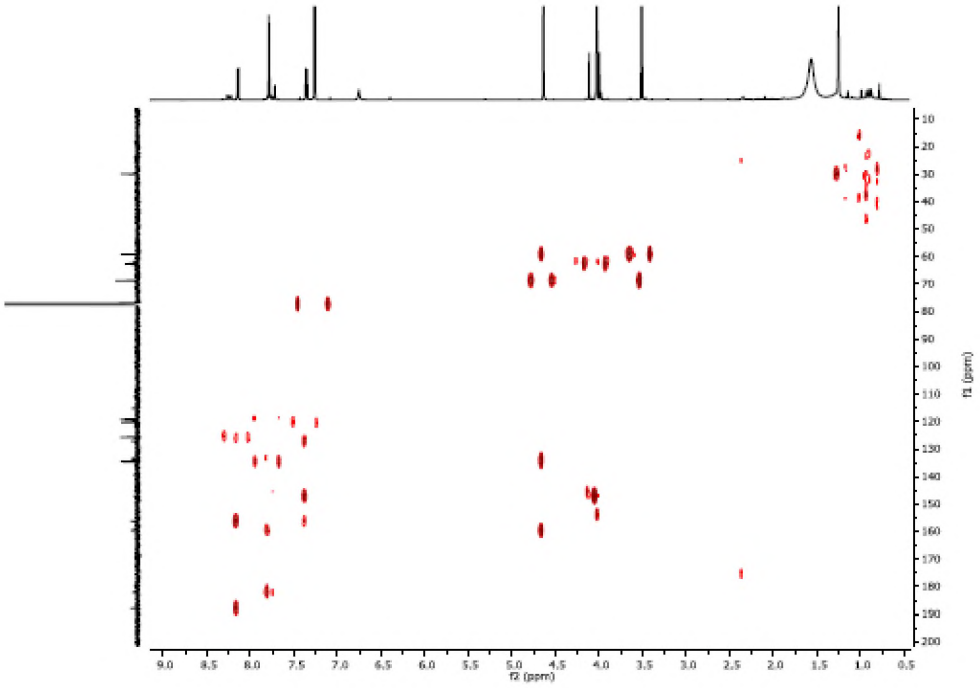

Appendix 5.5.5 **HSQC NMR for compound 5**

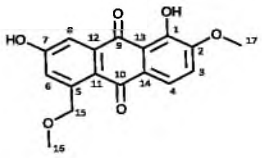

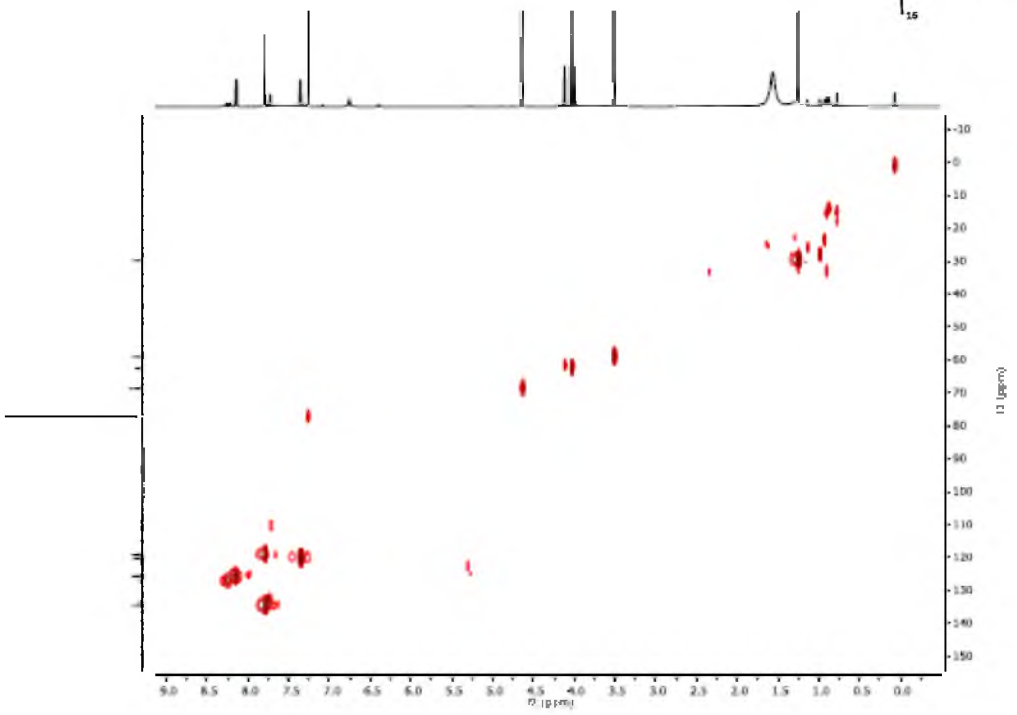

Appendix 5.5.6(a) **NOESY NMR for compound 5**

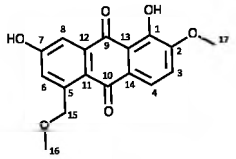

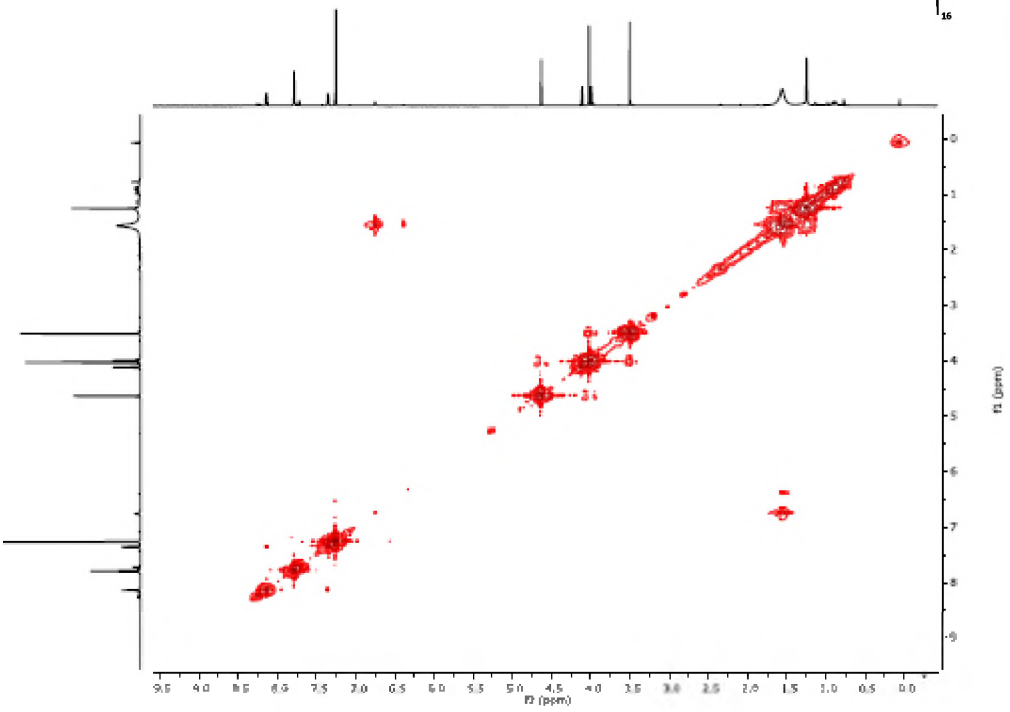

Appendix 5.5.6(b) **NOESY NMR for compound 5**

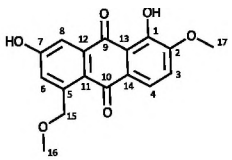

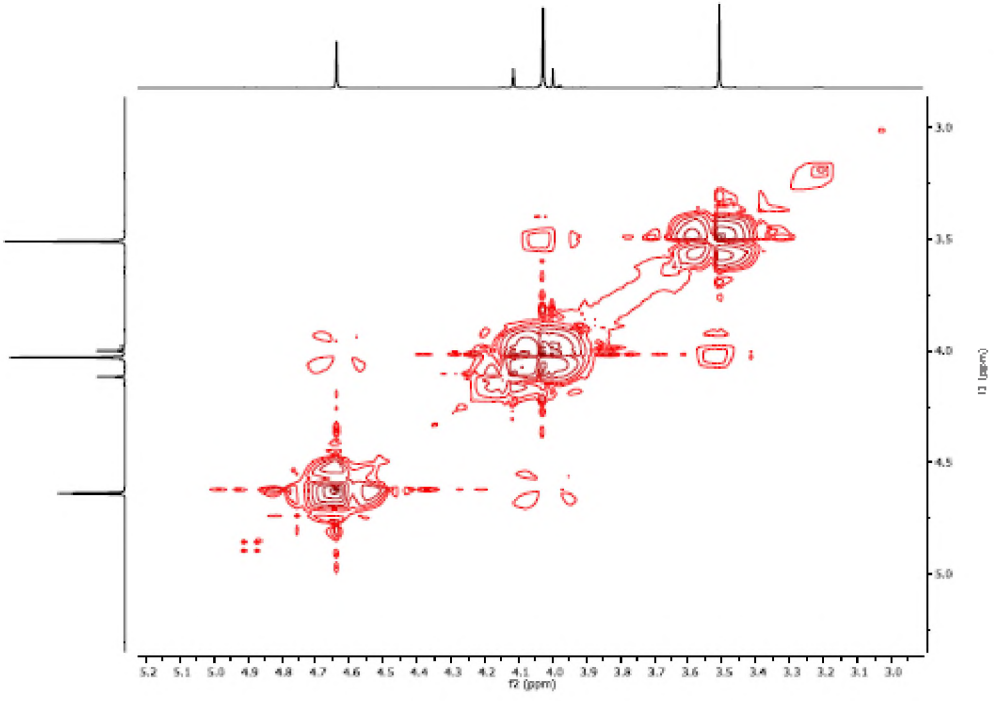

Appendix 5.6 **NMR for compound 6**

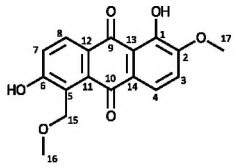

Appendix 5.6.1 **DEPT 135 NMR for compound 6**

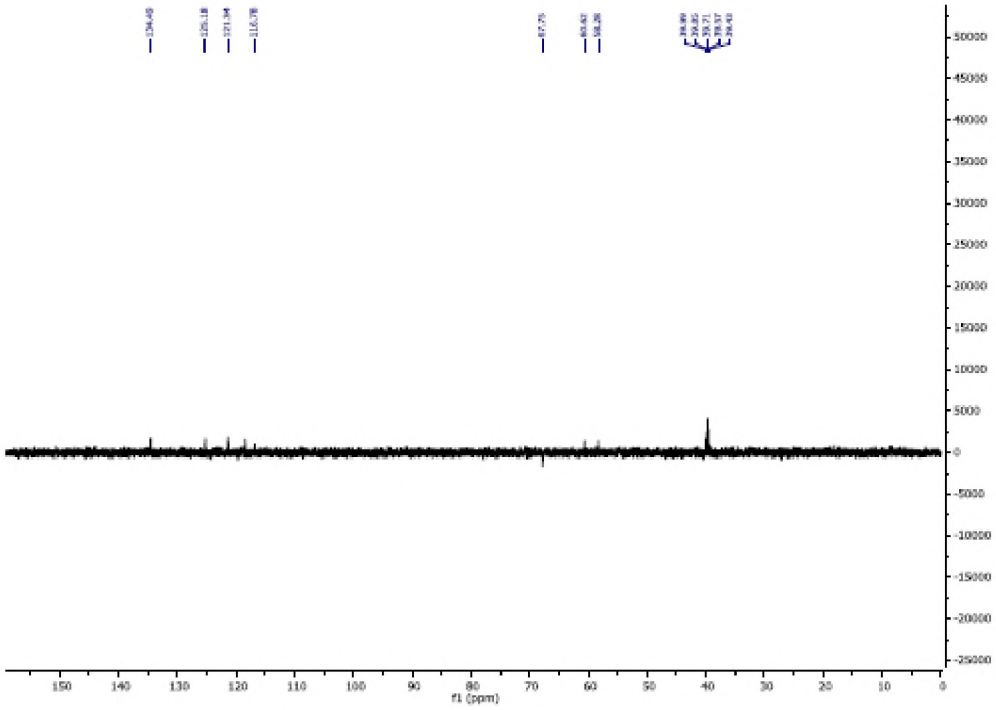

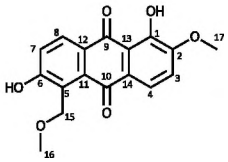

Appendix 5.6.2 **^{13}C & DEPT 135 NMR for compound 6**

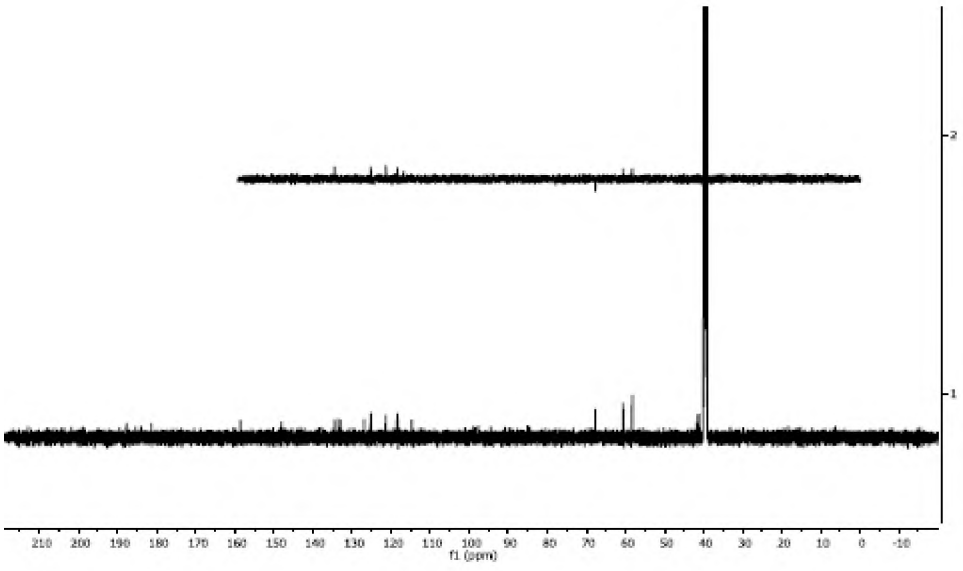

Appendix 5.6.3 COSY NMR for compound 6

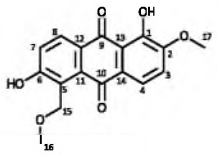

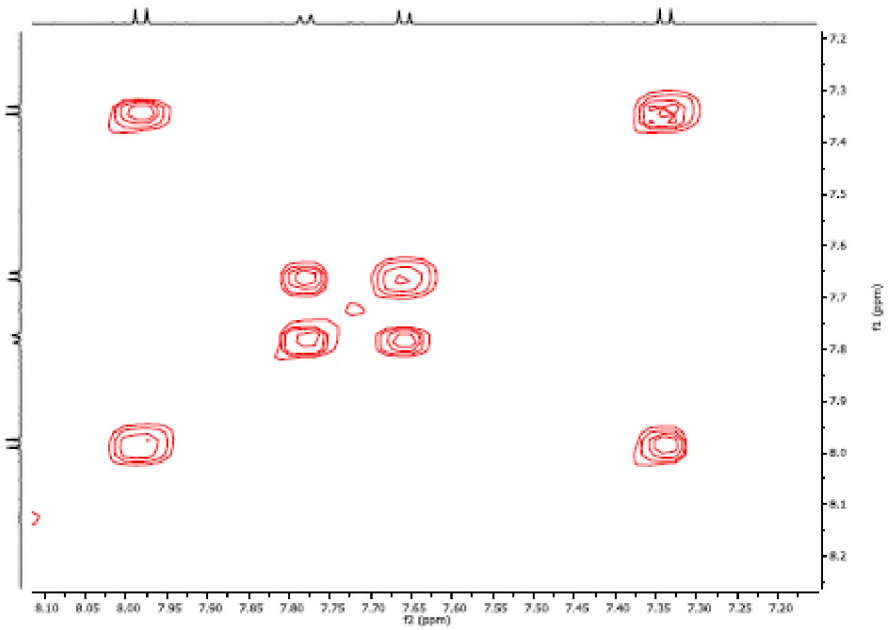

Appendix 5.6.4 HMBC NMR for compound 6

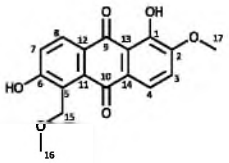

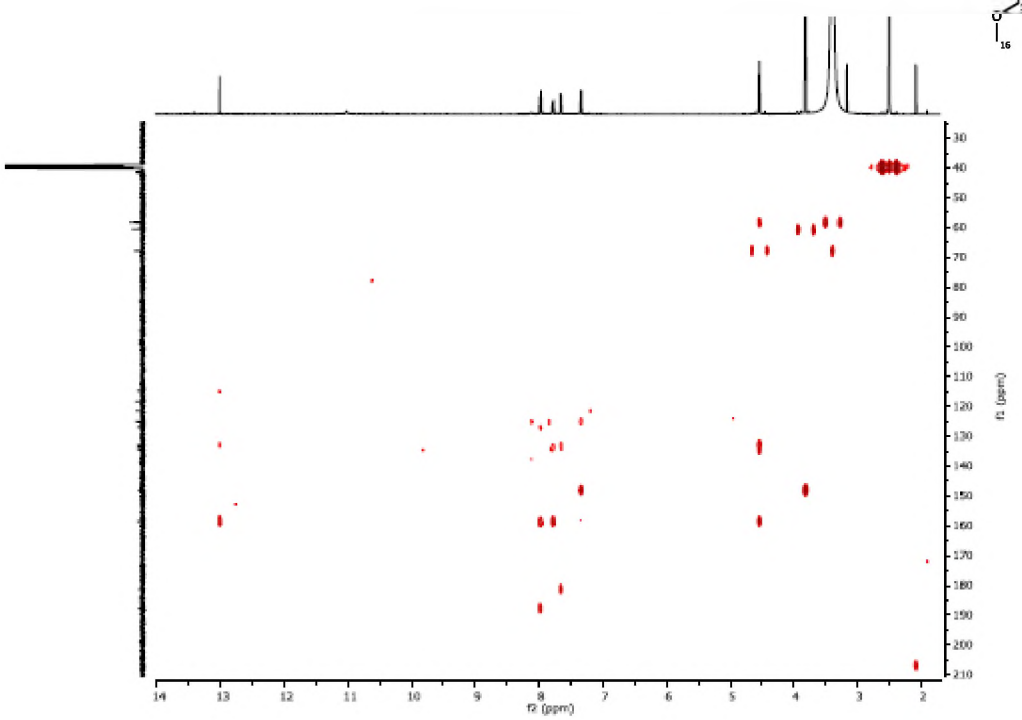

Appendix 5.6.5(a) **HSQC NMR for compound 6**

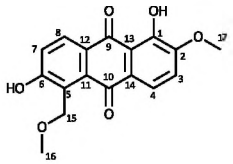

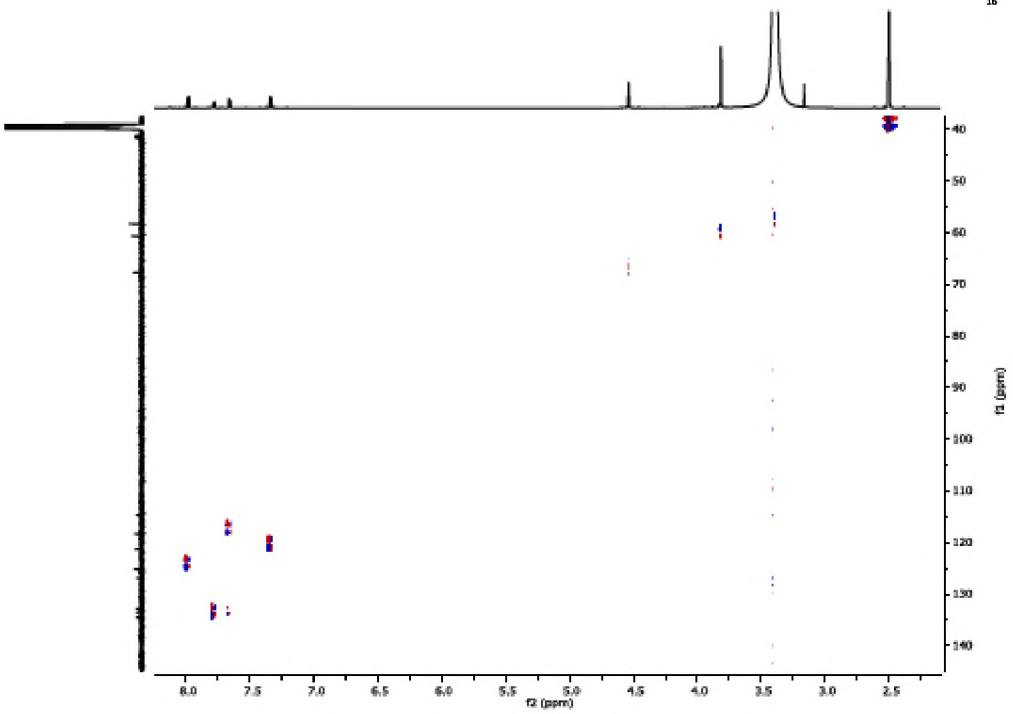

Appendix 5.6.5(b) **HSQC NMR for compound 6**

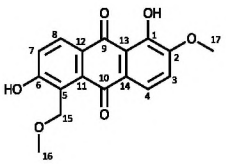

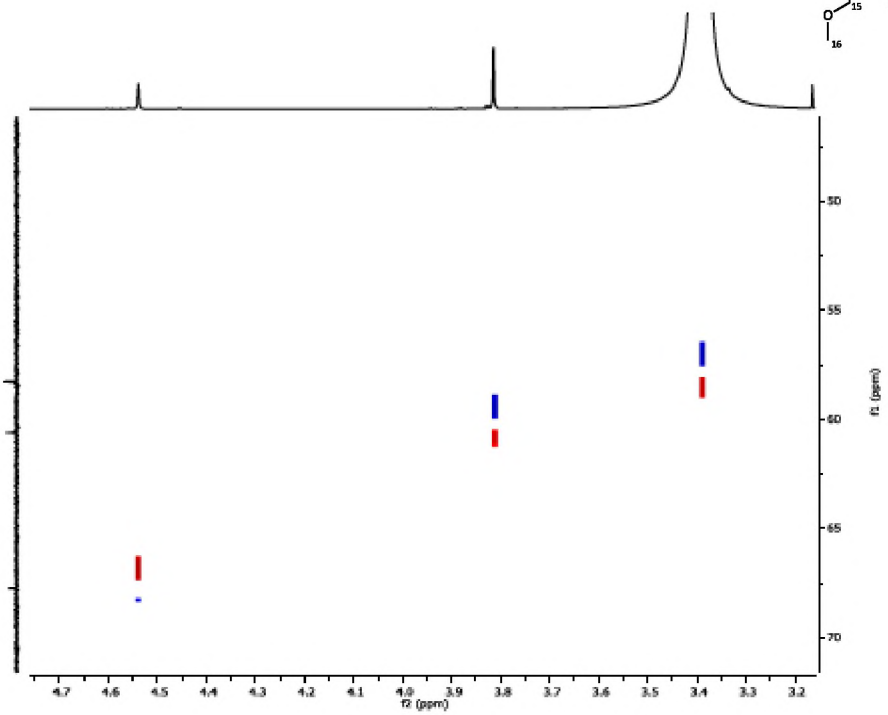

Appendix 5.6.6 NOESY NMR for compound 6